



저작자표시-비영리-변경금지 2.0 대한민국

이용자는 아래의 조건을 따르는 경우에 한하여 자유롭게

- 이 저작물을 복제, 배포, 전송, 전시, 공연 및 방송할 수 있습니다.

다음과 같은 조건을 따라야 합니다:



저작자표시. 귀하는 원저작자를 표시하여야 합니다.



비영리. 귀하는 이 저작물을 영리 목적으로 이용할 수 없습니다.



변경금지. 귀하는 이 저작물을 개작, 변형 또는 가공할 수 없습니다.

- 귀하는, 이 저작물의 재이용이나 배포의 경우, 이 저작물에 적용된 이용허락조건을 명확하게 나타내어야 합니다.
- 저작권자로부터 별도의 허가를 받으면 이러한 조건들은 적용되지 않습니다.

저작권법에 따른 이용자의 권리는 위의 내용에 의하여 영향을 받지 않습니다.

이것은 [이용허락규약\(Legal Code\)](#)을 이해하기 쉽게 요약한 것입니다.

[Disclaimer](#)

석사학위논문

The effects of the angiogenesis inhibitor ALS-L1023
on type 2 diabetes mellitus
in high fat diet-induced female obese mice

목 원 대 학 교 대 학 원

생물학과 동물학전공

임 혜 숙

2014년 6월

The effects of the angiogenesis inhibitor ALS-L1023
on type 2 diabetes mellitus
in high fat diet-induced female obese mice

지도교수 윤 미 정

이 논문을 이학석사학위 논문으로 제출함


2014년 6월


목 원 대 학 교 대 학 원

생 물 학 과

임 혜 숙

임혜숙의 석사학위 논문을 인준함

주심위원 尹 美 貞  (인)

부심위원 김 룬 라  (인)

부심위원 陰 眞 星  (인)

2014년 6월

목 원 대 학 교 대 학 원

CONTENTS

CONTENTS	I
LIST OF FIGURES	v
LIST OF TABLES	vii
ABBREVIATIONS	ix
ABSTRACT	1
1. High fat diet-fed female sham C57BL/6J mice	2
2. High fat diet-fed female OVX C57BL/6J mice	3
I. INTRODUCTION	6
II. MATERIALS AND METHODS	25
1. Preparation of ALS-L1023	25
2. Animal treatments	25
3. Blood analysis	26
4. Oral glucose tolerance test	28
5. Histological analysis	28
6. Immunohistochemistry	29
7. RT-PCR	30
8. Statistics	30
III. RESULTS	33

1. Female sham C57BL/6J mice	
1.1. Regulation of body weight, food intake, adipose tissue mass, and adipocyte size by ALS-L1023 in high fat diet-fed female sham mice	33
1.1.1. Body weight	33
1.1.2. Food intake	33
1.1.3. Adipose tissue mass and adipocyte size	35
1.2. Effects of ALS-L1023 on glucose and insulin levels	35
1.2.1. Glucose and insulin levels	35
1.2.2. OGTT	38
1.3. Effects of ALS-L1023 on pancreatic islet morphology and insulin-secreting cells	38
1.3.1. Histological evaluation of pancreatic islet morphology	40
1.3.2. Immunohistochemical finding : insulin	40
1.4. Effects of ALS-L1023 on pancreatic steatosis	40
1.4.1. Histological evaluation of pancreatic steatosis	40
1.4.2. mRNA expression of pancreatic genes related to fatty acid oxidation	43
1.4.3. mRNA expression of pancreatic genes related to lipogenesis	43
1.5. Effects of ALS-L1023 on pancreatic inflammation	46
1.5.1. Histological evaluation of pancreatic inflammation	46
1.5.2. mRNA expression of pancreatic gene related to inflammation	46
1.6. Effects of ALS-L1023 on pancreatic fibrosis	46

1.6.1. Histological evaluation of pancreatic fibrosis	46
1.6.2. mRNA expression of pancreatic genes related to fibrosis	50
1.7. Effect of ALS-L1023 on mRNA expression of pancreatic genes related to β-cell apoptosis	50
2. Female OVX C57BL/6J mice	
2.1. Regulation of body weight, adipose tissue mass, adipocyte size, and food intake by ALS-L1023 in high fat diet-fed female OVX mice	55
2.1.1. Body weight	55
2.1.2. Adipose tissue mass and adipocyte size	55
2.1.3. Food intake	58
2.2. Effects of ALS-L1023 on glucose and insulin levels	58
2.2.1. Glucose and insulin levels	58
2.2.2. OGTT	58
2.3. Effects of ALS-L1023 on pancreatic islet morphology and insulin-secreting cells	61
2.3.1. Histological evaluation of pancreatic islet morphology	61
2.3.2. Immunohistochemical finding : insulin	61
2.4. Effects of ALS-L1023 on pancreatic steatosis	64
2.4.1. Histological evaluation of pancreatic steatosis	64
2.4.2. mRNA expression of pancreatic genes related to fatty acid oxidation ·	64
2.4.3. mRNA expression of pancreatic genes related to lipogenesis	64
2.5. Effects of ALS-L1023 on pancreatic inflammation	68

2.5.1. Histological evaluation of pancreatic inflammation	68
2.5.2. mRNA expression of pancreatic gene related to inflammation	68
2.6. Effects of ALS-L1023 on pancreatic fibrosis	68
2.6.1. Histological evaluation of pancreatic fibrosis	71
2.6.2. mRNA expression of pancreatic genes related to fibrosis	71
2.7. Effects of ALS-L1023 on mRNA expression of pancreatic genes related to β-cell apoptosis	71
IV. DISCUSSION	76
V. REFERENCE	88
국문 요약	98
1. 고지방식이 암컷 비만마우스	99
2. 난소가 제거된 고지방식이 암컷 비만마우스	100

LIST OF FIGURES

Figure 1. Contribution of genetic predisposition and environment factors in the pathogenesis of type 2 diabetes	10
Figure 2. Structure of the pancreas	17
Figure 3. (A) The receptor of insulin and (B) the actions of insulin to stimulate uptake of blood glucose	18
Figure 4. Pathogenesis of insulin resistance and β -cell failure in type 2 diabetes mellitus	21
Figure 5. Effects of ALS-L1023 on body weight (A), and body weight gain (B), and food intake (C) in high fat diet-fed female sham mice	34
Figure 6. Effects of ALS-L1023 on adipose tissue mass	36
Figure 7. Effects of ALS-L1023 on visceral adipocyte histology	37
Figure 8. Effects of ALS-L1023 on serum glucose and insulin levels	39
Figure 9. Effects of ALS-L1023 on pancreatic islet structures	41
Figure 10. Effects of ALS-L1023 on insulin-positive cells in pancreas	42
Figure 11. Effects of ALS-L1023 on pancreatic steatosis	44
Figure 12. Effects of ALS-L1023 on mRNA expression of pancreatic genes related to fatty acid oxidation	45
Figure 13. Effects of ALS-L1023 on mRNA expression of pancreatic genes related to lipogenesis	47
Figure 14. Effects of ALS-L1023 on pancreatic inflammation	48

Figure 15. Effects of ALS-L1023 on mRNA expression of pancreatic gene related to inflammation	49
Figure 16. Effects of ALS-L1023 on pancreatic fibrosis	51
Figure 17. Effects of ALS-L1023 on mRNA expression of pancreatic genes related to fibrosis	52
Figure 18. Effects of ALS-L1023 on mRNA expression of pancreatic genes related to β -cell apoptosis	54
Figure 19. Effects of ALS-L1023 on body weight (A), and body weight gain (B), and food intake (C) in high fat diet-fed female OVX mice ..	56
Figure 20. Effects of ALS-L1023 on adipose tissue mass	57
Figure 21. Effects of ALS-L1023 on visceral adipocyte histology	59
Figure 22. Effects of ALS-L1023 on serum glucose and insulin levels	60
Figure 23. Effects of ALS-L1023 on pancreatic islet structures	62
Figure 24. Effects of ALS-L1023 on insulin-positive cells in pancreas	63
Figure 25. Effects of ALS-L1023 on pancreatic steatosis	65
Figure 26. Effects of ALS-L1023 on mRNA expression of pancreatic genes related to fatty acid oxidation	67
Figure 27. Effects of ALS-L1023 on mRNA expression of pancreatic genes related to lipogenesis	67
Figure 28. Effects of ALS-L1023 on pancreatic inflammation	69
Figure 29. Effects of ALS-L1023 on mRNA expression of pancreatic gene related to inflammation	70

Figure 30. Effects of ALS-L1023 on pancreatic fibrosis	72
Figure 31. Effects of ALS-L1023 on mRNA expression of pancreatic genes related to fibrosis	73
Figure 32. Effects of ALS-L1023 on mRNA expression of pancreatic genes related to β -cell apoptosis	74

LIST OF TABLES

Table 1. Overweight and obesity as defined by the World Health

Organization 7

Table 2. The experimental groups 27

Table 3. Composition of experimental diets 27

Table 4. PCR primers and conditions used for RT-PCR 31

ABBREVIATIONS

- T2D : Type 2 diabetes mellitus
- Sham-operated : Sham
- Ovariectomized : OVX
- HFD : High fat diet
- LFD : Low fat diet
- TG : Tryglyceride
- FA : Fatty acid
- MMP : Matrix metalloproteinase
- OGTT : Oral glucose tolerance test
- α -SMA : α -smooth muscle actin
- FAS : Fatty acid synthase
- PPAR α : Peroxisome proliferator-activated receptor α
- PPAR γ : Peroxisome proliferator-activated receptor γ
- MCAD : Medium chain acyl-CoA dehydrogenase
- VLCAD : Very long chain acyl-CoA dehydrogenase
- AMPK α 1 : AMP-activated protein kinase α 1
- AMPK α 2 : AMP-activated protein kinase α 2
- CPT-1 : Carnitine palmitoyltransferase I
- SREBP-1c : Sterol regulatory elements binding proteins
- ACC : Acetyl-CoA carboxylase
- C/EBP α : CCAAT-enhancer-binding protein α
- aP2 : Adipocyte protein 2
- CD68 : Cluster of Differentiation 68
- Bax : Bcl-2-associated X protein
- p53 : Tumor protein p53
- Bcl-2 : β -cell lymphoma 2
- Bcl-xL : β -cell lymphoma-extra 1

Abstract

The effects of the angiogenesis inhibitor ALS-L1023
on type 2 diabetes mellitus in high fat diet-induced female obese mice

Hyesook Lim

Department of Biology

The Graduate School of Mokwon University, Daejeon, Korea

Supervised by Professor Michung Yoon

Obesity is the most frequent and most studied of all the risk factors for type 2 diabetes mellitus (T2D). In particular, visceral obesity is deeply associated with T2D. T2D is a metabolic disorder that is characterized by high blood glucose in the context of chronic insulin resistance and relative insulin deficiency. Moreover, obesity and T2D are differentially regulated, depending on the presence of the ovarian steroid hormone estrogen. Therefore, this study was undertaken to investigate whether the angiogenesis inhibitor ALS-L1023 regulates T2D in animal models of human female T2D, such as high fat diet (HFD)-induced female sham-operated (sham) and ovariectomized (OVX) C57BL/6J mice and to determine the cellular and molecular mechanisms involved in this process. The results of this study are as follows.

1. High fat diet-fed female sham C57BL/6J mice

Here, this study investigated the regulation of T2D by the angiogenesis inhibitor ALS-L1023, which reduces adipose tissue growth and development, in diet-induced female obese mice.

- 1) HFD increased body weight gain, adipose tissue weight and adipocyte size compared with low fat diet (LFD). However, ALS-L1023 reduced body weight gain, adipose tissue mass and adipocyte size compared with HFD.
- 2) HFD-fed obese mice exhibited insulin resistance as shown by increased insulin and glucose levels. Whereas, 0.8% ALS-L1023 treatment decreased the serum glucose and insulin levels compared with HFD.
- 3) HFD-induced obese female sham mice displayed impaired glucose tolerance compared with the LFD-fed mice. However, 0.8% ALS-L1023 improved the impaired glucose tolerance caused by HFD.
- 4) Compared with LFD-fed mice, the pancreatic islet size was markedly increased in HFD-fed mice. Cells inside the pancreatic islets showed hyperplasia in HFD-fed mice. In contrast, the size of pancreatic islets was decreased to that of pancreatic islets in LFD-fed mice after 0.8% ALS-L1023 treatment. Similarly, ALS-L1023 increased the intensity of insulin-positive cells in pancreas compared with HFD alone.
- 5) ALS-L1023-treated mice exhibited decreased pancreatic lipid accumulation compared with obese control mice. In contrast, 0.8% ALS-L1023 downregulated the mRNA expression of lipogenic genes (i.e. aP2, SREBP-1c, and ACC), whereas

0.8% ALS-L1023 upregulated the mRNA expression of genes involved in β -oxidation (i.e. MCAD, CPT-1, PPAR α , AMPK α 1, and AMPK α 2).

- 6) Administration of ALS-L1023 reduced pancreatic mast cells compared with HFD alone. ALS-L1023 downregulated the mRNA expression of the inflammatory gene CD68.
- 7) ALS-L1023 reduced pancreatic fibrosis compared with HFD alone. Similarly, ALS-L1023 downregulated the mRNA expression of fibrogenic genes (i.e. α -SMA and collagen α 1).
- 8) The mRNA expression of the pancreatic apoptotic inducer p53 was decreased in ALS-L1023-treated mice compared with HFD-fed mice. By contrast, the mRNA expression of the pancreatic apoptotic inhibitor Bcl-xL was increased in ALS-L1023-treated mice compared with HFD-fed mice.

2. High fat diet-fed female OVX C57BL/6J mice

Gonadal hormones estrogens are important regulators of body weight, body fat distribution, glucose metabolism and insulin resistance. Since they have a dramatically increased risk for developing obesity, type 2 diabetes and the metabolic syndrome. So, OVX C57BL/6J mice are suitable for the animal model of postmenopausal women. When women enter menopause, the present findings support the idea that the combination of ovariectomy with a HFD in C57BL/6 mice leads to increased adiposity, dyslipidemia, and proinflammatory cytokines. Therefore, this study aimed to examine the effects of ALS-L1023 on obesity and obesity-related T2D in this mouse model.

- 1) HFD increased body weight gain and adipose tissue weight, and adipocyte size. However, 0.4% ALS-L1023 reduced body weight gain and adipose tissue mass and adipocyte size. In contrast, adipocyte size was decreased in the 0.8% ALS-L1023 treat mice compared with high fat-fed mice although body weight gain and adipose tissue mass were not decreased.
- 2) Analysis of HE-stained adipose tissue section revealed that ALS-L1023 at concentrations of 0.4% and 0.8% markedly decreased the size of visceral adipocytes in HFD-fed mice.
- 3) Blood glucose levels were not different between HFD and HFD supplemented with ALS-L1023 groups. Moreover, ALS-L1023-treated mice increased insulin levels compared with HFD-fed mice.
- 4) HFD-fed OVX mice displayed impaired glucose tolerance compared with the LFD-fed mice. However, 0.8% ALS-L1023 decreased at 30 min during oral glucose tolerance test compared with HFD-fed mice.
- 5) Compared with LFD-fed mice, the pancreatic islet size was markedly increased HFD-fed mice. Cells inside the pancreatic islets showed hyperplasia in HFD-fed mice. In contrast, the size of pancreatic islets was improved to that of the pancreatic islets in LFD-fed mice after 0.4% ALS-L1023 treatment, but not after 0.8% ALS-L1023 treatment. Consistent with the serum insulin levels, ALS-L1023 increased insulin-positive cells in pancreas compared with HFD alone.
- 6) ALS-L1023-treated mice showed decreased pancreatic lipid accumulation compared with HFD-fed control mice. Consistently, 0.8% ALS-L1023

downregulated the mRNA expression of lipogenic genes (i.e. C/EBP α , aP2, and SREBP-1c), whereas ALS-L1023 did not affect the expression of genes associated with fatty acid β -oxidation (i.e. MCAD, VLCAD, AMPK α 1, and AMPK α 2).

- 7) Administration of ALS-L1023 reduced pancreatic mast cells compared with HFD alone. ALS-L1023 downregulated the mRNA expression of the inflammatory gene CD68.
- 8) ALS-L1023 reduced pancreatic fibrosis compared with HFD alone. Similarly, ALS-L1023 downregulated the mRNA expression of fibrogenic genes (i.e. α -SMA and collagen α 1).
- 9) The mRNA expression of the pancreatic apoptotic inducers Bax and p53 was decreased in ALS-L1023-treated mice compared with HFD-fed mice. Whereas, the mRNA expression of the pancreatic apoptotic inhibitor Bcl-2 was increased in ALS-L1023-treated mice compared with HFD-fed mice.

In conclusion, these results demonstrate that the angiogenesis inhibitor ALS-L1023 may prevent HFD-induced obesity and T2D in both female sham and OVX mice, and that these processes are regulated probably through the inhibition of pancreatic steatosis, inflammation, fibrosis, and apoptosis. In this study, HFD-induced obesity and T2D were more eminent in OVX mice than in sham mice. The effects of ALS-L1023 on obesity and T2D are greater in sham mice with functioning ovaries compared with OVX mice, maybe due to high estradiol concentrations in female sham mice.

I. INTRODUCTION

1. T2D

Type 2 diabetes mellitus (T2D, formerly noninsulin-dependent diabetes mellitus or adult-onset diabetes) is a metabolic disorder that is characterized by high blood glucose in the context of chronic insulin resistance and relative insulin deficiency (Kumar *et al.*, 2005). This is in contrast to type 1 diabetes mellitus, in which there is an absolute insulin deficiency due to destruction of islet cells in the pancreas (David *et al.*, 2011). The classic symptoms are excess thirst, frequent urination, and constant hunger. T2D makes up about 90% of cases of diabetes with the other 10% due primarily to type 1 diabetes and gestational diabetes. Obesity is thought to be the primary cause of T2D in people who are genetically predisposed to the disease.

1.1. Obesity and T2D

A perplexing byproduct of contemporary human behaviour related to feeding and physical activity is an increasing accumulation of body fat compared with lean mass. The incidence of obesity [defined as having a body mass index (BMI) of greater than 30 kg per m², Table 1] is increasing dramatically in virtually all societies of the world, and with it come important pathological consequences such as T2D and cardiovascular disease (National Institutes of Health, 1998; Flier *et al.*, 2008). Rates of T2D have increased markedly since 1960 in parallel with obesity : As of 2010 there are

Table 1. Overweight and obesity as defined by the World Health Organization

Category	Body Mass Index
Normal	18.5–24.9 kg/m ²
Overweight	25–29.9 kg/m ²
Obesity class I	30–34.9 kg/m ²
Obesity class II	35–39.9 kg/m ²
Obesity class III	≥ 40 kg/m ²

Body mass index = weight (kg)/height² (m²).

approximately 285 million people with the disease compared to around 30 million in 1985 (Smyth et al., 2006; Shlomo et al., 2012). Long-term complications from high blood sugar can include heart disease, strokes, diabetic retinopathy where eyesight is affected, kidney failure which may require dialysis, and poor circulation in the limbs leading to amputations.

Obesity is the most frequent and most studied of all the risk factors for T2D. While in the whole population prevalence of diabetes mellitus has been somewhere between 3 - 6%, in the population having obesity the prevalence of diabetes has been estimated at 20%. With regard to importance of obesity in pathogenesis, T2D is divided into non-obese and obese variants. The latter form is more common and accounts for approximately 80% of all cases of T2D. The risk of clinical manifestation of T2D shows a close relationship to the degree and duration of obesity. In most obese persons insulin secretion is excessive (from the beginning mainly postprandial hyperinsulinemia is present). In spite of it, however, it is insufficient for increased demands of insulin evoked by peripheral insulin resistance. In theory hyperinsulinemia could induce secondary insulin resistance by downregulation of insulin receptors. This results in hyperglycemia. It is possible that in some individuals prolonged hyperglycemia could lead to the increase of insulin resistance and to the impairment of β -cell function. It gradually leads to β -cell exhaustion and their irreversible damage. This hypothesis is supported by the finding that after the reduction of excess body weight the clinical and laboratory symptoms of diabetes are reduced. Insulin resistance in patients with T2D may be the result of two separate factors. Because insulin insensitivity occurs in obesity without

hyperglycemia, increased adiposity undoubtedly plays an important role in the insulin resistance of obese patients with T2D. However, nonobese relatives of persons with T2D may have hyperinsulinemia and diminished insulin sensitivity, proving that obesity is not the sole cause of insulin resistance (Hulín et al., 1997). Considerable efforts have been made in recent years to find effective preventive measures for a stop or even a reversal of the increase in T2D. Ample evidence has been accumulated indicating that a reduction of intraabdominal fat reduces the incidence of the disease (Tuomilehto et al., 2001). Also, a pharmacological intervention with agents that reduce blood glucose levels, e.g. metformin or the glucosidase inhibitor acarbose, reduces the incidence of diabetes in cohorts with impaired glucose tolerance. Thus, T2D can be considered a largely preventable disease (Knowler et al., 2002; Chiasson et al., 2002; Joost, 2008).

1.2. Pathogenesis and risk factors of T2D

Over the last decade, major advances have been made in our understanding of the pathophysiology and molecular biology of T2D (Scheen, 1996; DeFronzo, 1996). T2D is a bipolar disease characterized by a defect in both insulin secretion and insulin action whose complex interaction leads to a progressive increase of plasma glucose levels (Kahn, 2003). It is also well established that the development of T2D results from an interaction of a subject's genetic makeup and their environment, and that with the increasing prevalence of obesity, the prevalence of T2D is reaching epidemic proportions (Figure 1) (Scheen, 2001). Various organs play a crucial role in the

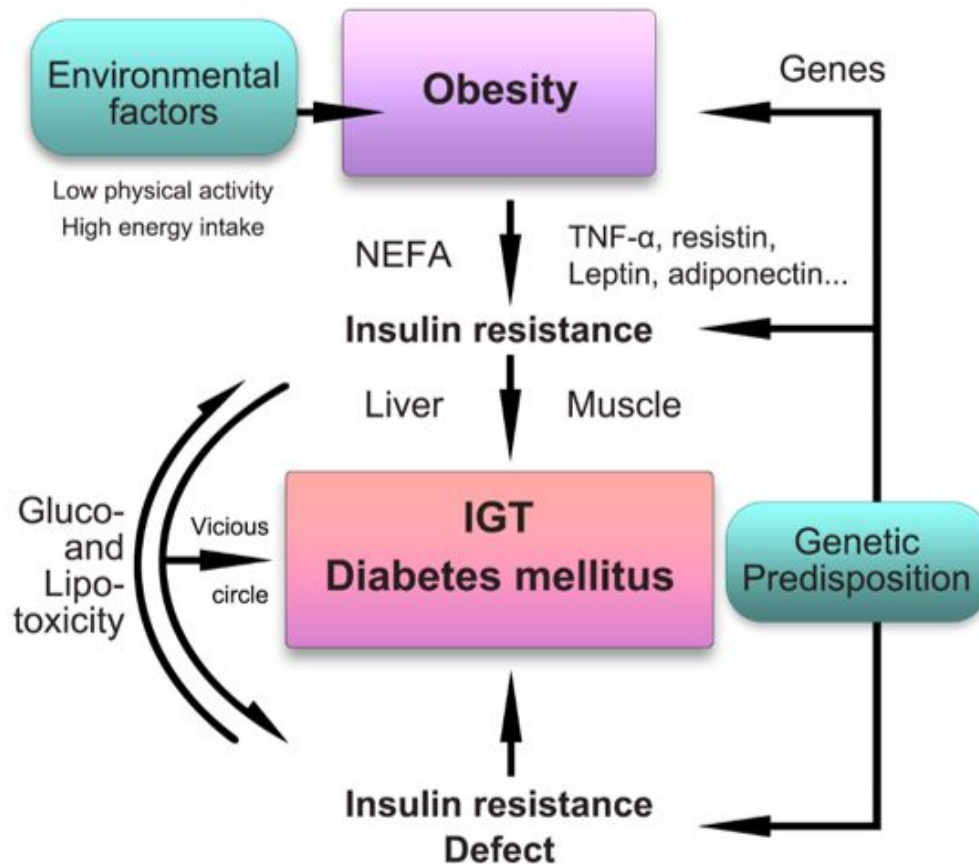


Figure 1. Contribution of genetic predisposition and environment factors in the pathogenesis of type 2 diabetes (T2D). Interplay between defective insulin secretion and insulin resistance leading to a vicious circle explaining the progression from impaired glucose tolerance (IGT) to T2D and the progressive aggravation of the disease. Adapted from Scheen (2003).

pathophysiology of T2D (Gerich, 1998). Disruption of the cross-talk between endocrine pancreas, liver, skeletal muscle, adipose tissue and, presumably, gut and central nervous system may lead to alteration of glucose homeostasis and T2D. While most patients with T2D are overweight or obese, the role of fat was initially neglected in the pathophysiology of the disease (DeFronzo, 1998). Its role was highlighted almost a decade ago, especially the interactions of non-esterified fatty acids (FA) with glucose metabolism (Reaven, 1995; Scheen, 2003).

Excess adiposity is considered the most important factor in the pathogenesis of T2D. In all mouse models of T2D, obesity is essential for the development of hyperglycaemia. In human T2D, the anthropometric parameters body weight, body mass index (BMI) and waist circumference are major predictors of the individual disease risk (Schulze et al., 2005; Colditz et al., 1995; Wang et al., 2005). This risk increase is mainly conferred by the intraabdominal and intrahepatic fat depots, whereas the subcutaneous fat appears to be indifferent (Bajaj et al., 2004; Bajaj et al., 2003; Stumvoll et al., 2004). In mouse models of diabetes and insulin resistance, enhanced hepatic lipogenesis is a key pathophysiological feature (Lan et al., 2003; Becker et al., 2004). Intrahepatic triglycerides (TG) are believed to cause insulin resistance and are therefore directly linked with the pathophysiology of diabetes; even a small reduction significantly lowers the diabetes risk (Joost, 2008; Petersen et al., 2005).

1.3. Metabolic syndrome in females

Obesity, as defined by World Health Organization (Table 1), is more prevalent

in women than in men. The latest National Health and Nutrition Examination Survey data estimate that approximately two thirds of women 40 to 60 years of age are overweight or obese (Ogden et al., 2006). Body weight increases with age, irrespective of the baseline weight in normal and obese individuals alike, Weight gain during menopausal transition has been scrutinized as a major contributing factor to midlife body weight (Polotsky¹ and Polotsky, 2010). Menopausal transition is associated with significant weight gain (2 to 2.5 kg over 3 years on average), which is not dissimilar to that in premenopausal women of like age. Concomitantly, there is an increase in abdominal adiposity and a decrease in energy expenditure, phenomena that have been postulated to explain the higher risk of metabolic syndrome and increases in cholesterol and TGs. Hypertension and diabetes become more prevalent with age (Polotsky¹ and Polotsky, 2010).

Women are usually diagnosed with T2D beyond the age of forty. Taking this fact into consideration menopause can play a role in complicating T2D. Menopause usually occurs between the ages of forty-eight and fifty-two (Rosenthal, 2005). We already know that obesity is a problem in postmenopausal women this fact is due to the decline in growth hormone and the loss of estrogen. The decrease in these two hormones may explain the rapid increase of fat (Mantzoros, 2006). Menopausal women with T2D are also at greater risk for cardiovascular disease. “Cardiovascular disease is the number one killer of women with diabetes, suppressing both breast and ovarian cancer” (Childs, 2006). The risk for developing heart disease in a diabetic patient is two to three times higher than the risk for patients without diabetes. The greater risk for cardiovascular

disease is due to the decrease in estrogen and can also be due to blood vessel damage. To reduce the risk of cardiovascular disease a women with T2D should reduce her intake of certain fats including saturated fats and TGs and increase the intake of other fats including unsaturated fats and omega-3 oils (Revis and Keene, 2006).

2. Pancreas and T2D

Diabetes mellitus is the most common endocrine disorder. However, it is not an individual nosological unit. This term denotes a diabetic syndrome comprising an etiologically and clinically heterogenous group of pathological states, the common and permanent symptom of which is hyperglycemia originating secondary to long-lasting absolute or relative insulin deficiency or to its insufficient effect in target tissues, usually in the presence of a relative or absolute excess of glucagon. Absolute insulin deficiency or its insufficient effect in peripheral tissues causes a disorder of glucose metabolism. When the insulin deficiency is extreme this hormonal abnormality is responsible for the tendency to develop ketoacidosis. The impaired glucose utilization is subsequently associated with the origin of disorder of fat and protein metabolism, as well as with the disorder of water and electrolyte metabolism. Therefore, a complex metabolic disorder originates. In the period of overt diabetes mellitus this complex metabolic disturbance is manifested by hyperglycemia, glycosuria, increased protein catabolism, and ketoacidosis (Hulín *et al.*, 1997).

2.1. Structure of pancreas

The pancreas is both exocrine and endocrine glands that lies in the abdomen, specifically the upper, left abdomen. It is found below the stomach, surrounded by the duodenum. The human pancreas is typically 5.75–9.5 cm long (Kumar et al., 2005). The pancreas is divided into a head, which rests against the second and first part of the duodenum, a body, which passes underneath the base of the stomach, and a tail, which ends adjacent to the spleen. The head of the pancreas surrounds the superior mesenteric artery, which emerges from it.

The exocrine component of the pancreas, often called simply the exocrine pancreas, is the portion of the pancreas that performs exocrine functions. It has ducts that are arranged in clusters called acini (singular acinus).

The islets of Langerhans are the regions of the pancreas that contain its endocrine (i.e., hormone-producing) cells. The islets of Langerhans constitute approximately 1% to 2% of the mass of the pancreas. There are about one million islets distributed throughout the pancreas of a healthy adult human, each of which measures about 0.2 mm in diameter. Each is separated from the surrounding pancreatic tissue by a thin fibrous connective tissue capsule which is continuous with the fibrous connective tissue that is interwoven throughout the rest of the pancreas (Mark et al., 2009). The combined mass of the islets is 1 to 1.5 g.

In the human adult the islets consist of three major and three minor cell types. The three main types are B, A, and D cells making up about 95% of the islet cell population. The β -cells account for about 70% of the islet cell population and produce insulin. The α -cells

account for about 20% of the islet cell population and secrete glucagon. The delta cells secrete somatostatin and make up about 5% of the islet cell population. In immunohistochemical studies that employ specific antibodies to individual hormones, the existence of the three rare cell types has been proved. The three minor cell types are PP cells, D1 cells, and gastrin cells. The PP cells produce a unique pancreatic polypeptide (PP). The D1 cells elaborate vasoactive intestinal polypeptide (VIP). The gastrin cells synthesize pancreatic gastrin. According to their effect, pancreatic polypeptide, vasoactive intestinal polypeptide, pancreatic gastrin, and somatostatin belong to the group of gastrointestinal hormones (Hulín et al., 1997).

2.2. Physiology of pancreas

The pancreas is a soft, glandular organ that has both exocrine and endocrine functions. The endocrine function is performed by clusters of cells called the pancreatic islets, or islets of Langerhans, that secrete the hormones insulin and glucagon into the blood. As an exocrine gland, the pancreas secretes pancreatic juice through the pancreatic duct into the duodenum. Within the lobules of the pancreas are the exocrine secretory units, called acini. Each acinus consists of a single layer of acinar epithelial cells surrounding a lumen, into which the constituents of pancreatic juice are secreted (Fox, 2013). Pancreatic juice contains bicarbonate and about 20 different digestive enzymes. These enzymes include (1) amylase, which digests starch; (2) trypsin, which digests protein; and (3) lipase, which digests TGs. It should be noted that the complete digestion of food

molecules in the small intestine requires the action of both pancreatic enzymes and brush border enzymes. Evidence suggests that bicarbonate is secreted into the pancreatic juice by the cells that line the ductules, rather than by the acinar cells (Figure 2A) (Fox, 2013).

The endocrine portion of the pancreas consists of scattered clusters of cells called the pancreatic islets or islets of Langerhans (Fox, 2013) The Pancreatic islets secrete two major hormones, insulin and glucagon. Insulin promotes the lowering of blood glucose and the storage of energy in the form of glycogen and fat. Glucagon has antagonistic effects that raise the blood glucose concentration (Fox, 2013).

On a microscopic level, the most conspicuous cells in the islets are the α and β -cells (Figure 2B) (Fox, 2013). The α -cells secrete the hormone glucagon, and the β -cells secrete insulin. There are more than twice as many insulin-secreting β -cells as α -cells in each islet. Insulin is the primary hormone regulating the plasma glucose concentration. After a carbohydrate meal or sugary drink, the plasma glucose level rises. This rise in plasma glucose stimulates the β -cells of the islets to secrete increased amounts of insulin. Insulin then binds to its receptors in the plasma membrane of its target cells, and, through the action of signaling molecules, causes intracellular vesicles containing GLUT4 carrier proteins to translocate to the plasma membrane (Figure 3B) (Fox, 2013). These carrier proteins promote the facilitated diffusion of glucose into the cells of insulin's target organs—primarily the skeletal muscle, liver, and adipose tissue.

The insulin receptor consists of two alpha and two beta subunits (Figure 3A) (Fox, 2013). The beta subunits span the plasma membrane; the alpha subunits are located on

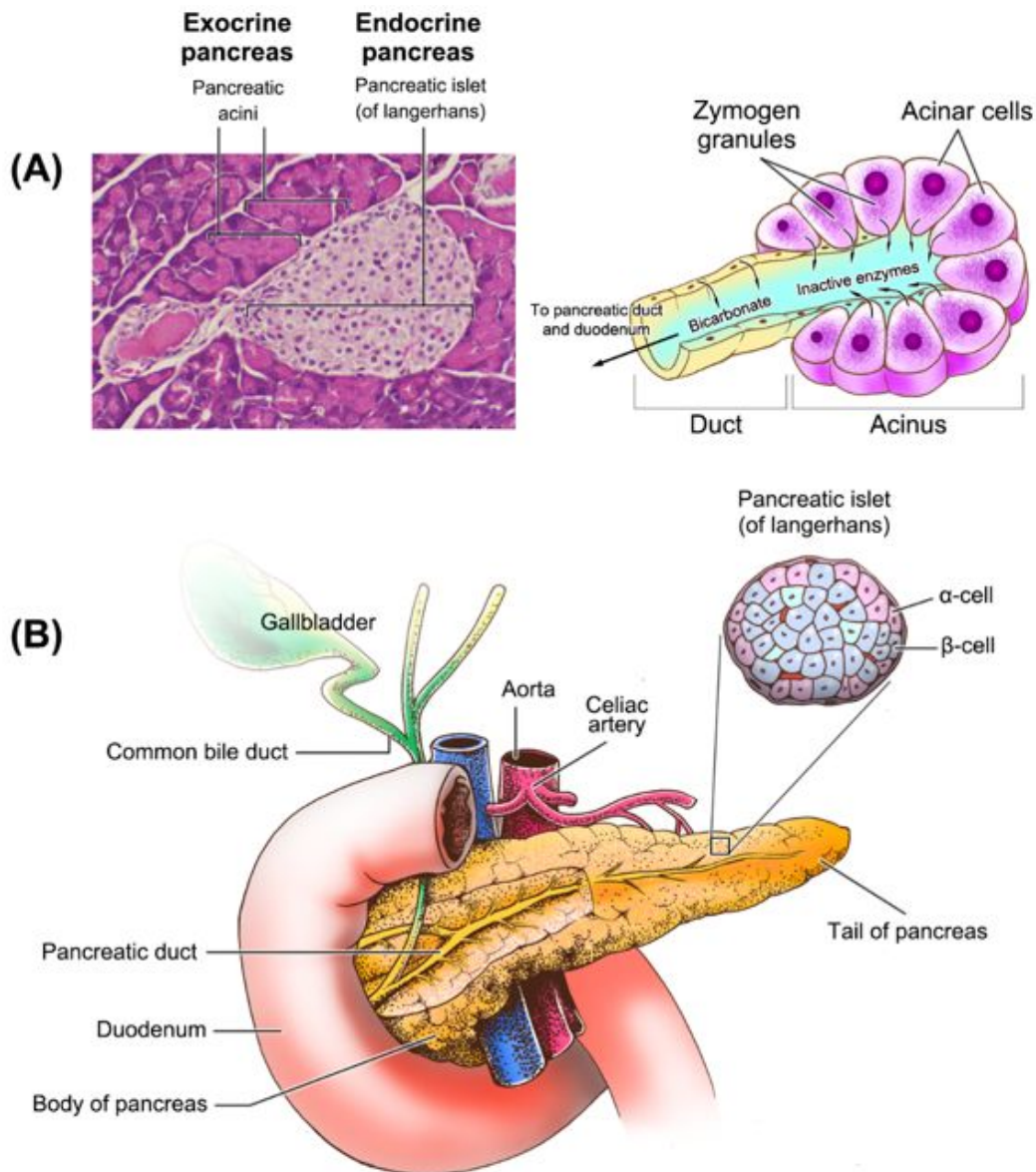


Figure 2. The structure of pancreas. (A) The pancreas is both exocrine and endocrine glands. (B) The pancreas and associated pancreatic islets (islets of Langerhans). Adapted from Fox (2013).

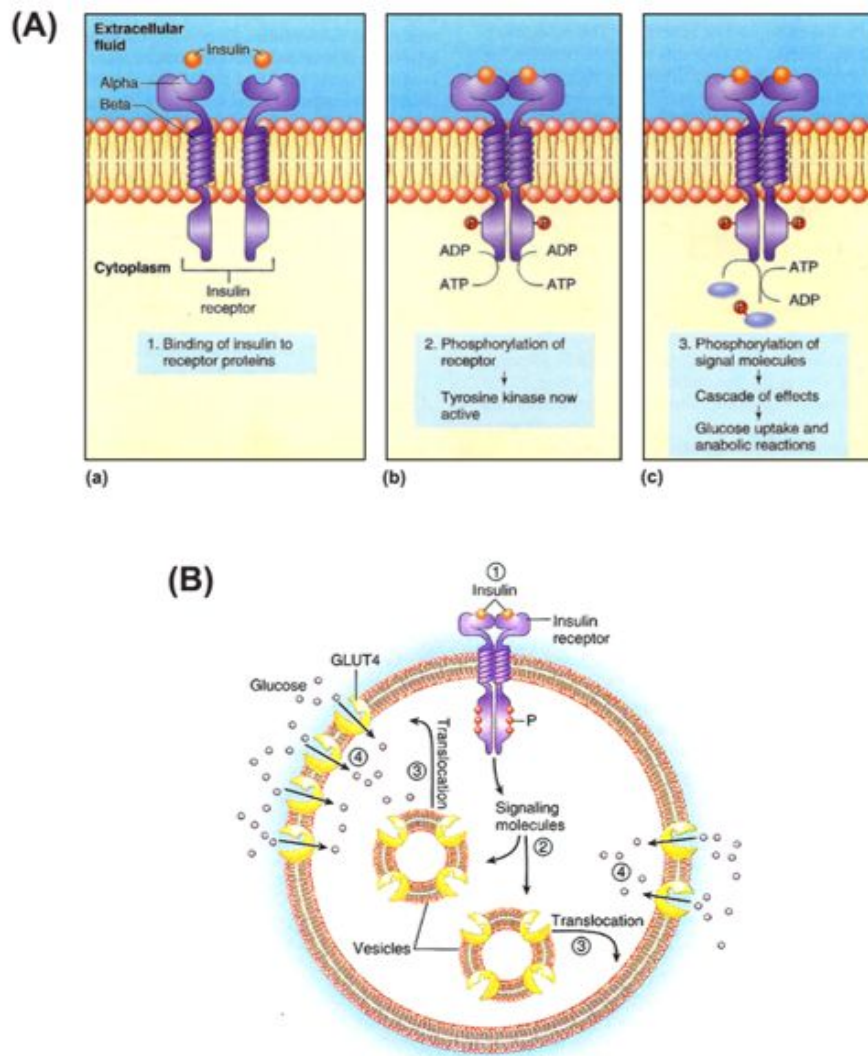


Figure 3. (A) The receptor of insulin and (B) the actions of insulin to stimulate uptake of blood glucose. Adapted from Fox (2013).

the extracellular side of the plasma membrane and contain the ligand (insulin) binding sites. When insulin binds to the alpha subunits, the beta subunits are stimulated to phosphorylate each other in a process called autophosphorylation. This activates the tyrosine kinase activity of the insulin receptor. The activated insulin receptor then phosphorylates insulin receptor substrate proteins, which provide an enzymatic docking station that activates a variety of other signaling molecules. These signaling molecules cause the insertion of transport carrier proteins for glucose into the plasma membrane (Figure 3B) (Fox, 2013), and so promote the uptake of plasma glucose into tissue cells. In this way, insulin promotes the lowering of the plasma glucose concentration. Some signaling molecules activate other second-messenger systems within the target cells, allowing insulin and growth factors to regulate different aspects of the metabolism of their target cells (Fox, 2013).

Glucagon, secreted by the α -cells of the pancreatic islets, acts antagonistically to insulin—it promotes effects that raise the plasma glucose concentration. Glucagon secretion is stimulated by a fall in the plasma glucose concentration and insulin secretion that occurs when a person is fasting. Under these conditions, glucagon stimulates the liver to hydrolyze glycogen into glucose (a process called glycogenolysis), allowing the liver to secrete glucose into the blood (Fox, 2013). Also, insulin indirectly stimulates the activity of the enzyme glycogen synthetase in skeletal muscle and liver, which promotes the conversion of intracellular glucose into which promotes the conversion of intracellular glucose into glycogen for storage. Insulin thereby causes glucose to leave the plasma and enter the target cells, where it is converted into the

energy storage molecules of glycogen (in skeletal muscles and liver) and fat (in adipose tissue). Through these effects, insulin lowers the blood glucose concentration (Fox, 2013) as it promotes anabolism. The ability of the β -cells to secrete insulin, and the action of insulin to lower the plasma glucose concentration, are tested in an oral glucose tolerance test (OGTT) for diabetes mellitus.

Insulin promotes glucose and amino acid transport and stimulates glycogen, fat and protein synthesis in its target organs—primarily the liver, skeletal muscle, and adipose tissue (Fox, 2013).

2.3. Islet β -cell failure in T2D

It is generally accepted that T2D is caused by the combination of insulin resistance and a progressive failure of pancreatic β -cells (Kahn, 1998). According to a plausible scenario (Figure 4), insulin resistance occurs when adipose cells reach a critical size and adipose tissue stores become limited. Ectopic TGs and FAs then produce insulin resistance in liver and muscle. In addition, a chronic inflammatory state, caused by immune cell infiltration into adipose tissue in obesity, appears to contribute to insulin resistance. Ectopic lipids also appear to affect β -cell function ('lipotoxicity'), probably in combination with the exposure of cells to high glucose concentrations ('glucotoxicity'). This pathogenesis unfolds when a polygenic susceptibility interacts with exogenous factors such as nutrition and physical activity. Therefore, T2D is the paradigm of a complex disease which has a genetic basis but is precipitated by exogenous factors (Diamond, 2003; Joost, 2008).

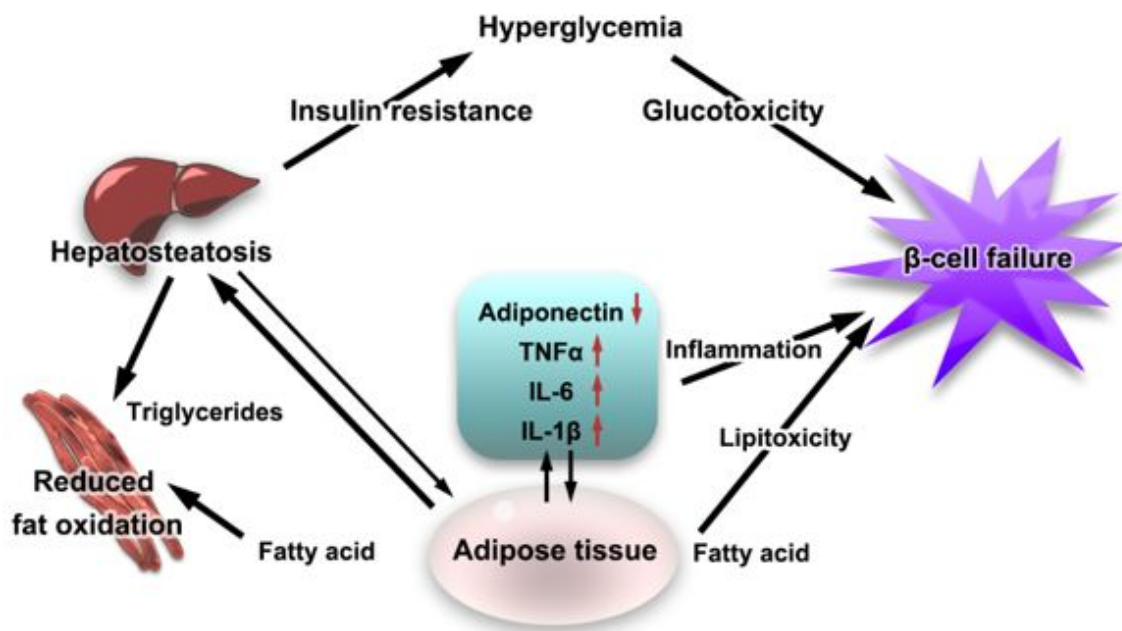


Figure 4. Pathogenesis of insulin resistance and β -cell failure in T2D.
 Adapted from Kumar *et al.* (2005).

Convincing data have indicated that excess ectopic lipid accumulation is a causal factor in the development of diabetes (Joost, 2008). It has been suggested that accumulation of ectopic lipids in other tissues such as muscle and islets is also involved in the pathogenesis of diabetes. Thus, intraabdominal and intrahepatic fat stores might be a marker for the accumulation of TGs in β -cells that was suggested to produce islet cell failure (lipotoxicity) (Joost, 2008). Incorporation of excess TGs in pancreatic islets can trigger apoptosis of β -cells (Unger, 2003). When lipids accumulate in non-adipose tissues during over-nutrition, FAs cause the formation of ceramide. Ceramide is a toxic lipid and probably the cause of lipoapoptosis (Unger, 2003). Alternatively, it has been postulated that elevation of post-prandial and post-absorptive blood glucose levels damage the pancreatic β -cell (glucotoxicity).

According to this hypothesis, the β -cell is very sensitive to oxidative damage, or is sensitized by a low anti-oxidative capacity (Leahy, 1990). It was suggested that elevated blood glucose concentrations lead to formation of reactive oxygen radicals which cause loss of essential transcription factors such as MafA, and an irreversible cell damage (Brownlee, 2003; Harmon *et al.*, 2005). This hypothesis is supported by numerous experimental findings: Long-term culture of β -cells in the presence of high glucose concentrations affects their function (Robertson *et al.*, 1992). In db/db or NZO mice, diabetes (defined as histologically assessed β -cell damage) can be delayed or prevented by feeding a high-protein or high-fat, carbohydrate-free diet (Leiter *et al.*, 1981; Leiter *et al.*, 1983; Jürgens *et al.*, 2006). Thus, carbohydrates are essential for β -cell destruction in mouse models of diabetes, and lipotoxicity appears to co-operate

with glucotoxicity in this pathogenesis (Poitout and Robertson, 2002).

Obesity is associated with a massive infiltration of adipose tissue with immune cells such as macrophages, and it has been suggested that the pathogenesis of T2D has an immunological component in that cytokines released from adipose tissue play a causal role in the insulin resistance and β -cell failure (Spranger *et al.*, 2003). Consequently, serum levels of inflammatory cytokines or other biomarkers of inflammatory processes such as IL-6 and C-reactive protein (CRP) are elevated long before the onset of overt T2D (Kolb *et al.*, 2005). It should be noted, however, that adipose tissue inflammation was fully dissociated from the development of diabetes under a carbohydrate-free diet (Jürgens *et al.*, 2006). Thus, inflammatory cytokines may contribute to the pathogenesis of diabetes, but are not a sufficient factor (Joost, 2008).

4. A C57BL/6J mouse strain as a T2D mouse model

T2D model by simply feeding high fat feed to non obese, non diabetic C57BL/6J mouse strain was initially developed in Japan and is now available at Jackson laboratory, Bar Harbor. It is characterized by marked obesity, hyperinsulinaemia, insulin resistance and glucose intolerance (Surwit *et al.*, 1988). In addition, they exhibit marked fasting as well as basal hyperglycaemia in contrast to normal basal glucose level seen in C57BL/6J (*ob/ob*) mice. They manifest most of the characteristic features of the patients with genetic predisposition to develop T2D when they become obese.

This animal model represents both genetic and environmental risk factors in contrast to C57BL/6J (*ob/ob*) mouse in which onset of symptoms

is highly genetically determined. Further, its usefulness for drug testing has been reported in the literature as these mice treated with orally active inhibitor of dipeptidyl peptidase-IV (LAF237) are shown to have normalized glucose tolerance in association with augmented insulin secretion (Winzell and Ahrén, 2004; Srinivasan and Ramarao, 2007).

5. ALS-L1023

ALS-L1023 is a lemon balm (*Melissa officinalis* L.; Labiatae) leaf extract. Lemon balm is widely used as a medicinal plant for treatment of headache, neuralgia and fever and has been reported to regulate herpes virus, insomnia and Alzheimer's disease (Kim et al., 2006; Dimitrova et al., 1993; Akhondzadeh et al., 2003). Further, the researcher have found that ALS-L1023, which exhibits anti-angiogenic and MMP inhibitory activities, reduced adipose tissue mass nutritionally induced obese mice (submitted), suggesting that ALS-L1023 may inhibit obesity - related T2D. Therefore, the present study was undertaken to determine whether the angiogenesis inhibitor ALS-L1023 can regulate T2D in high fat-fed sham-operated (sham) and ovariectomized (OVX) female mice and to investigate the mechanisms involved in this process.

The present study shows that ALS-L1023 not only reduces body weight and visceral adipose tissue mass, but also inhibits insulin resistance and pancreatic β -cell failure, steatosis, inflammation, and fibrosis in both sham and OVX mice. In addition, these effects were more effective in sham mice than in OVX mice.

II. MATERIALS AND METHODS

1. Preparation of ALS-L1023

ALS-L1023 was manufactured by activity-guided fractionation from the leaves of *Melissa officinalis* L. (Alfred Galke GmbH, Harz, Germany). The dried *Melissa* leaves were extracted with aqueous ethanol, and the extract was filtered and concentrated. The concentrated ethanol extract was further fractionated with ethyl acetate, after which it was concentrated and dried to obtain ALS in a dried powder form. The quality of ALS was controlled by standardization with two reference compounds by high performance liquid chromatography. ALS exhibited enhanced antiangiogenic and MMP inhibitory activities compared with that of water extract or ethanol extract of *Melissa* leaves.

2. Animal treatments

For all experiments, eight-week-old female mice (C57BL/6J) were housed and bred at Mokwon University with a standard 12-h light/dark cycle. Prior to the administration of special diets, mice were fed standard rodent chow and *water ad libitum*. Two experiments were carried out to study the effects of ALS-L1023 on obesity and T2D. Experiment 1 was done in female mice with functioning ovaries. The mice were randomly divided into four groups (n=5/group) and then fed for 16 weeks a low fat diet (LFD, 10% kcal% fat, Daehan Biolink, Eumseong, Korea), a high fat

diet (HFD, 45% kcal% fat, FEEDLAB, Guri, Korea), or the same HFD supplemented with ALS-L1023 at doses of 0.4% or 0.8% for 16 weeks (Table 1). Experiment 2 was done in ovariectomized (OVX) mice. OVX mice were randomly divided into four groups (n=5/group) and then received for 16 weeks a low fat diet (LFD, 10% kcal% fat, Daehan Biolink, Eumseong, Korea), a high fat diet (HFD, 45% kcal% fat, FEEDLAB, Guri, Korea), or the same HFD supplemented with ALS-L1023 at doses of 0.4% or 0.8% for 16 weeks (Table 2).

In all experiments, body weights were measured three times a week using a top-loading balance and the person measuring the body weight blinded to each treatment group. Animals were sacrificed by cervical dislocation, and tissues were harvested, weighed, snap frozen in liquid nitrogen and stored at -80°C until use. Portions were prepared for histology. Blood was collected after 4-hr fast from the retroorbital sinus into tubes, and serum was separated and stored at -80°C until analysis. All animal experiments were approved by the Institutional Animal Care and Use Committees of Mokwon University, and followed National Research Council Guidelines.

3. Blood analysis

Glucose and Insulin were measured using a glucometer (Accu-Chek[®] Performa, Roche Diagnostic, Mannheim, Germany) and a ELISA kit (Insulin-Rat/Mouse ELISA Kit, Millipore, USA) respectively.

Table 2. The experimental groups

Mouse models	Groups	Treatments
Female Sham-operated mouse	LFD	LFD (10 kcal% fat)
	HFD	HFD (45 kcal% fat)
	HFD + ALS (0.4%)	HFD + ALS-L1023 (0.4 %, w/w)
	HFD + ALS (0.8%)	HFD + ALS-L1023 (0.8 %, w/w)
Female ovariectomized mouse	LFD	LFD (10 kcal% fat)
	HFD	HFD (45 kcal% fat)
	HFD + ALS (0.4%)	HFD + ALS-L1023 (0.4 %, w/w)
	HFD + ALS (0.8%)	HFD + ALS-L1023 (0.8 %, w/w)

Table 3. Composition of experimental diets

Ingredient	LFD		HFD	
	g (w/w)	kcal	g (w/w)	kcal
Carbohydrate	46 %	61 kcal%	41 %	35 kcal%
Protein	22 %	29 kcal%	24 %	20 kcal%
Fat	3.5%	10 kcal%	24 %	45 kcal%

4. Oral glucose tolerance test

After 16 weeks of treatment, oral glucose tolerance test (OGTT) was performed on mice after a 16-h overnight fast. The mice were gavaged with glucose (2g/kg body weight, dissolved in water). Blood glucose levels were assessed by collecting tail blood, and glucose levels were measured immediately before and 30, 60, 90, 120 and 150 min after glucose administration.

5. Histological analysis

The pancreas was fixed in 10% phosphate-buffered formalin for 1 day and processed in a routine manner for paraffin section. Sections were cut at 5 μ m, deparaffinized and dehydrated. Sections were then stained with microscopic examination.

For H&E staining, sections were incubated with hematoxylin solution for 3 min and washed with tap water for 10 min at room temperature. After an eosin step for 2 min 30 sec at room temperature, sections were dehydrated with 80%, 90%, 95%, and 100% ethanol and dealcoholized with xylene in rotation.

For Masson's trichrome staining, tissue were fixed with Bouin's solution for 5 min at 56°C. After washing with tap water, sections were incubated with Weigert's iron hematoxylin solution for 10 min at room temperature. After a washing step, sections were incubated with Biebrich scarlet acid fuchsin solution for 10 min, phosphotungstic acid solution for 15 min, aniline blue solution for 10 min and 1% acetic acid for 3 min at

room temperature. Finally, sections were incubated with 95% and 100% ethanol and xylene step by step.

For toluidine blue staining, sections were incubated with toluidine blue solution for 3 min at room temperature, dehydrated with 95% and 100% ethanol and dealcoholized with xylene. The histological variation in the stained tissues were analyzed with an image analysis system (Image Pro-Plus, Media Cybernetics, Silver Spring, MD, USA).

6. Immunohistochemistry

Immunohistochemical staining was performed using Mouse on Mouse™ basic kit (BMK-2202, Vector laboratories, Burlingame, CA, USA) and Vectastain® Elite ABC kits (PK-6100, Vector laboratories). Paraffin embedded tissues were sectioned at 5 μ m thickness. After deparaffinization, sections were incubated with 10 mM sodium citrate buffer for 20 min at 95°C and then cooled for 20 min at room temperature. They were then exposed to 3% H₂O₂ at room temperature. After blocking with mouse IgG blocking reagent (Vector laboratories) for 1 h at room temperature, sections were incubated with a primary antibody against insulin (1:1400, I2018, Sigma-Aldrich) for 2 h at room temperature. Sections were incubated with biotinylated anti-mouse IgG (Vector laboratories) as a secondary antibody for 10 min at room temperature. After washing, sections were visualized using ImmPACT™ DAB (SK-4105, Vector laboratories, Burlingame, CA, USA) for 8 min at room temperature. The sections were analyzed using a Olympus DP70 camera.

7. RT-PCR

Total cellular RNA was prepared from the pancreas tissues using Trizol reagent (TR-118, Molecular Research Center, Cincinnati, OH, USA). After 2 μ g total RNA was reverse-transcribed with Moloney murine leukemia virus reverse transcriptase (M-MLV RT, DR01601, Doctor Protein, Seoul, Korea) and Oligo-dT (O1024-050, GenDEPOT, Barker, USA), cDNA was generated. Briefly, RNA was mixed with M-MLV RT, M-MLV RT buffer, dNTP and oligo-dT mixture, and incubated for 40 min at 50°C. Synthesized cDNA fragments were amplified by a PCR process in an MJ Research Thermocycler (Waltman, MA, USA) and MJ Mini™ Gradient Thermal Cycler (PTC-1148, Bio-rad, CA, USA). PCR primers used to determine the mRNA expression of each gene were shown in Table 3. Simply, cDNA was mixed with PCR primers, HelixAmp™ Ready-2X-Go (PMD008L, Nanohelix, Daejeon, Korea). The PCR condition consisted of 25-30 cycles denaturation for 30 sec at 94°C, annealing for 30 sec at 55-59°C and elongation for 30 sec at 72°C. The PCR products were analyzed by electrophoresis on a 1 % agarose gel. Relative expression levels were indicated as ratio of target gene cDNA vs β -actin cDNA. The results determined by image analyzer (Syngene, Cambridge, UK).

8. Statistics

Unless otherwise noted, all values are expressed as mean \pm standard deviation (SD). All data were analyzed by unpaired student's t-test for statistically significant differences between groups using SigmaPlot 2001 (SPSS, Chicago, IL, USA).

Table 4. PCR primers and conditions used for RT-PCR

Gene	Gene Bank	primer sequence	cDNA size (bp)	Tm / cycle
PPAR α	NM_001113418	Forward : 5'-gcagctcgtacaggtcatca-3' Reverse : 5'-ctcttcatcccaagcgtag-3'	202	58 / 34
CPT-1	L07736	Forward : 5'-tatgtgaggatgctgcttcc-3' Reverse : 5'-ctcggagagctaagcttgc-3'	629	52 / 32
AMPK α 1	NM_001013367	Forward : 5'-agagggccgcaataaaagat-3' Reverse : 5'-tgttgtagcagcagctgagg-3'	177	58 / 35
AMPK α 2	NM_178143	Forward : 5'-cgctctagtctcctcatcag-3' Reverse : 5'-atgtcacacgctttgctctg-3'	219	55 / 33
MCAD	NM_007382	Forward : 5'-gacatttgaaaagctgtagtg-3' Reverse : 5'-tcacgagctatgatcagcctctg-3'	321	58 / 35
VLCAD	NM_017366	Forward : 5'-cgtcagagggtgactttgatgg-3' Reverse : 5'-catggactcagtcacatactgc-3'	269	55 / 33
SREBP-1c	NM_011480	Forward : 5'-cttctggagacatcgcaaac-3' Reverse : 5'-ggtagacaacagccgcac-3'	278	58 / 33
FAS	NM_007988	Forward : 5'-cttgggtgctgactacaacc-3' Reverse : 5'-gccctccgtacactcactc-3'	163	57 / 30
aP2	NM_024406	Forward : 5'-caaaatgtgtgatgcctttgtg-3' Reverse : 5'-ctcttcccttggctcatgcc-3'	416	59 / 32
C/EBP α	NM_007678	Forward : 5'-atccagagggactggagtt-3' Reverse : 5'-aagtccttagccggagggaagc-3'	373	59 / 32
PPAR γ	NM_001127330	Forward : 5'-attctggcccaccaacttcgg-3' Reverse : 5'-tggaagcctgatgctttatcccca-3'	339	58 / 32
ACC	NM_133360	Forward : 5'-gggctacctctaattggtctt-3' Reverse : 5'-ctacctgatggtaaatggga-3'	439	58 / 32
CD68	NM_001291058	Forward : 5'-aacaggacctacatcagagc-3' Reverse : 5'-ctgtagccttagagagagca-3'	218	58 / 28
α -SMA	NM_007392	Forward : 5'-ctggagaagagctacgaactgc-3' Reverse : 5'-ctgatccacatctgctggaagg-3'	368	55 / 28
TGF- β	NM_011577	Forward : 5'-accgcaacaacgccatctat-3' Reverse : 5'-gtaacgccaggaattgttgc-3'	200	59 / 28
Collagen α 1	NM_007742	Forward : 5'-gcccgaacccaaggaaaagaagc-3' Reverse : 5'-ctgggaggcctcgggtggacattag-3'	148	55 / 30
Bax	NM_007527.3	Forward : 5'-ggtttcatccaggatcgagcagg-3' Reverse : 5'-acaaagatgggtcactgtctgcc-3'	446	59 / 39
p53	AB017816.1	Forward : 5'-gggacagccaagtctgttatg-3' Reverse : 5'-ggagtcttccagtgtgatgat-3'	432	58 / 33

Bcl-2	NM_009741,3	Forward : 5'-tcgctaccgtcgtgacttc-3' Reverse : 5'-aaacagaggtcgcatgctg-3'	313	58 / 30
Bcl-xL	L35049,1	Forward : 5'-gttgtaacctgcttgctggcgcgg-3' Reverse : 5'-agcttgtaggagagaaagtcgacc-3'	200	58 / 32
β -actin	BC138614	Forward : 5'-tggaatcctgtggcatccatgaaac-3' Reverse : 5'-taaaacgcagctcagtaacagtcg-3'	349	58 / 25

III. RESULTS

1. Female sham C57BL/6J mice

1.1. Regulation of body weight, food intake, adipose tissue mass, and adipocyte size by ALS-L1023 in high fat diet-fed female sham mice

1.1.1. Body weight

Since T2D is deeply associated with obesity, we examined the effects of ALS-L1023 on body weight in female sham mice. Female sham mice were fed with a LFD (LFD), a HFD or the same HFD supplemented with ALS-L1023 for 17 weeks. After 17 weeks of a LFD, the body weight was 24.8 ± 1.24 g (Figure 5A). By contrast, the body weight of mice fed a HFD was increased to 34.3 ± 5.44 g, whereas mice received a HFD supplemented with 0.4% ALS and 0.8% ALS-L1023 showed body weight of 27.1 ± 2.33 g and 28 ± 1.07 g, respectively. 0.4% and 0.8 % ALS-L1023 treatment decreased body weight gain by 50% ($p<0.05$) and 43% ($p<0.05$), respectively, compared with HFD alone (Figure 5B).

1.1.2. Food intake

During 16 weeks, food intake was higher in the HFD-fed sham mice than in LFD-fed lean mice, but no significant difference was observed in food intake between the

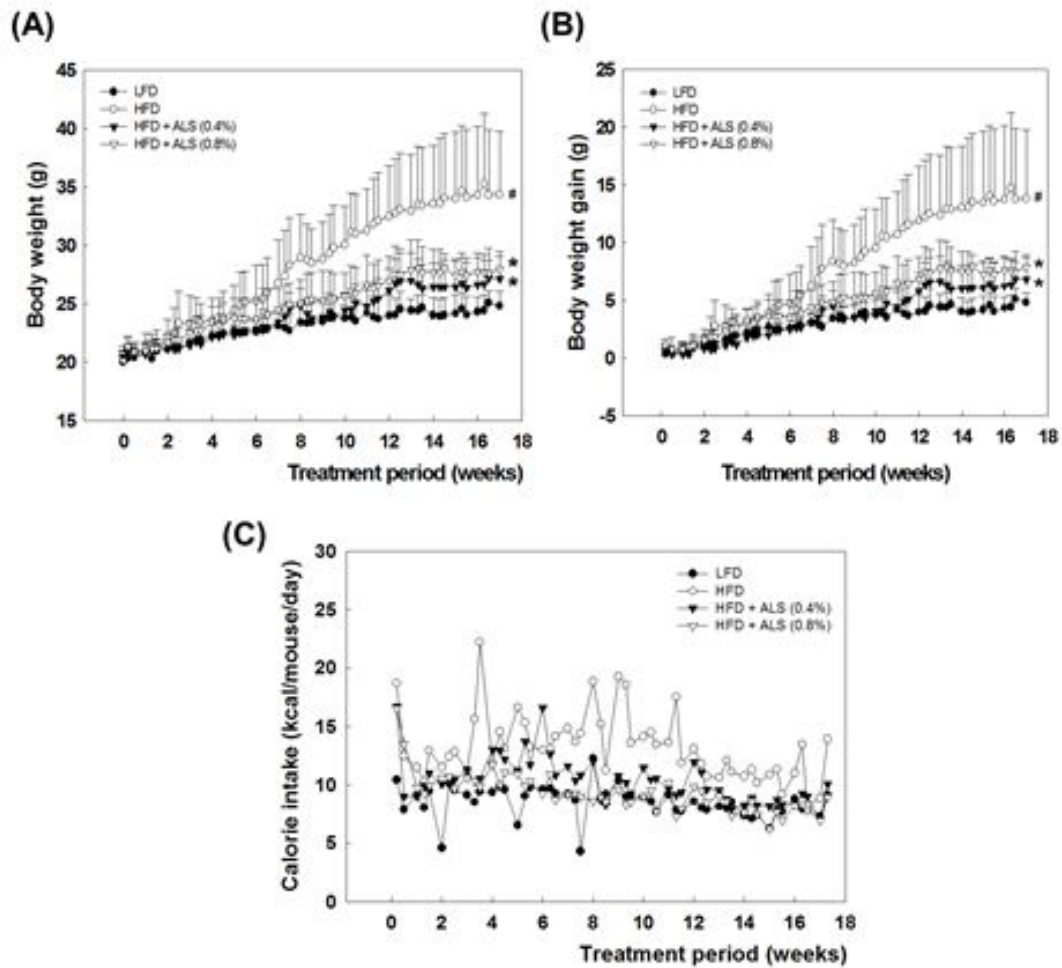


Figure 5. Effects of ALS-L1023 on body weight (A), and body weight gain (B), and food intake (C) in high fat diet-fed female sham mice. Mice (n=5/group) were fed a LFD, a HFD, or the same HFD supplemented with either 0.4% or 0.8% ALS-L1023 for 17 weeks. All values are expressed as mean \pm SD. # $p < 0.05$ compared with LFD. * $p < 0.05$ compared with HFD.

HFD-treated and ALS-treated mice (Figure 5C).

1.1.3. Adipose tissue mass and adipocyte size

Adipose tissue mass was also significantly decreased by ALS-L1023 treatment in HFD-fed sham mice (Figure 6). As shown in Figure 6B, the total adipose tissue mass in 0.4% and 0.8% ALS-L1023 treated mice was 39% and 42% lower, respectively, than that of HFD-treated mice. Visceral adipose tissue mass was reduced by 42% and 47% after 0.4% and 0.8 % ALS-L1023 treatment (Figure 6C). These results suggest that ALS-L1023 may effectively reduces body weight and adipose tissue mass in without appetite suppression HFD-induced obese mice.

Analysis of HE-stained adipose tissue section revealed that ALS-L1023 markedly decreased the size of visceral adipocytes (Figure 7). ALS-L1023 at concentrations of 0.4% and 0.8% decreased the average size of visceral adipocytes by 30% and 37%, in HFD-fed mice, respectively (Figure 7B), indicating that reductions in body weight and adipose tissue mass can be correlated with a reduction in the size of adipocytes following ALS-L1023 treatment. In addition, adipocyte numbers in a fixed area ALS-L1023 compared with HFD alone.

1.2. Effects of ALS-L1023 on glucose, and insulin levels

1.2.1. Glucose and insulin levels

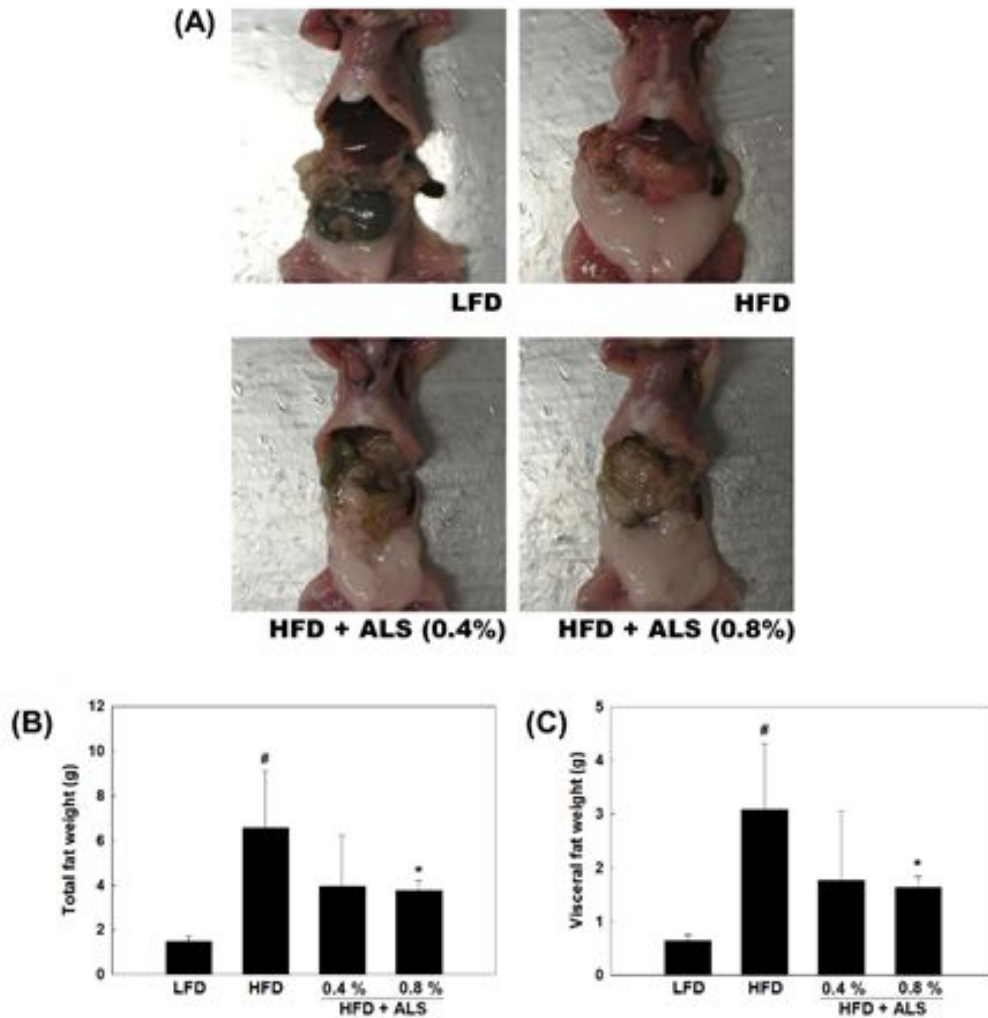


Figure 6. Effects of ALS-L1023 on adipose tissue mass. Female sham C57BL/6J mice were fed a LFD, a HFD, or the same HFD supplemented with either 0.4% or 0.8% ALS-L1023 for 17 weeks. (A) Ventrotomy image, (B) total adipose tissue mass, and (C) visceral adipose tissue mass. All values are expressed as mean \pm SD. [#] $p < 0.05$ compared with LFD. ^{*} $p < 0.05$ compared with HFD.

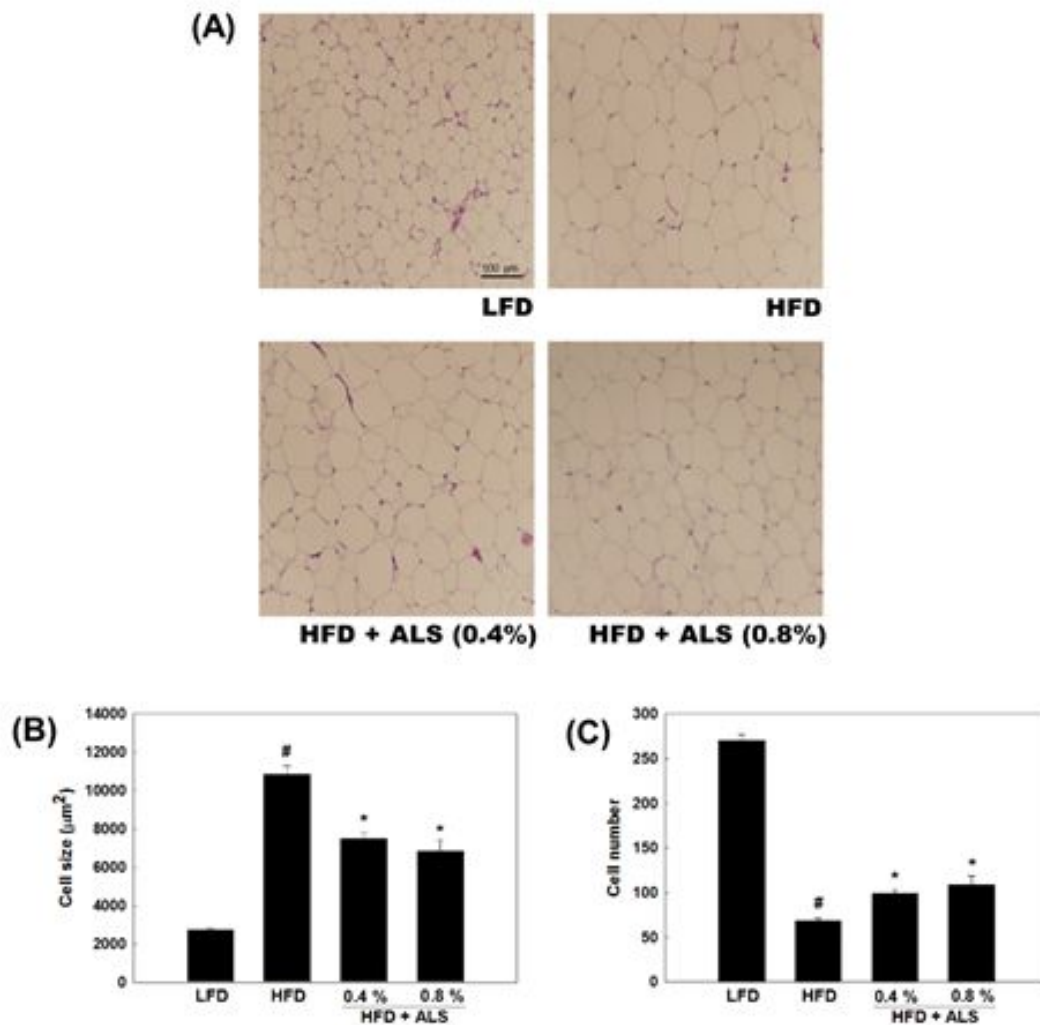


Figure 7. Effects of ALS-L1023 on visceral adipocyte histology. Female sham C57BL/6J mice were fed a LFD, a HFD, or the same HFD supplemented with either 0.4% or 0.8% ALS-L1023 for 17 weeks. (A) HE-stained sections of visceral adipocytes are shown (original magnification X100), (B) the size of visceral adipocytes and (C) the number of visceral adipocytes in a fixed area (1,000,000 μm²) was measured and values are expressed as mean ± SD. [#]*p*<0.05 compared with LFD. ^{*}*p*<0.05 compared with HFD.

C57BL/6J mice are susceptible to HFD and develop glucose intolerance more readily than other strains (Ahrén *et al.*, 1999). Thus, it was hypothesized that ALS-L1023 treatment regulates serum glucose and insulin levels in female sham obese mice.

As shown in Figure 8A, blood glucose levels was increased by 7% after 17 weeks in the HFD-fed mice compared with LFD-fed mice. However, 0.4% and 0.8% ALS-L1023 treatment decreased by 8% and 12%, respectively, compared with HFD-fed mice. Moreover, HFD-fed obese mice exhibited insulin resistance as shown by significantly increased insulin levels and increased glucose levels. HFD-fed mice increased insulin levels by 240%, compared with the LFD-fed mice, whereas, 0.8% ALS-L1023 treatment significantly decreased the serum insulin levels by 60% (Figure 8B, $p < 0.05$).

1.2.2. OGTT

The female sham mice with HFD induced obesity displayed impaired glucose tolerance compared with the LFD-fed mice (Figure 8C, $p < 0.05$). However, 0.4% ALS-L1023 supplement improved the impaired glucose tolerance at 120 min ($p < 0.05$) compared with HFD-fed mice. Similarly, 0.8% ALS-L1023 supplement significantly improved the impaired glucose tolerance at 30 and 90 min ($p < 0.05$), indicating that ALS-L1023 may improve glucose tolerance in obese mice.

1.3. Effects of ALS-L1023 on pancreatic islet morphology and insulin-secreting cells

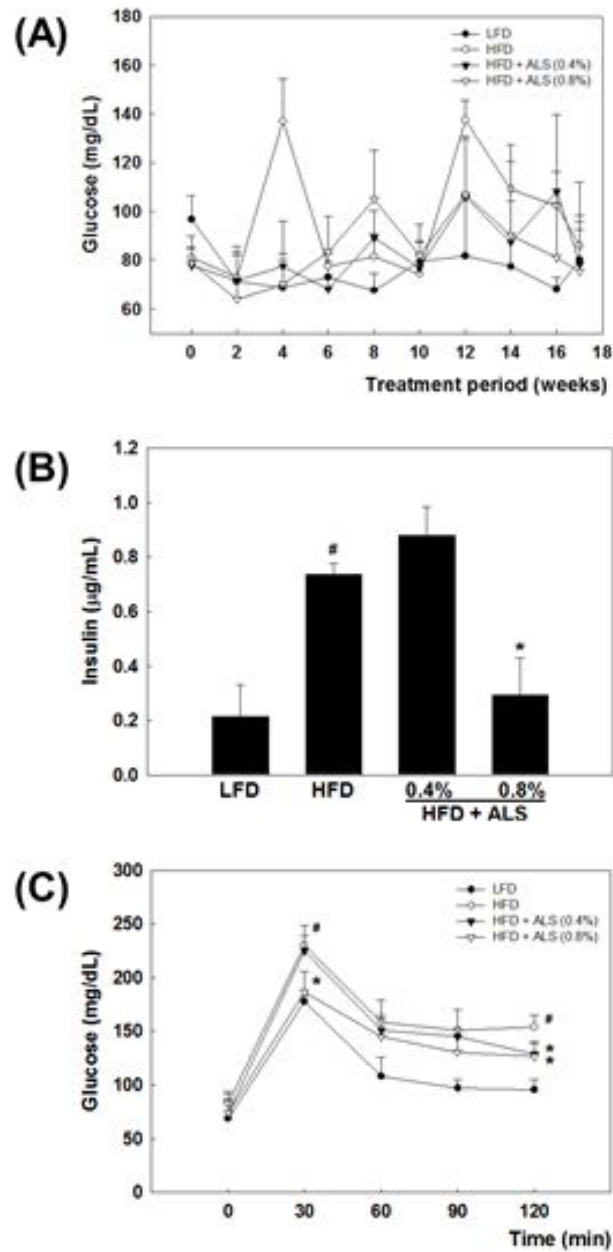


Figure 8. Effects of ALS-L1023 on serum glucose and insulin levels. Female sham C57BL/6J mice were fed a LFD, a HFD, or the same HFD supplemented with either 0.4% or 0.8% ALS-L1023 for 17 weeks. (A) Fasting blood glucose levels. (B) Serum insulin levels. (C) OGTT at 18 weeks following ALS-L1023 treatment. [#] $p < 0.05$ compared with LFD. ^{*} $p < 0.05$ compared with HFD.

1.3.1. Histological evaluation of pancreatic islet morphology

The size and morphology of pancreatic islet was determined by a hematoxylin and eosin staining method. The LFD-fed mice showed a normal pancreatic islet structure, whereas the size of pancreatic islets was markedly increased in HFD-fed mice compared with LFD-fed mice. Cells inside the pancreatic islets showed hyperplasia and acinar cells around the islets were modified in HFD-fed mice. (Figure 9) In contrast, the size of pancreas was decreased to the size of the pancreas in LFD-fed mice after 0.8% ALS-L1023 treatment. ALS-L1023-treated group showed improved islet morphology (Figure 9).

1.3.2. Immunohistochemical finding : insulin

Immunohistochemistry was performed to determine insulin-secretion in pancreatic β -cells by using an anti-insulin antibody. Insulin-positive areas in pancreatic islets were increased, but insulin-positive intensity was reduced in HFD-fed mice compared with LFD mice. By contrast, a marked elevation in the insulin content of islets was observed in ALS-L1023-treated mice compared with HFD-fed mice (Figure 10).

1.4. Effects of ALS-L1023 on pancreatic steatosis

1.4.1. Histological evaluation of pancreatic steatosis

To determine whether ALS-L1023 regulates obesity-induced pancreatic steatosis, we studied the effects of ALS-L1023 on pancreatic lipid accumulation in female sham

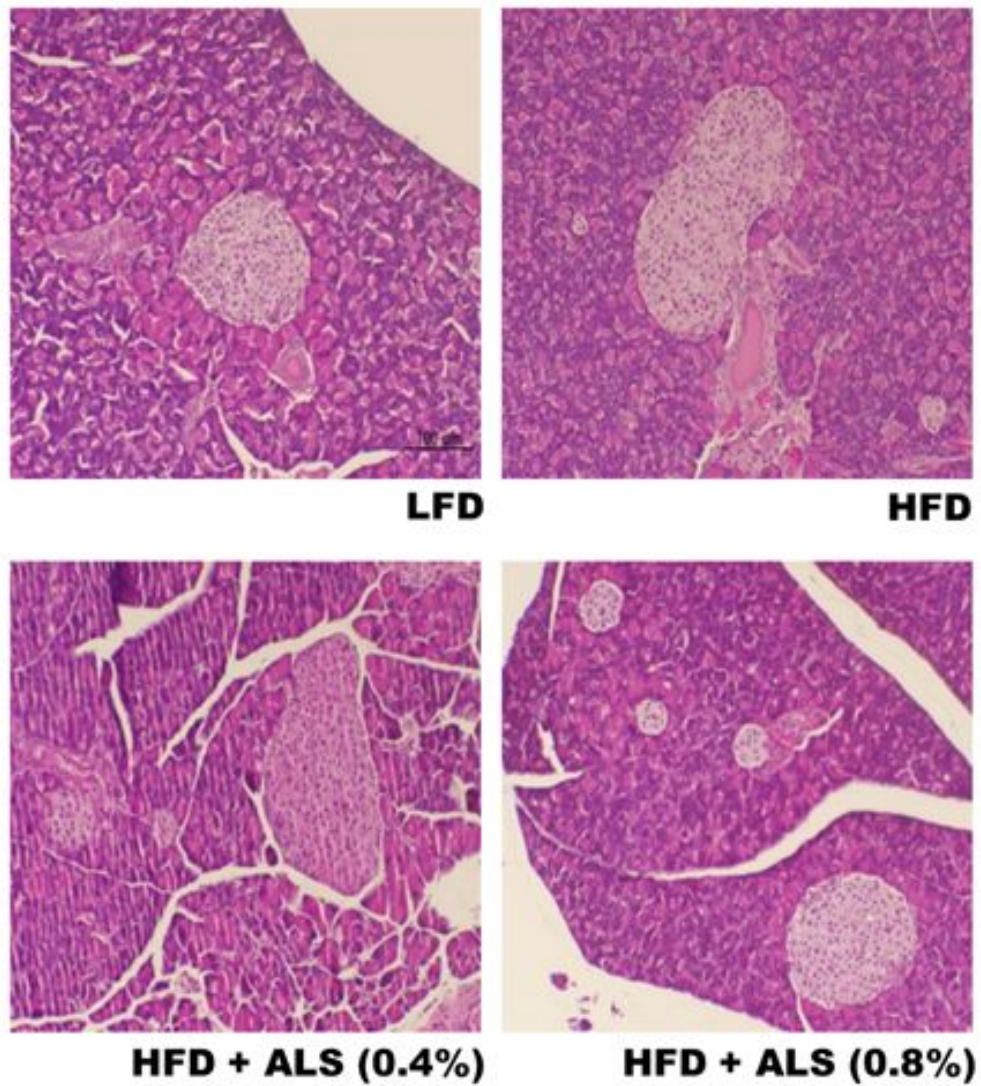


Figure 9. Effects of ALS-L1023 on pancreatic islet structures. Female sham C57BL/6J mice were fed a LFD, a HFD, or the same HFD supplemented with either 0.4% or 0.8% ALS-L1023 for 17 weeks. Pancreas sections were stained with Hematoxylin and Eosin. Original magnification X100.

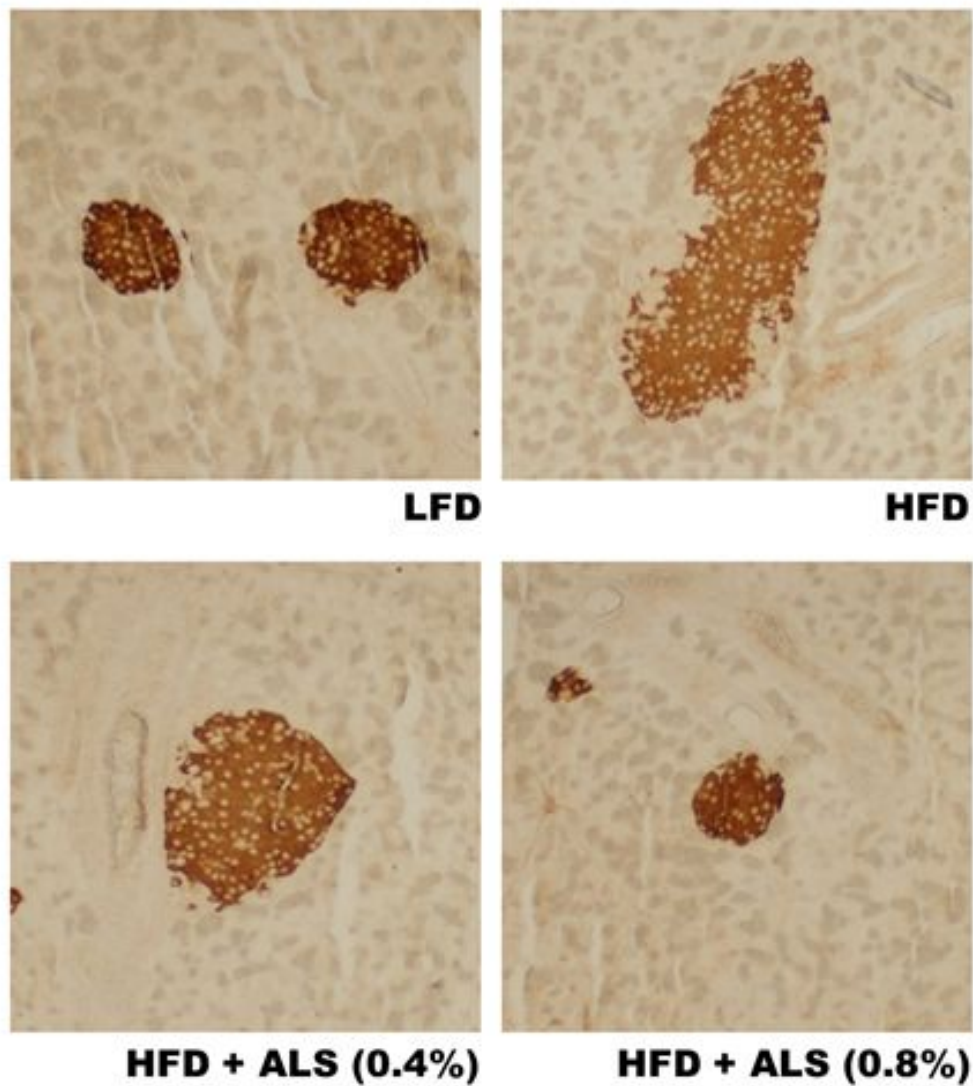


Figure 10. Effects of ALS-L1023 on insulin-positive cells in pancreas. Female sham C57BL/6J mice were fed a LFD, a HFD, or the same HFD supplemented with either 0.4% or 0.8% ALS-L1023 for 17 weeks. Representative pancreas sections stained with an antibody against insulin are shown in dark brown color. Original magnification X100.

mice. The pancreatic accumulation of lipids was determined by a Masson's trichrome staining method. ALS-L1023-treated mice showed lower pancreatic lipid accumulation than HFD-fed mice (Figure 11). These results show that ALS-L1023 may improve pancreatic steatosis.

1.4.2. mRNA expression of pancreatic genes related to FA oxidation

To determine whether changes in the expression of FA oxidation genes are associated with the reduction of pancreatic steatosis, mRNA levels of FA oxidation genes were measured after ALS-L1023 treatment. PPAR α , CPT-1, and VLCAD mRNA levels were increased by 39%, 26% and 9% in 0.4% ALS-L1023-treated mice, respectively, compared with HFD-fed mice although MCAD mRNA levels were not increased. PPAR α , CPT-1, MCAD and VLCAD mRNA levels in 0.8% ALS-L1023 treated mice were also increased by 45% ($p<0.05$), 46% ($p<0.05$), 24% ($p<0.05$), and 5%, respectively, than in HFD-fed mice (Figure 12).

1.4.3. mRNA expression of pancreatic genes related to lipogenesis

To determine whether changes in the expression of lipogenic genes are associated with the reduction of pancreatic steatosis, mRNA levels of lipogenic genes were measured after ALS-L1023 treatment. Compared with LFD-fed mice, HFD-fed mice had increased mRNA levels of SREBP-1c, FAS, and ACC mRNA levels by 35%, 17%, and 44%, respectively. However, 0.4% ALS-treated mice had decreased SREBP-1c,

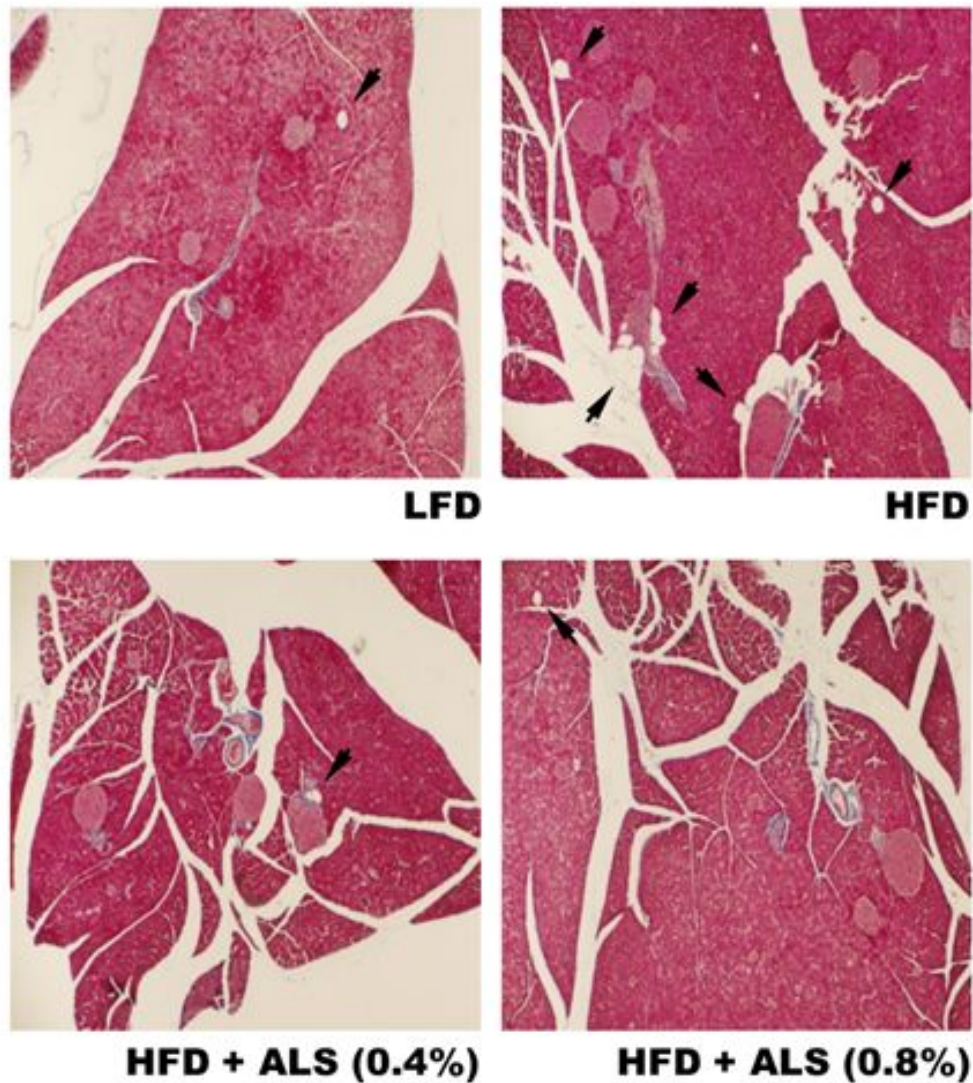


Figure 11. Effects of ALS-L1023 on pancreatic steatosis. Female sham C57BL/6J mice were fed a LFD, a HFD, or the same HFD supplemented with either 0.4% or 0.8% ALS-L1023 for 17 weeks. A photomicrograph of mouse pancreatic tissue of the high fat group showing lipid droplets (black arrow). Pancreas sections were stained with Masson's trichrome. Original magnification X40.

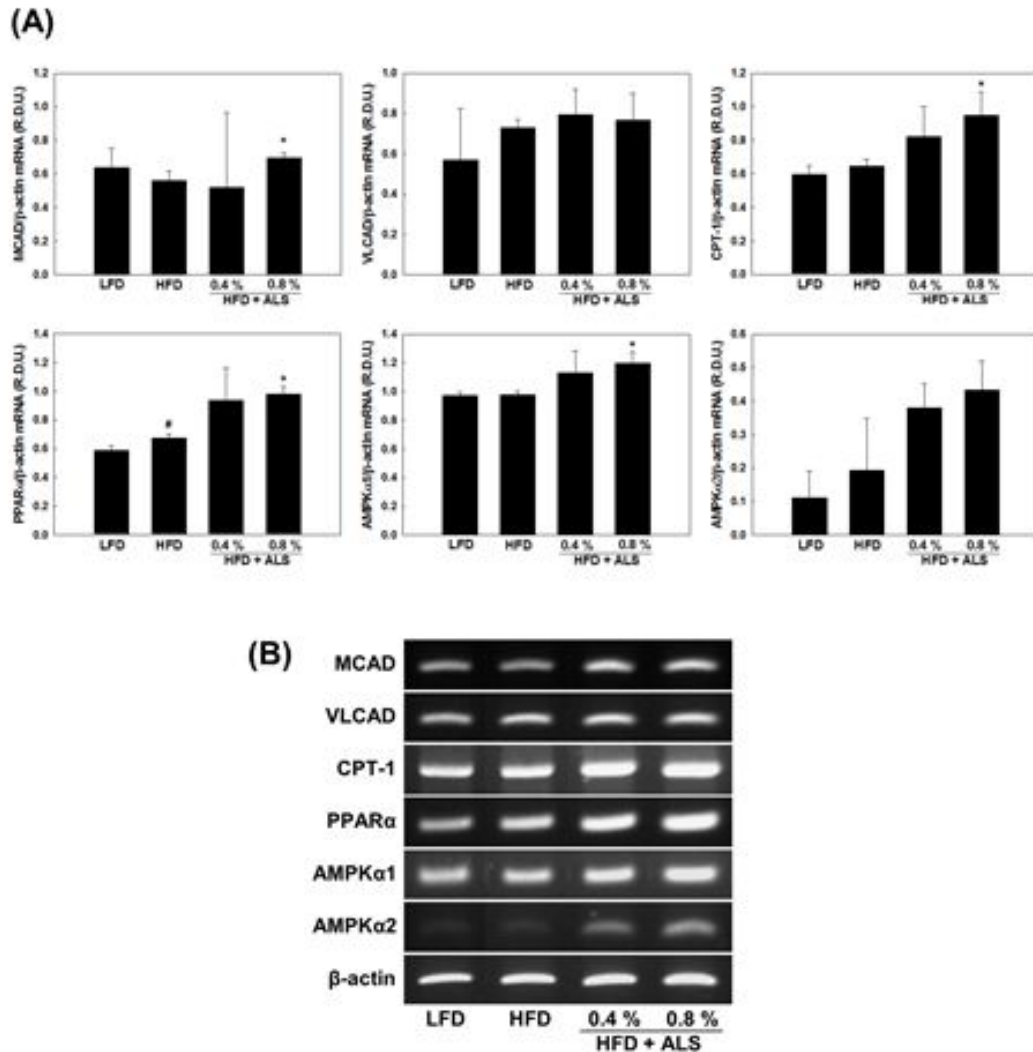


Figure 12. Effects of ALS-L1023 on mRNA expression of pancreatic genes related to FA oxidation. (A) Female sham C57BL/6J mice were fed a LFD, a HFD, or the same HFD supplemented with either 0.4% or 0.8% ALS-L1023 for 17 weeks. MCAD, VLCAD, CPT-1, PPAR α , AMPK α 1, and AMPK α 2 and VLCAD mRNA levels were measured by RT-PCR. All values are expressed as mean \pm SD of R.D.U. (relative density units) using β -actin as a reference. # p <0.05 compared with LFD. * p <0.05 compared with HFD. (B) Representative RT-PCR bands from one of three independent experiments are shown.

and ACC by 4%, and 10%, respectively, compared with HFD-fed mice although FAS mRNA levels were not decreased. SREBP-1c, FAS, ACC mRNA levels in 0.8% ALS-L1923 treated mice were also decreased by 33%, 5%, and 21%, respectively, than in HFD-fed mice (Figure 13).

1.5. Effects of ALS-L1023 on pancreatic inflammation

1.5.1. Histological evaluation of pancreatic inflammation

Pancreatic inflammation in female sham mice was examined by using a toluidine blue staining method, which detects mast cells. Toluidine blue staining showed that pancreatic inflammation was increased in the HFD-fed mice compared with LFD-mice, whereas pancreatic inflammation in the ALS-L1023-treated mice was reduced compared with HFD-fed mice (Figure 14).

1.5.2. mRNA expression of pancreatic gene related to inflammation

CD68 are associated with pancreatic inflammation. CD68 mRNA levels was increased by 27% ($P < 0.05$) in HFD-fed mice compared with LFD-fed mice. By contrast, CD68 mRNA levels was significantly decreased by 12% ($p < 0.05$) and 12% ($p < 0.05$) in 0.4% and 0.8% ALS-L1023 treated mice compared with HFD-fed mice, respectively (Figure 15).

1.6. Effects of ALS-L1023 on pancreatic fibrosis

1.6.1. Histological evaluation of pancreatic fibrosis

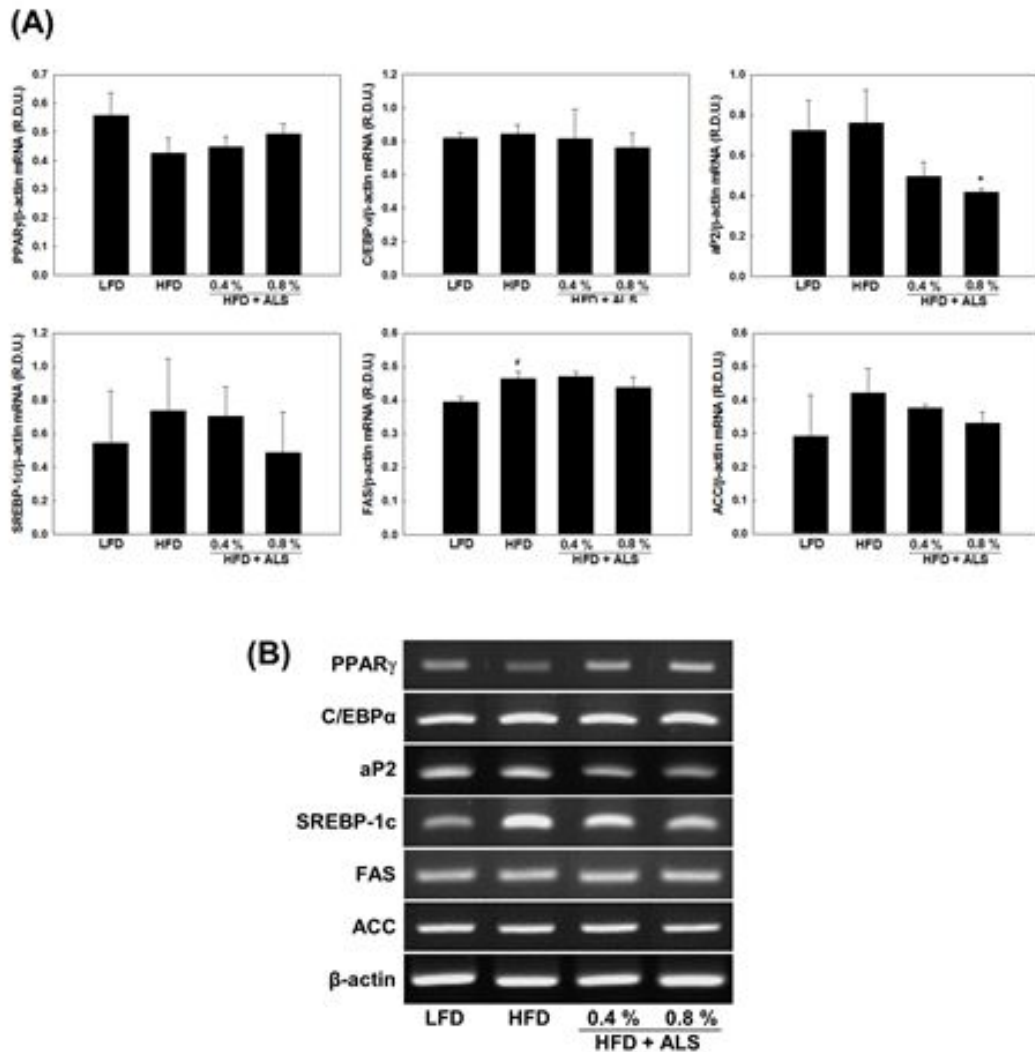


Figure 13. Effects of ALS-L1023 on mRNA expression of pancreatic genes related to lipogenesis. (A) Female sham C57BL/6J mice were fed a LFD, a HFD, or the same HFD supplemented with either 0.4% or 0.8% ALS-L1023 for 17 weeks. PPAR γ , C/EBP α , aP2, SREBP-1c, FAS, and ACC mRNA levels were measured by RT-PCR. All values are expressed as mean \pm SD of R.D.U. (relative density units) using β -actin as a reference. # p <0.05 compared with LFD. * p <0.05 compared with HFD. (B) Representative RT-PCR bands from one of three independent experiments are shown.

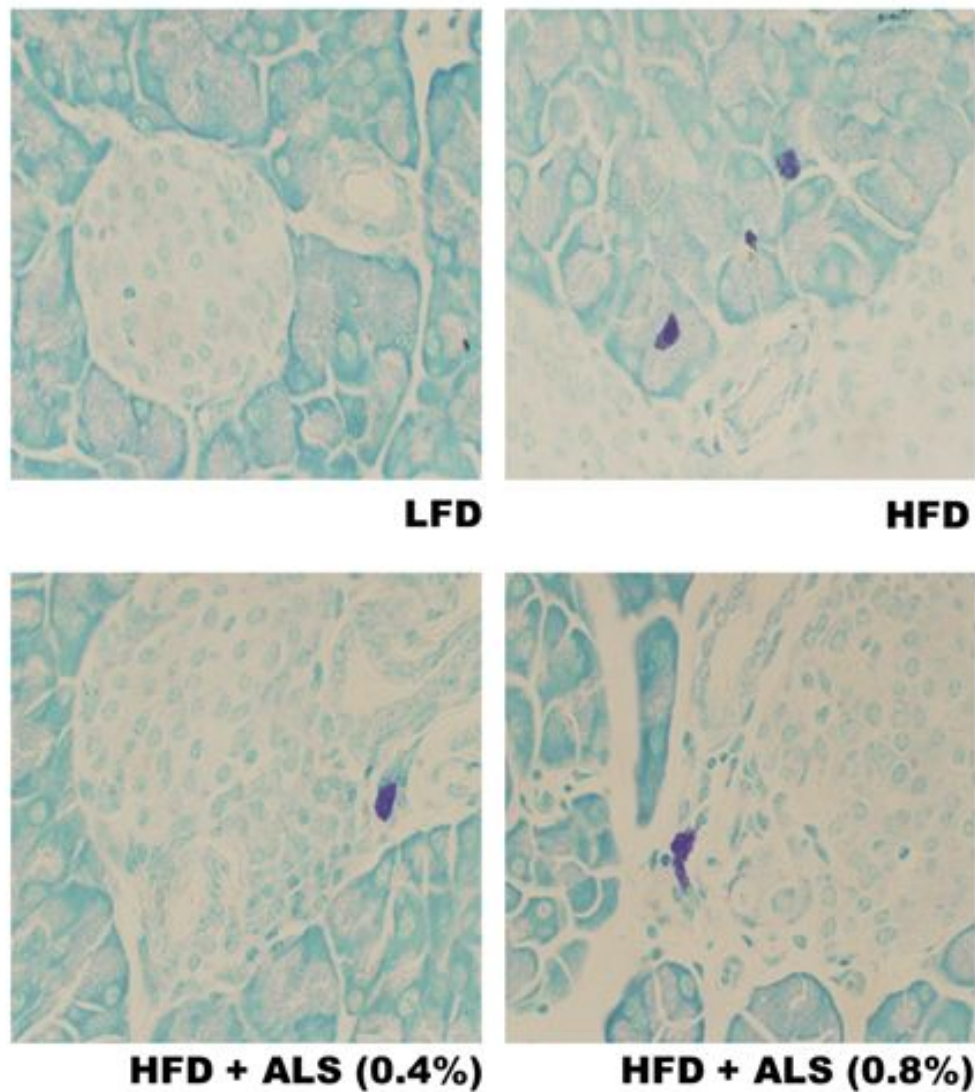


Figure 14. Effects of ALS-L1023 on pancreatic inflammation. Female sham C57BL/6J mice were fed a LFD, a HFD, or the same HFD supplemented with either 0.4% or 0.8% ALS-L1023 for 17 weeks. Representative toluidine blue stained sections of pancreas are shown in purple color. Original magnification X400.

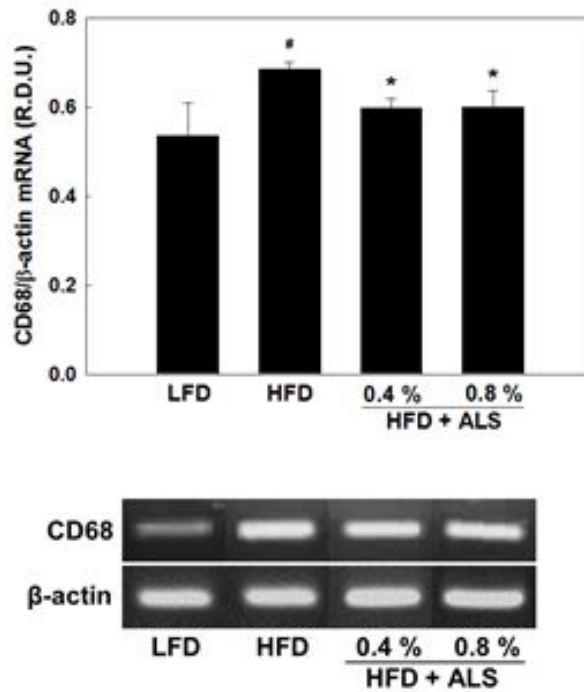


Figure 15. Effects of ALS-L1023 on mRNA expression of pancreatic gene related to inflammation. (A) Female sham C57BL/6J mice were fed a LFD, a HFD, or the same HFD supplemented with either 0.4% or 0.8% ALS-L1023 for 17 weeks. CD68 mRNA levels were measured by RT-PCR. All values are expressed as mean \pm SD of R.D.U. (relative density units) using β -actin as a reference. [#] $p < 0.05$ compared with LFD. ^{*} $p < 0.05$ compared with HFD. (B) Representative RT-PCR bands from one of three independent experiments are shown.

Pancreatic fibrosis was examined by Masson's trichrome staining in mice fed a HFD. Pancreatic fibrosis was worsened in HFD-fed mice compared with LFD-fed mice (Figure 16). In contrast, HFD supplemented with ALS-L1023 decreased pancreatic fibrosis (Figure 16). These results show that ALS-L1023 in female sham pancreas effectively reduces pancreatic fibrosis.

1.6.2. mRNA expression of pancreatic genes related to fibrosis

Pancreatic fibrosis is induced by fibrogenic molecules, such as α -smooth muscle actin (α -SMA), transforming growth factor β 1 (TGF β 1), and collagen α 1. 0.4% ALS-L1023-treated mice had decreased mRNA levels of α -SMA and collagen α 1 by 6% and 27% ($p < 0.05$), respectively, compared with HFD-treated mice. 0.8% ALS-L1023 also decreased α -SMA, TGF- β 1, and collagen α 1 gene expression by 18%, 15%, and 52% ($p < 0.05$), respectively (Figure 17).

1.7. Effect of ALS-L1023 on mRNA expression of pancreatic genes related to β -cell apoptosis

Chronic elevation of FAs has also been shown to be associated with increased β -cell apoptosis in rodents (Martinez *et al.*, 2008). The apoptosis gene p53 mRNA levels was decreased by 66% ($p < 0.05$) and 69% ($p < 0.05$) in 0.4% and 0.8% ALS-L1023 treated mice compared with HFD-fed mice, respectively. However, the apoptosis gene Bax mRNA levels was increased by 69% ($p < 0.05$) and 33% in 0.4% and 0.8% ALS-L1023

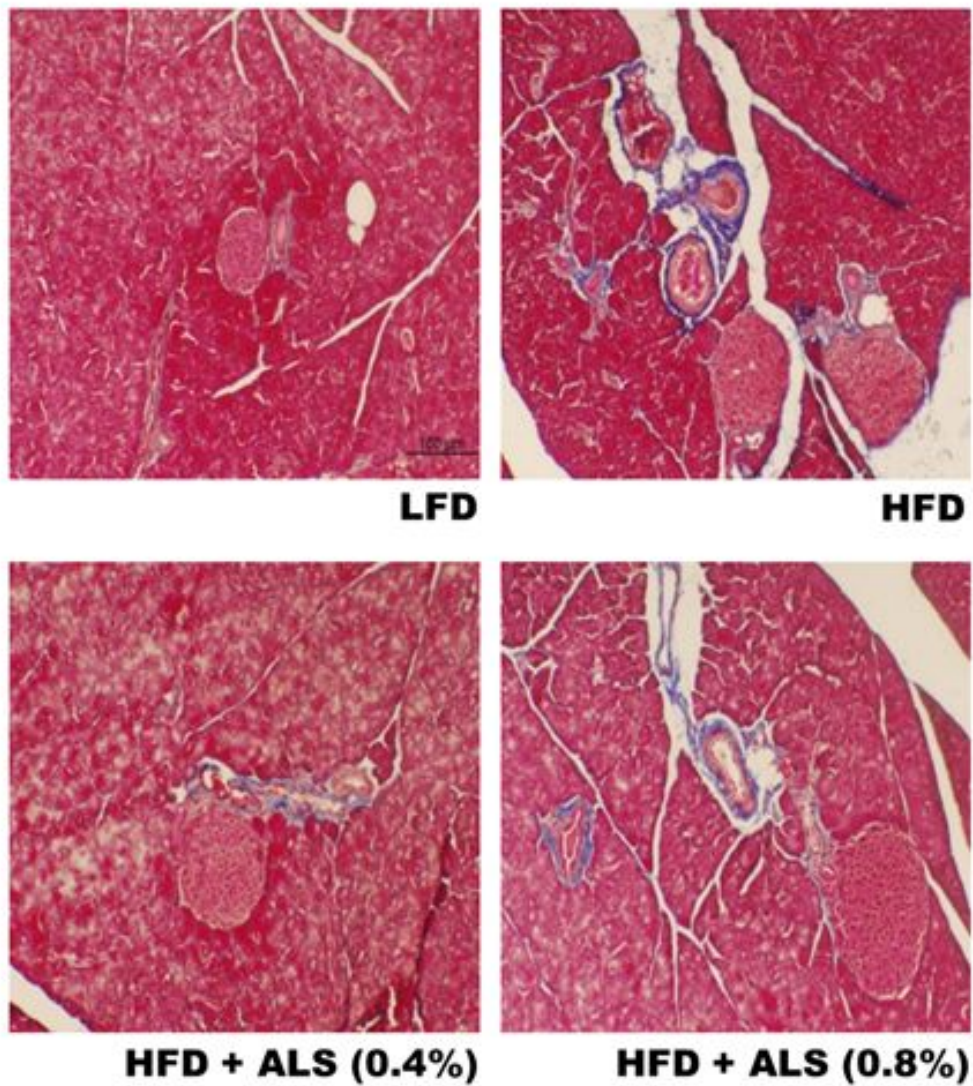


Figure 16. Effects of ALS-L1023 on pancreatic fibrosis. Female sham C57BL/6J mice were fed a LFD, a HFD, or the same HFD supplemented with either 0.4% or 0.8% ALS-L1023 for 17 weeks. Representative Masson's trichrome stained sections of pancreas are shown in blue color. Original magnification X100.

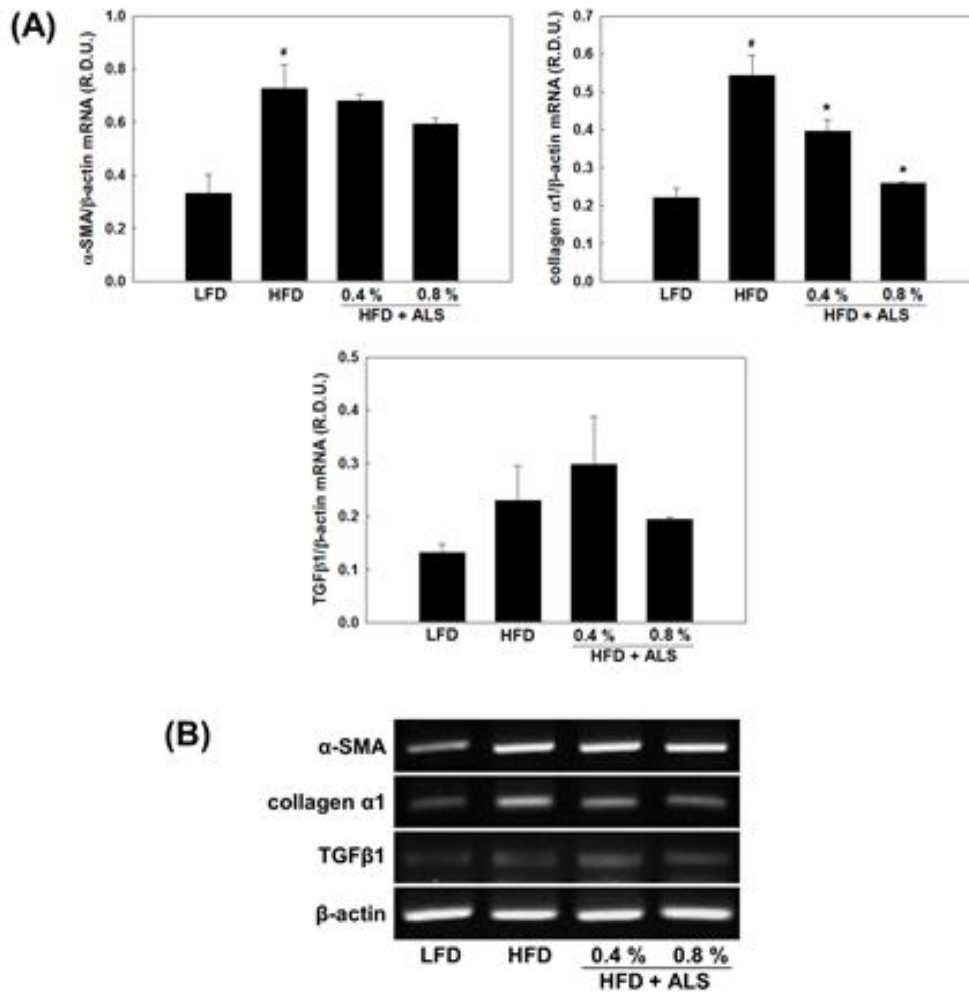


Figure 17. Effects of ALS-L1023 on mRNA expression of pancreatic genes related to fibrosis. (A) Female sham C57BL/6J mice were fed a LFD, a HFD, or the same HFD supplemented with either 0.4% or 0.8% ALS-L1023 for 17 weeks. α -SMA, collagen α 1, and TGF β 1 mRNA levels were measured by RT-PCR. All values are expressed as mean \pm SD of R.D.U. (relative density units) using β -actin as a reference. # p <0.05 compared with LFD. * p <0.05 compared with HFD. (B) Representative RT-PCR bands from one of three independent experiments are shown.

treated mice compared with HFD-fed mice, respectively (Figure 18).

The apoptosis inhibitor gene Bcl-xL mRNA levels was elevated 98% ($p<0.05$) and 67% ($p<0.05$) in 0.4% and 0.8% ALS-L1023 treated mice compared with HFD-fed mice, respectively. In contrast, Bcl-2 mRNA levels was decreased by 14% ($p<0.05$) and 28% ($p<0.05$) in 0.4% and 0.8% ALS-L1023 treated mice compared with HFD-fed mice, respectively (Figure 18).

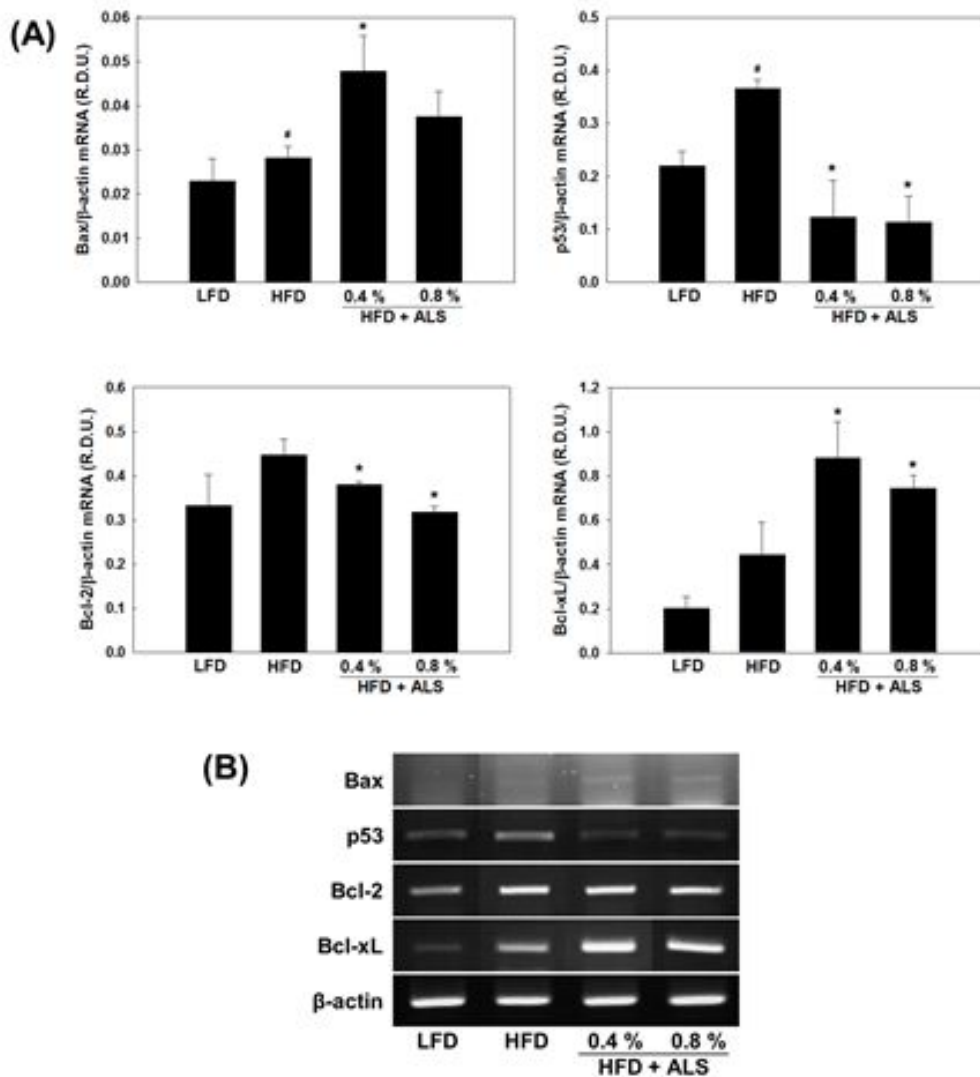


Figure 18. Effects of ALS-L1023 on mRNA expression of pancreatic genes related to β -cell apoptosis. (A) Female sham C57BL/6J mice were fed a LFD, a HFD, or the same HFD supplemented with either 0.4% or 0.8% ALS-L1023 for 17 weeks. Bax, p53, Bcl-2 and Bcl-xL mRNA levels were measured by RT-PCR. All values are expressed as mean \pm SD of R.D.U. (relative density units) using β -actin as a reference. # $p < 0.05$ compared with LFD. * $p < 0.05$ compared with HFD. (B) Representative RT-PCR bands from one of three independent experiments are shown.

2. Female OVX C57BL/6J mice

2.1. Regulation of body weight, adipose tissue mass, adipocyte size, and food intake by ALS-L1023 in high fat diet-fed female OVX mice

2.1.1. Body weight

Female OVX mice received a LFD, a HFD or the same HFD supplemented with ALS-L1023 for 16 weeks. After 16 weeks of a LFD, the body weight was 28 ± 1.96 g. By contrast, the body weight of mice fed a HFD was increased to 39 ± 2.31 g, whereas mice received a 0.4% ALS-L1023 showed body weight of 34 ± 1.58 g, compared with HFD (Figure 19A). 0.4% ALS-L1023 treatment significantly decreased body weight gain by 22% ($p < 0.05$), compared with HFD (Figure 19B). However, the body weight and body weight gain were not different between HFD and HFD supplemented with 0.8% ALS-L1023 group (Figure 19B).

2.1.2. Adipose tissue mass and adipocyte size

Adipose tissue mass was also significantly decreased by ALS-L1023 treatment in HFD-fed OVX mice (Figure 20). As shown in Figure 21B, the total adipose tissue mass in 0.4% ALS-L1023 treated mice was 21% ($p < 0.05$) lower than that of HFD-treated mice. Visceral adipose tissue mass was reduced by 20% after 0.4% ALS-L1023 treatment (Figure 20C).

Analysis of HE-stained adipose tissue section revealed that ALS-L1023 markedly decreased the size of visceral adipocytes. ALS-L1023 at concentrations of 0.4%

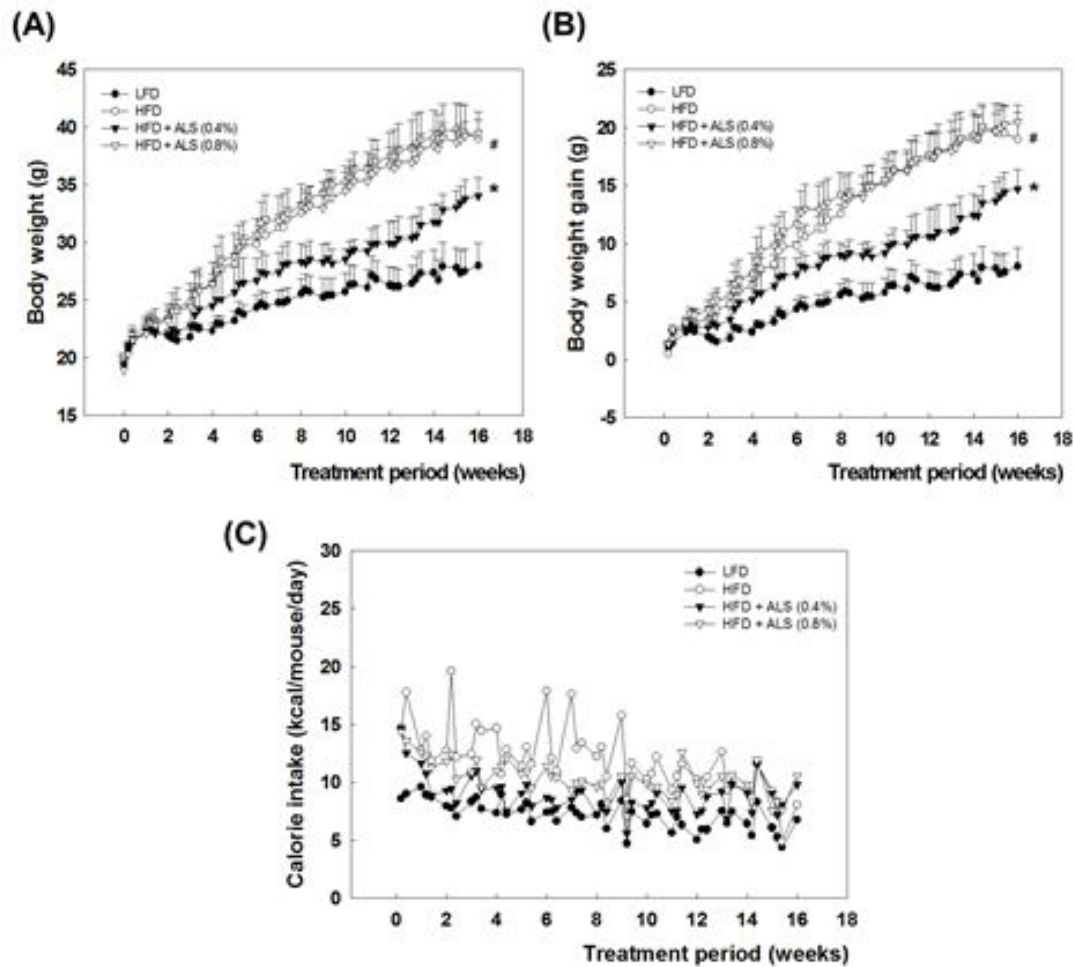


Figure 19. Effects of ALS-L1023 on body weight (A), and body weight gain (B), and food intake (C) in high fat diet-fed female OVX mice. Mice (n=5/group) were fed a LFD, a HFD, or the same HFD supplemented with either 0.4% or 0.8% ALS-L1023 for 16 weeks. All values are expressed as mean \pm SD. #p<0.05 compared with LFD. *p<0.05 compared with HFD.

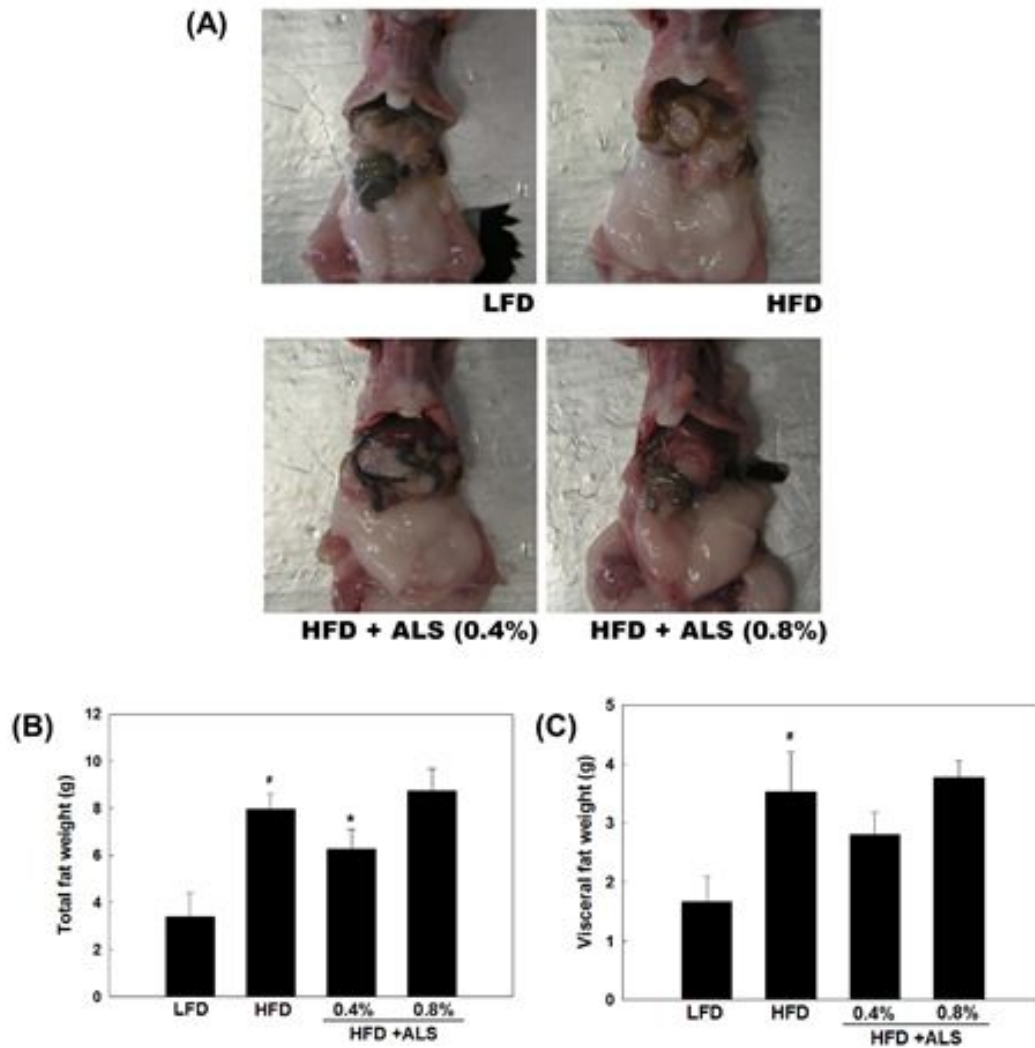


Figure 20. Effects of ALS-L1023 on adipose tissue mass. Female OVX C57BL/6J mice were fed a LFD, a HFD, or the same HFD supplemented with either 0.4% or 0.8% ALS-L1023 for 16 weeks. (A) Ventrotomy image, (B) total adipose tissue mass, and (C) visceral adipose tissue mass. All values are expressed as mean \pm SD. [#] $p < 0.05$ compared with LFD. ^{*} $p < 0.05$ compared with HFD.

and 0.8% decreased the average size of visceral adipocytes by 26% ($p<0.05$) and 22% ($p<0.05$), in HFD-fed mice, respectively (Figure 21B).

2.1.3. Food intake

During 16 weeks, food intake was higher in the HFD-fed OVX mice than in LFD-fed lean mice, but no significant difference was observed in food intake between the HFD-treated and ALS-treated mice (Figure 19C).

2.2. Effects of ALS-L1023 on glucose, and insulin levels

2.2.1. Glucose and insulin levels

As shown in Figure 22A, blood glucose levels was not different between HFD and HFD supplemented with ALS-L1023 group. Serum insulin levels were 30% ($p<0.05$) higher in HFD-fed mice than in LFD-fed mice. Moreover, 0.4% and 0.8% ALS-L1023-treated mice increased insulin levels by 192%, and 190% ($p<0.05$) compared with the HFD-fed mice (Figure 22B, $p<0.05$).

2.2.2. OGTT

HFD-fed obese OVX mice displayed impaired glucose tolerance compared with the LFD-fed mice (Figure 22C, $p<0.05$). However, 0.8% and 0.4% ALS-L1023 improved the impaired glucose tolerance at 30 min by 30% ($p<0.05$) and 23%, compared with the HFD-fed mice (Figure 22C).

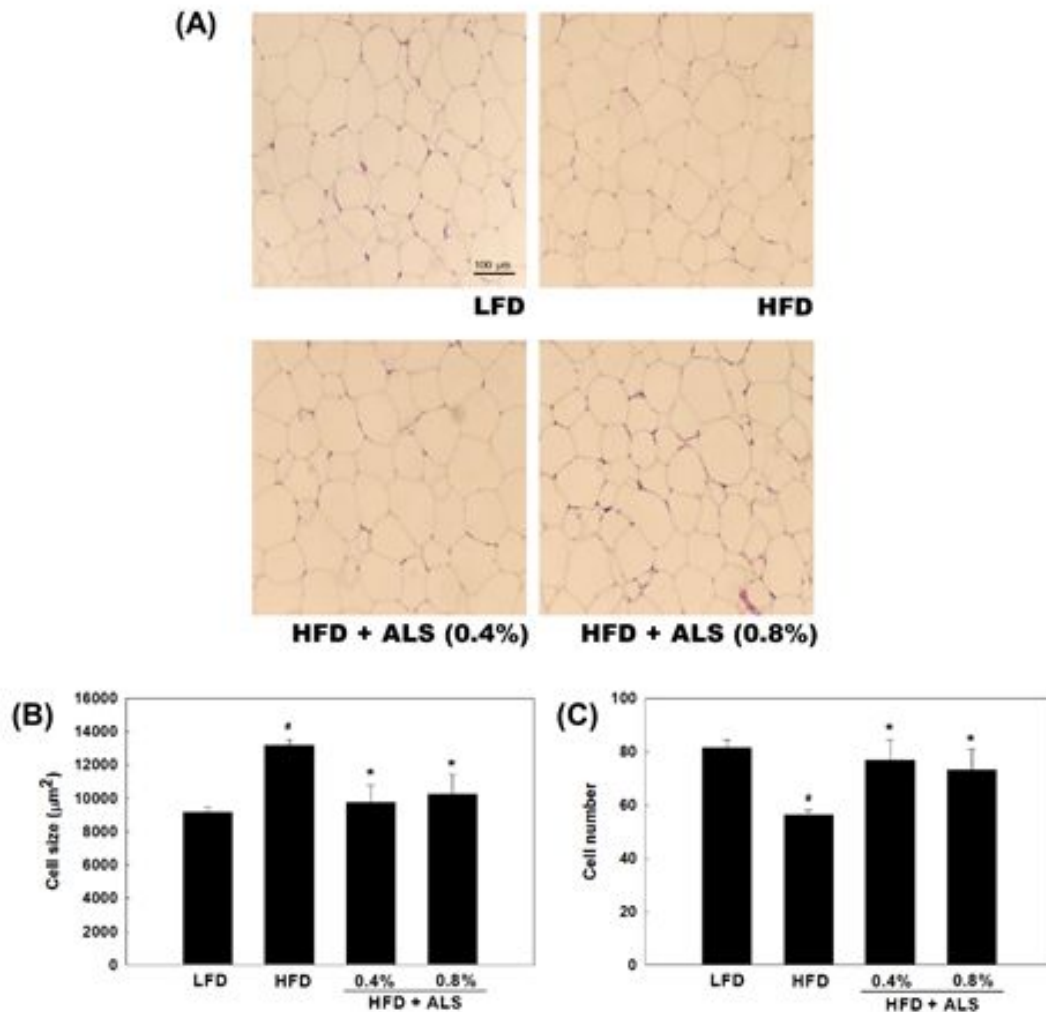


Figure 21. Effects of ALS-L1023 on visceral adipocyte histology. Female OVX C57BL/6J mice were fed a LFD, a HFD, or the same HFD supplemented with either 0.4% or 0.8% ALS-L1023 for 16 weeks. (A) HE-stained sections of visceral adipocytes are shown (original magnification X100), (B) the size of visceral adipocytes and (C) the number of visceral adipocytes in a fixed area (1,000,000 μm²) was measured and values are expressed as mean ± SD. #p<0.05 compared with LFD. *p<0.05 compared with HFD.

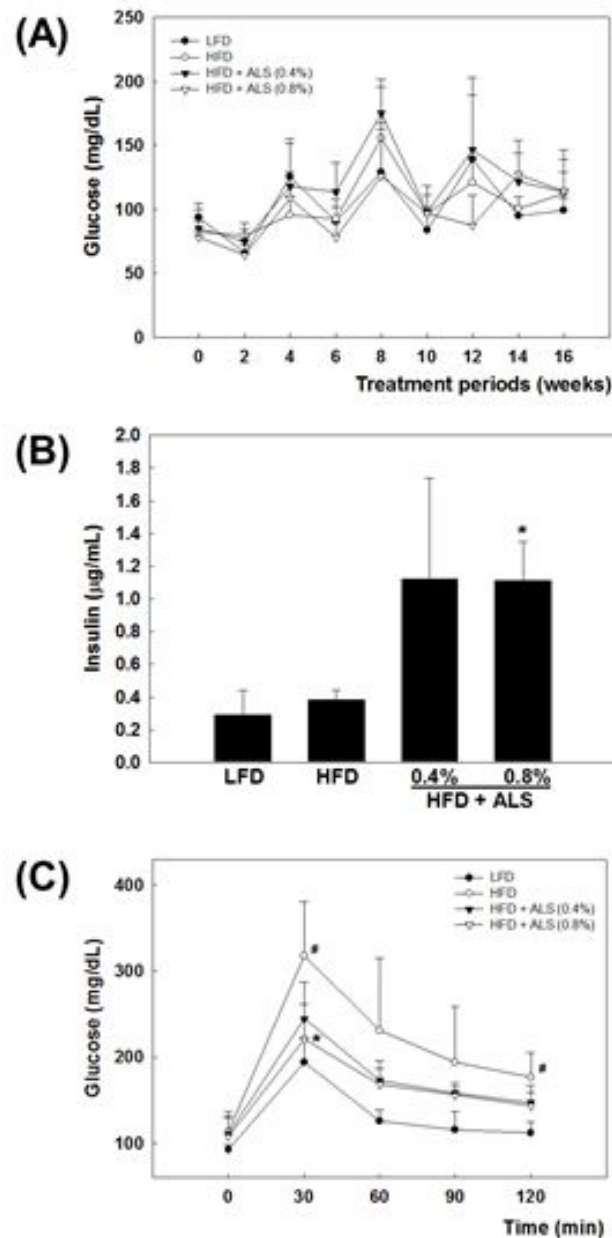


Figure 22. Effects of ALS-L1023 on serum glucose and insulin levels. Female OVX C57BL/6J mice were fed a LFD, a HFD, or the same HFD supplemented with either 0.4% or 0.8% ALS-L1023 for 16 weeks. (A): Fasting blood glucose levels. (B): Oral glucose tolerance test. (C): Serum insulin levels at 18 weeks following ALS-L1023 treatment. # $p < 0.05$ compared with LFD. * $p < 0.05$ compared with HFD.

2.3. Effects of ALS-L1023 on pancreatic islet morphology and insulin-secreting cells

2.3.1. Histological evaluation of pancreatic islet morphology

The size and morphology of pancreatic islet was determined by a hematoxylin and eosin staining method. The LFD-fed mice showed a normal pancreatic islet structure, whereas the size of pancreatic islets was markedly increased in HFD-fed mice compared with LFD-fed mice. Cells inside the pancreatic islets showed hyperplasia were modified in HFD-fed mice (Figure 23). In contrast, the pancreas morphology was restored to the pancreas morphology in LFD-fed mice after 0.4% ALS-L1023 treatment. 0.4% ALS-L1023-treated group showed improved islet morphology (Figure 23). However, pancreatic islet size of 0.8% ALS-L1023-treated group were not different between HFD-group.

2.3.2. Immunohistochemical finding : Insulin

Immunohistochemistry was performed to determine insulin secretion in pancreatic β -cells by using an anti-insulin antibody. Insulin-positive areas in pancreatic islets were was increased, but insulin-positive intensity was reduced in HFD-fed mice compared with LFD mice. By contrast, a marked elevation in the insulin content of islets was observed in 0.4% and 0.8% ALS-L1023-treated mice compared with HFD-fed mice (Figure 24). In addition, 0.4% ALS-L1023-treated group showed improved pancreatic islet structure.

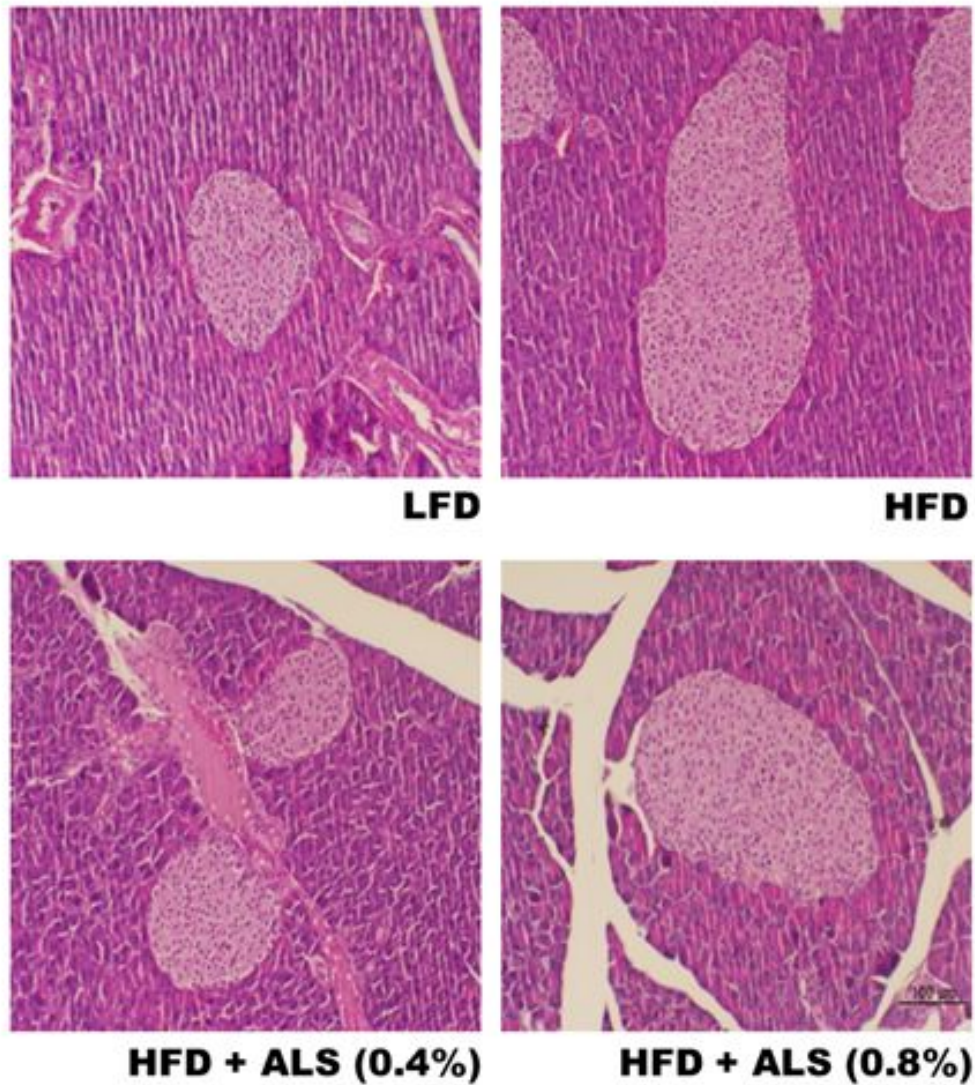


Figure 23. Effects of ALS-L1023 on pancreatic islet structures. Female OVX C57BL/6J mice were fed a LFD, a HFD, or the same HFD supplemented with either 0.4% or 0.8% ALS-L1023 for 16 weeks. Pancreas sections were stained with Hematoxylin and Eosin. Original magnification X100.

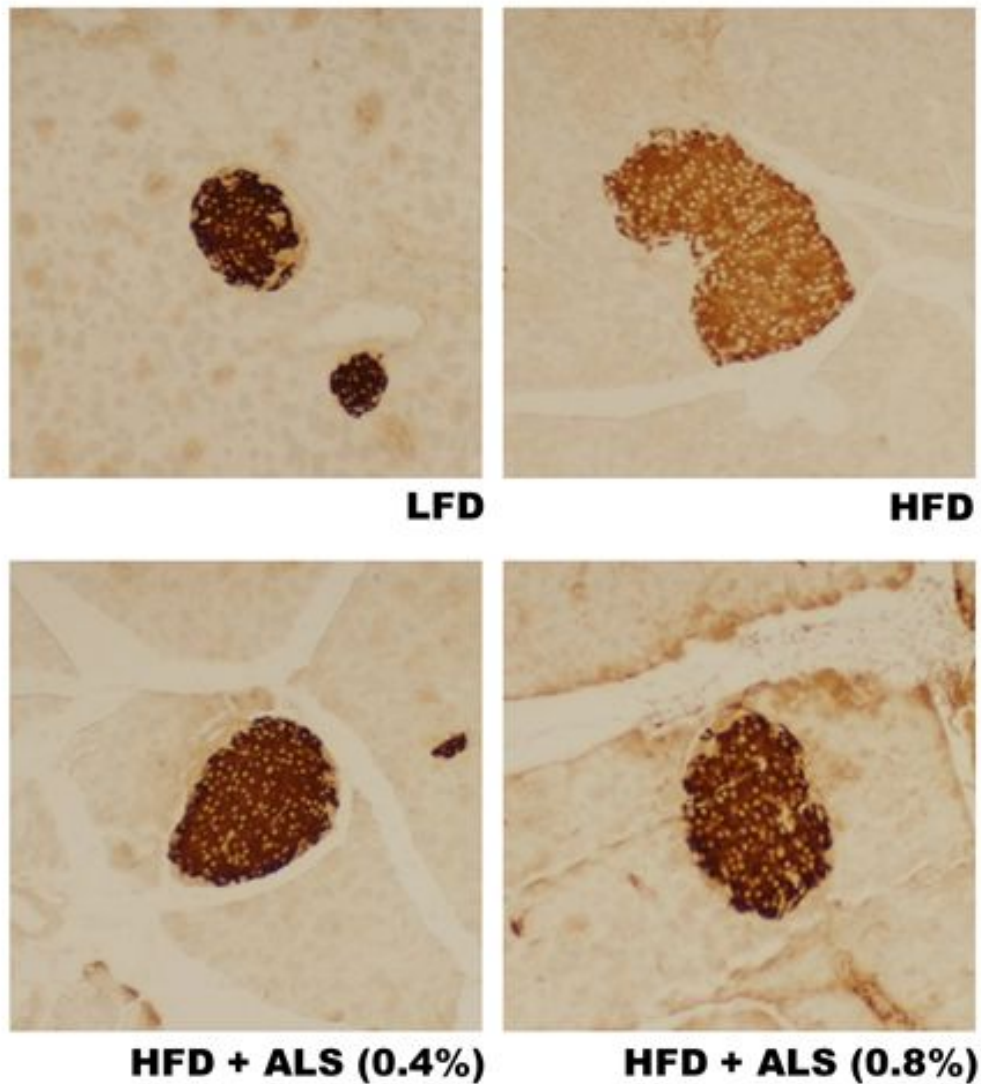


Figure 24. Effects of ALS-L1023 on insulin-positive cells in pancreas. Female OVX C57BL/6J mice were fed a LFD, a HFD, or the same HFD supplemented with either 0.4% or 0.8% ALS-L1023 for 16 weeks. Representative pancreas sections stained with an antibody against insulin are shown in dark brown color. Original magnification X100.

2.4. Effects of ALS-L1023 on pancreatic steatosis

2.4.1. Histological evaluation of pancreatic steatosis

The pancreatic accumulation of lipid was determined by a Masson's trichrome staining method. 0.4% and 0.8% ALS-L1023-treated mice showed lower pancreatic lipid accumulation than HFD-fed mice (Figure 25).

2.4.2. mRNA expression of pancreatic genes related to FA oxidation

The FA oxidation genes were measured after ALS-L1023 treatment. PPAR α , and CPT-1 mRNA levels were significantly increased by 15% ($p<0.05$), and 17% ($p<0.05$) in 0.4% ALS-L1023-treated mice, respectively, compared with HFD-fed mice. PPAR α and CPT-1 mRNA levels in 0.8% ALS-L1023 treated mice were also increased by 20% ($p<0.05$), and 14% respectively, than in HFD-fed mice (Figure 26). However, MCAD, VLCAD, AMPK α 1, and AMPK α 2 mRNA levels were not different between HFD and ALS-L1023-supplemented HFD group (Figure 26).

2.4.3. mRNA expression of pancreatic genes related to lipogenesis

Compared with HFD-fed mice, 0.4% ALS-L1023-treated mice had decreased mRNA levels of C/EBP α , and aP2 mRNA levels by 8% ($p<0.05$), and 11%, respectively. However, 0.4% ALS-L1023 treated mice had increased PPAR γ , SREBP-1c, FAS, and ACC mRNA levels by 29% ($p<0.05$), 26%, 38% ($p<0.05$), and 59%, respectively, compared with HFD-fed mice (Figure 27).

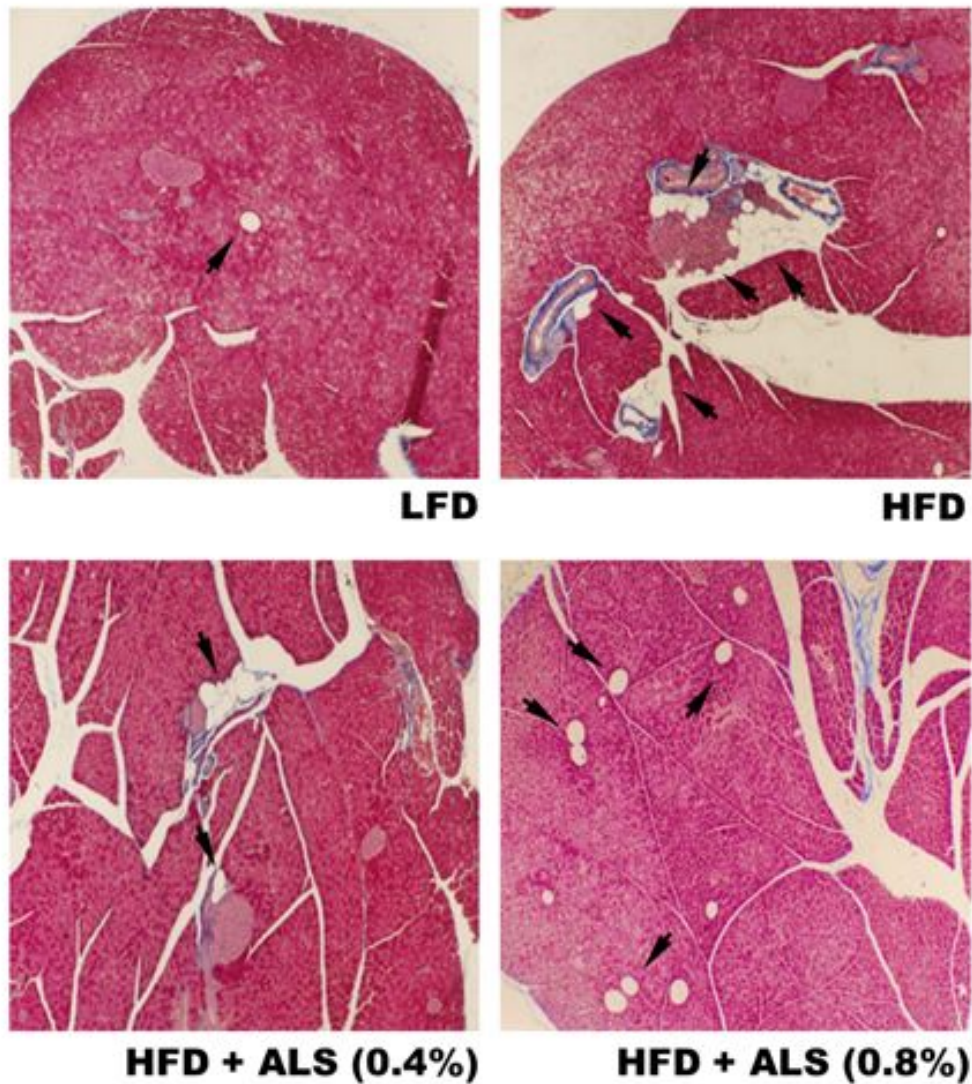


Figure 25. Effects of ALS-L1023 on pancreatic steatosis. Female OVX C57BL/6J mice were fed a LFD, a HFD, or the same HFD supplemented with either 0.4% or 0.8% ALS-L1023 for 16 weeks. A photomicrograph of mouse pancreatic tissue of the high fat group showing lipid droplets (black arrow). Pancreas sections were stained with Masson's trichrome. Original magnification X40.

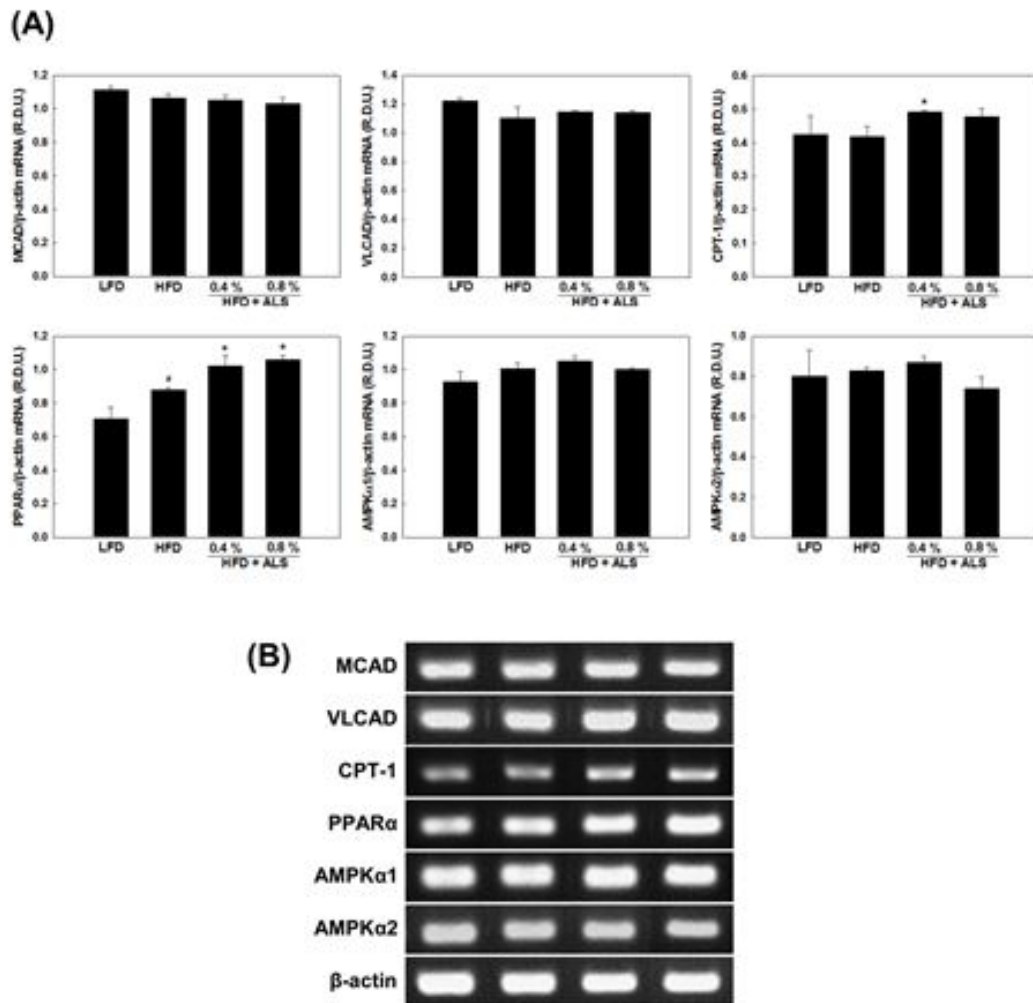


Figure 26. Effects of ALS-L1023 on mRNA expression of pancreatic genes related to FA oxidation. (A) Female OVX C57BL/6J mice were fed a LFD, a HFD, or the same HFD supplemented with either 0.4% or 0.8% ALS-L1023 for 16 weeks. MCAD and VLCAD, CPT-1, PPARα, AMPKα1, and AMPKα2, mRNA levels were measured by RT-PCR. All values are expressed as mean \pm SD of R.D.U. (relative density units) using β -actin as a reference. # p <0.05 compared with LFD. * p <0.05 compared with HFD. (B) Representative RT-PCR bands from one of three independent experiments are shown.

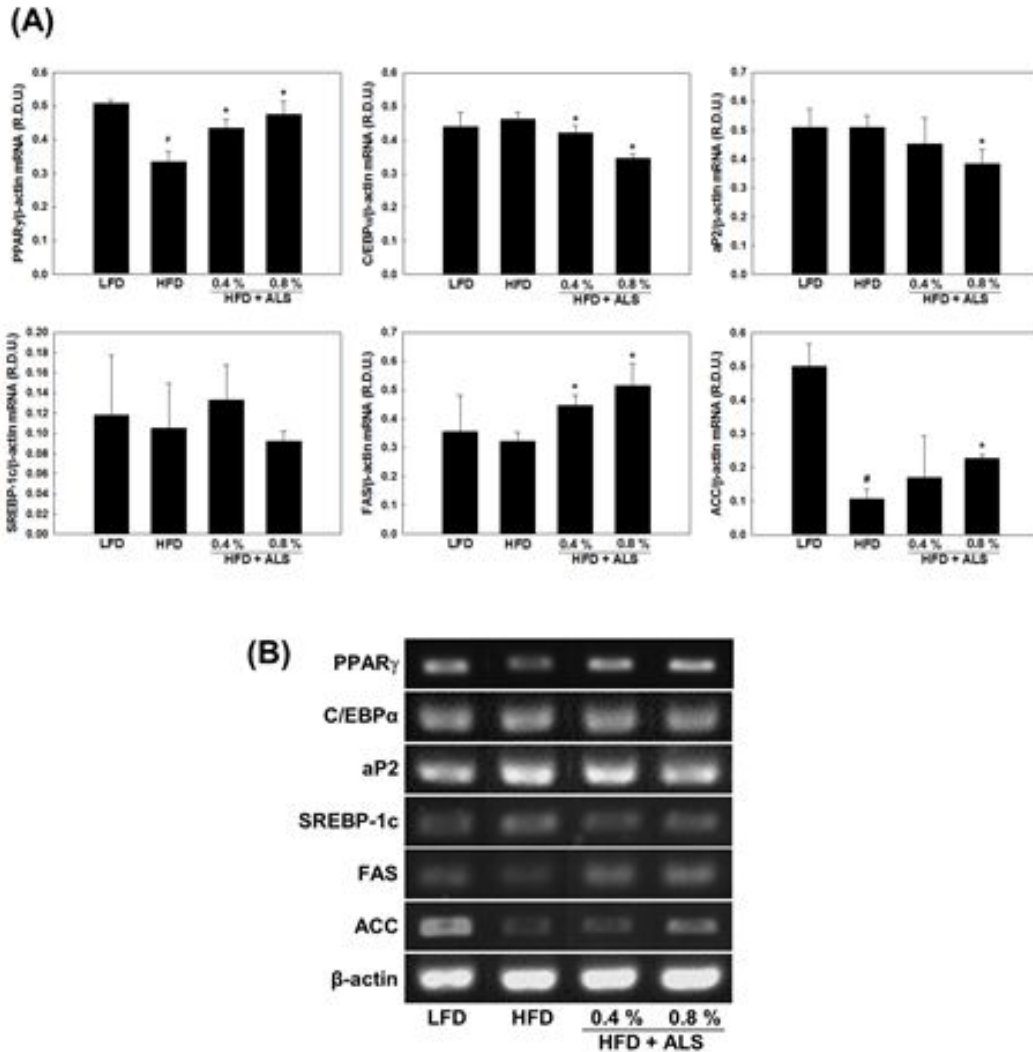


Figure 27. Effects of ALS-L1023 on mRNA expression of pancreatic genes related to lipogenesis. (A) Female OVX C57BL/6J mice were fed a LFD, a HFD, or the same HFD supplemented with either 0.4% or 0.8% ALS-L1023 for 16 weeks. PPAR γ , C/EBP α , aP2, SREBP1c, FAS, and ACC mRNA levels were measured by RT-PCR. All values are expressed as mean \pm SD of R.D.U. (relative density units) using β -actin as a reference. # p <0.05 compared with LFD. * p <0.05 compared with HFD. (B) Representative RT-PCR bands from one of three independent experiments are shown.

Compared with HFD-fed mice, 0.8% ALS-L1023-treated mice had decreased mRNA levels of C/EBP α , aP2, and SREBP-1c mRNA levels by 25% ($p<0.05$), 24% ($p<0.05$), and 12%, respectively. Although, 0.8% ALS-L1023 treated mice had significantly increased PPAR γ , FAS, and ACC by 41% ($p<0.05$), 60% ($p<0.05$), and 112% ($p<0.05$), respectively, compared with HFD-fed mice (Figure 27).

2.5. Effects of ALS-L1023 on pancreatic inflammation

2.5.1. Histological evaluation of pancreatic inflammation

Pancreatic inflammation in female OVX mice was examined by using a toluidine blue staining method, which detects mast cells. Toluidine blue staining showed that pancreatic inflammation was increased in the HFD-fed mice compared with LFD-mice, whereas pancreatic inflammation in the ALS-L1023-treated mice was reduced compared with HFD-fed mice (Figure 28).

2.5.2. mRNA expression of pancreatic gene related to inflammation

CD68 mRNA levels was increased by 8% in HFD-fed mice compared with LFD-fed mice. By contrast, CD68 mRNA levels was significantly decreased by 25% ($p<0.05$) and 46% ($p<0.05$) in 0.4% and 0.8% ALS-L1023 treated mice compared with HFD-fed mice, respectively (Figure 29).

2.6. Effects of ALS-L1023 on pancreatic fibrosis

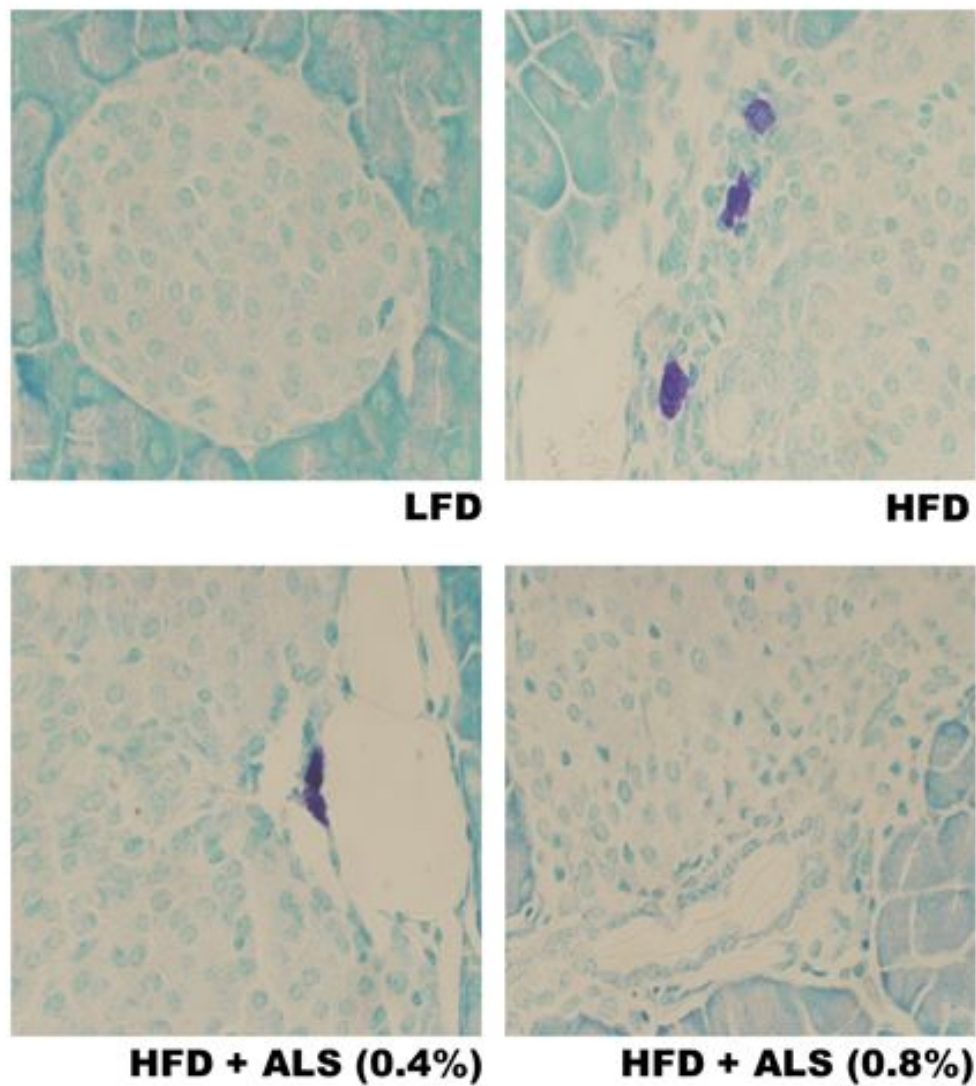


Figure 28. Effects of ALS-L1023 on pancreatic inflammation. Female OVX C57BL/6J mice were fed a LFD, a HFD, or the same HFD supplemented with either 0.4% or 0.8% ALS-L1023 for 16 weeks. Representative toluidine blue stained sections of pancreas are shown in purple color. Original magnification X400.

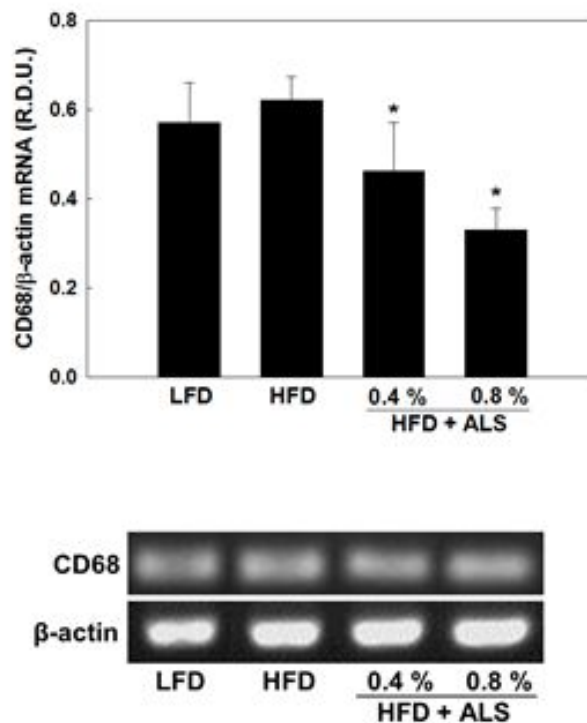


Figure 29. Effects of ALS-L1023 on mRNA expression of pancreatic gene related to inflammation. (A) Female OVX C57BL/6J mice were fed a LFD, a HFD, or the same HFD supplemented with either 0.4% or 0.8% ALS-L1023 for 16 weeks. CD68 mRNA levels were measured by RT-PCR. All values are expressed as mean \pm SD of R.D.U. (relative density units) using β -actin as a reference. # $p < 0.05$ compared with LFD. * $p < 0.05$ compared with HFD. (B) Representative RT-PCR bands from one of three independent experiments are shown.

2.6.1. Histological evaluation of pancreatic fibrosis

Pancreatic fibrosis was seriously worsened in HFD-fed mice compared with LFD-fed mice (Figure 30). In contrast, mice fed on a HFD supplemented with ALS-L1023 decreased pancreatic fibrosis compared with HFD-fed mice (Figure 30).

2.6.2. mRNA expression of genes related to pancreatic fibrosis

α -SMA, collagen $\alpha 1$, and TGF β 1 are associated with pancreatic fibrosis. 0.4% ALS-L1023-treated mice had decreased mRNA levels of α -SMA and collagen $\alpha 1$ by 45% ($p < 0.05$) and 48% ($p < 0.05$), respectively, compared with HFD-treated mice. 0.8% ALS-L1023 also decreased α -SMA and collagen $\alpha 1$ gene expression by 28%, and 42% ($p < 0.05$), respectively (Figure 31). However, TGF β 1 mRNA levels were not different between HFD and ALS-L1023-supplemented HFD group (Figure 31).

2.7. Effect of ALS-L1023 on mRNA expression of pancreatic genes related to β -cell apoptosis

The apoptosis inducers Bax and p53 mRNA levels were decreased by 51% ($p < 0.05$) and 23% in 0.4% ALS-L1023 treated mice compared with HFD-fed mice. 0.8% ALS-L1023 decreased Bax and p53 gene expression by 28%, and 42% ($p < 0.05$), respectively (Figure 32).

The apoptosis inhibitor Bcl-2 mRNA levels were increased by 30% and 21% in 0.4% and 0.8% ALS-L1023 treated mice, respectively, compared with HFD-fed mice.

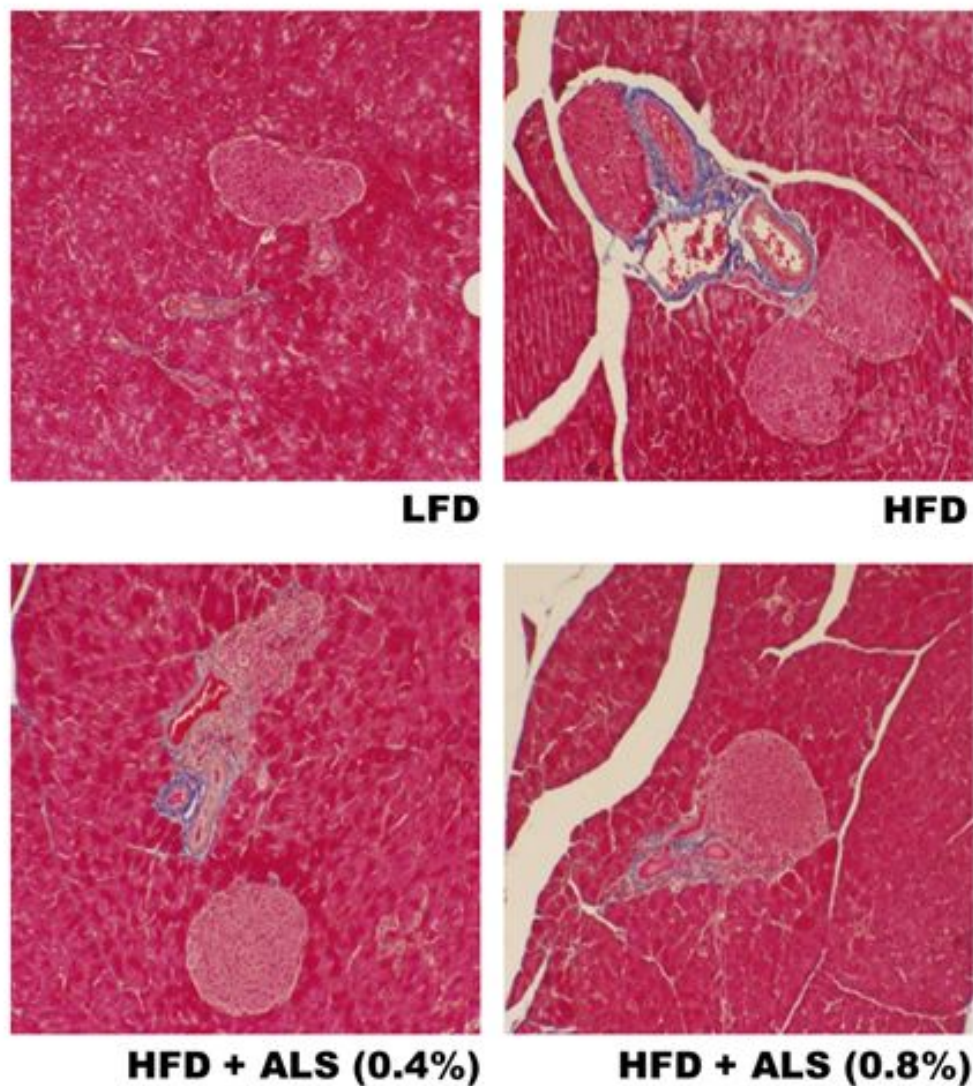


Figure 30. Effects of ALS-L1023 on pancreatic fibrosis. Female OVX C57BL/6J mice were fed a LFD, a HFD, or the same HFD supplemented with either 0.4% or 0.8% ALS-L1023 for 16 weeks. Representative Masson's trichrome stained sections of pancreas are shown in blue color. Original magnification X100.

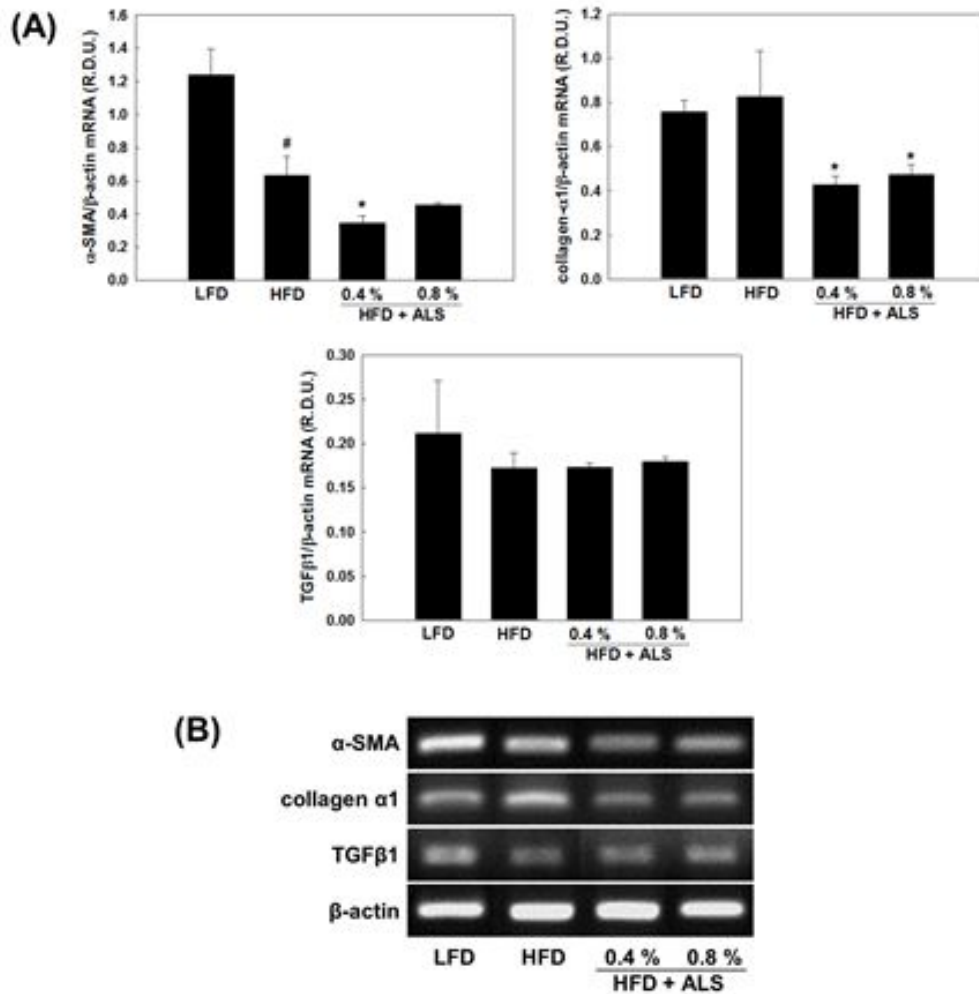


Figure 31. Effects of ALS-L1023 on mRNA expression of pancreatic genes related to fibrosis. (A) Female OVX C57BL/6J mice were fed a LFD, a HFD, or the same HFD supplemented with either 0.4% or 0.8% ALS-L1023 for 16 weeks. α-SMA, collagen α1, and TGFβ1 mRNA levels were measured by RT-PCR. All values are expressed as mean ±SD of R.D.U. (relative density units) using β-actin as a reference. [#]p<0.05 compared with LFD. ^{*}p<0.05 compared with HFD. (B) Representative RT-PCR bands from one of three independent experiments are shown.

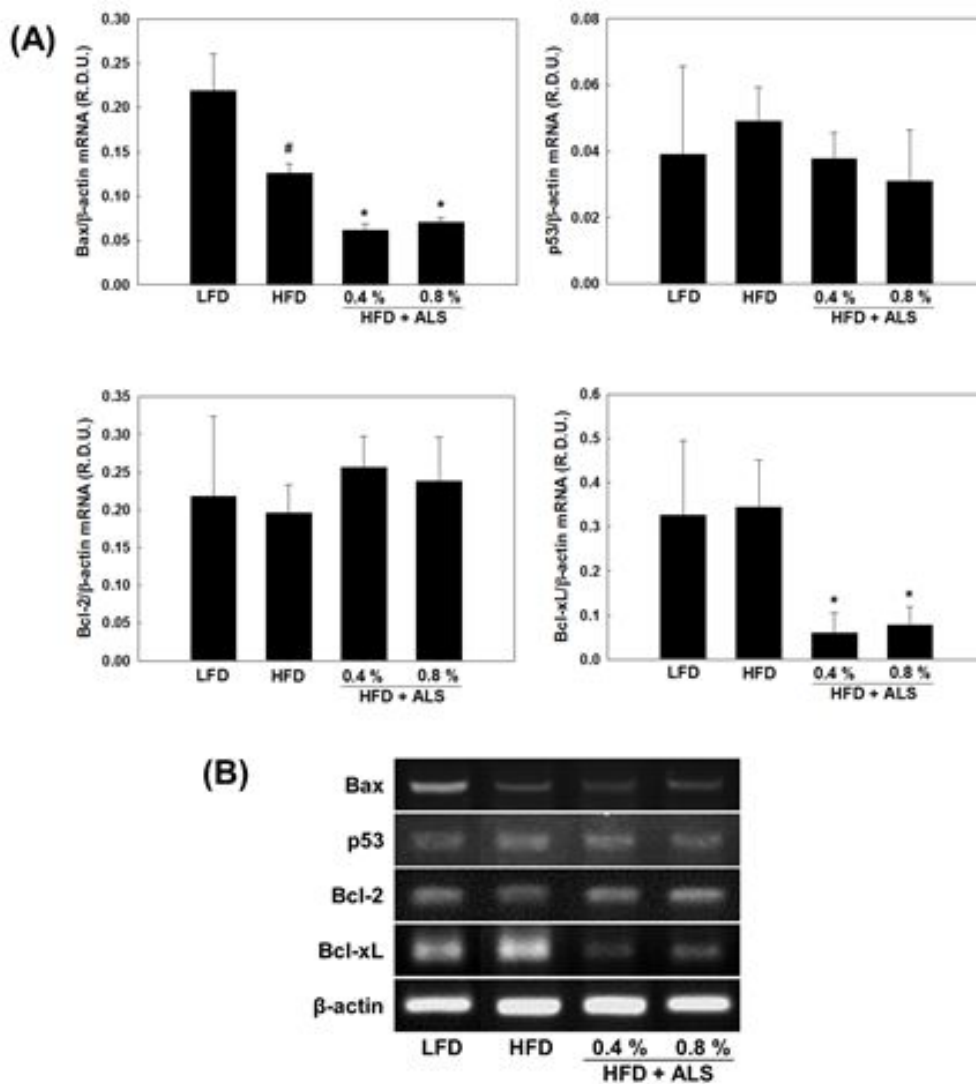


Figure 32. Effects of ALS-L1023 on mRNA expression of pancreatic genes related to β -cell apoptosis. (A) Female OVX C57BL/6J mice were fed a LFD, a HFD, or the same HFD supplemented with either 0.4% or 0.8% ALS-L1023 for 16 weeks. Bax, p53, Bcl-2 and Bcl-xL mRNA levels were measured by RT-PCR. All values are expressed as mean \pm SD of R.D.U. (relative density units) using β -actin as a reference. [#] $p < 0.05$ compared with LFD. ^{*} $p < 0.05$ compared with HFD. (B) Representative RT-PCR bands from one of three independent experiments are shown.

However, Bcl-xL mRNA levels were decreased 82% ($p<0.05$) and 77% ($p<0.05$) in 0.4% and 0.8% ALS-L1023 treated mice, respectively, compared with HFD-fed mice (Figure 32).

IV. DISCUSSION

T2D is a metabolic disorder that is characterized by high blood glucose in the context of chronic insulin resistance and relative insulin deficiency (Kumar *et al.*, 2005). Obesity is the most frequent and most studied of all the risk factors for T2D ((Hulín *et al.*, 1997). It is generally accepted that T2D is caused by the combination of insulin resistance and a progressive failure of pancreatic β -cells (Kahn, 1998). According to a plausible scenario, insulin resistance occurs when adipose cells reach a critical size and adipose tissue stores become limited (Figure 1). Ectopic TGs and FAs then produce insulin resistance in liver and muscle. In addition, a chronic inflammatory state, caused by immune cell infiltration into adipose tissue in obesity, appears to contribute to insulin resistance. Ectopic lipids also appear to affect β -cell function ('lipotoxicity'), probably in combination with the exposure of cells to high glucose concentrations ('glucotoxicity'). This pathogenesis unfolds when a polygenic susceptibility interacts with exogenous factors such as nutrition and physical activity. Therefore, T2D is the paradigm of a complex disease which has a genetic basis but is precipitated by exogenous factors (Diamond, 2003; Joost, 2008). Since it is known that ovarian steroids play in the control of body weight and adipose tissue mass, female mice were divided into two groups (sham and OVX), depending on the presence of functioning ovaries. For example, it is well known that OVX animals and postmenopausal women show increased body weight, adipose tissue mass and insulin resistance, indicating

the involvement of gonadal steroids in the modulation of obesity and T2D. (Wade, 1975; Geary and Asarian, 2001, Haifei and Kumar, 2012) Franck Mauvais-Jarvis *et al.* have shown that the gonadal steroid 17 β -estradiol protects β -cells from oxidative stress-induced apoptosis and stimulates insulin biosynthesis via estrogen receptors present in β -cells, with a predominant estrogen receptors effect (Le May *et al.*, 2006; Liu *et al.*, 2009; Wong *et al.*, 2010). The fact that both human and rodent females are relatively protected from obese forms of T2D with severe β -cell failure raises the possibility that activation of estrogen receptors may also improve lipid homeostasis in β -cells (Liu *et al.*, 2010; Le May *et al.*, 2006; Liu *et al.*, 2009; Wong *et al.*, 2010; Wong *et al.*, 2010; Pick *et al.*, 1998; Louet *et al.*, 2008; Tiano *et al.*, 2010). Decrease of estrogen levels upon senescence or ovariectomy in humans and rodents alter metabolic processes and cause an increase in adiposity (Wade *et al.*, 1985; Tunca *et al.*, 2013). Therefore, this study investigated the effects of the anti-angiogenic inhibitor ALS-L1023 on female obesity and T2D using HFD-fed female sham and OVX mice, which is an animal model of human pre- and postmenopausal women.

1. Female sham mice

The present study demonstrated that ALS-L1023 regulates T2D via improvement of obesity-associated insulin resistance and pancreatic morphology and inhibition of pancreatic steatosis, inflammation, fibrosis, and β -cell apoptosis in HFD-fed obese female sham mice. ALS-L1023 reduces body weight, body weight gain and adipose tissue mass. However, mice fed a HFD-supplemented with 0.4% or 0.8% ALS-L1023

for 17 weeks decreased body weight and body weight gain compared with HFD-fed mice. In parallel with reduction of body weight and body weight gain, ALS-L1023 decreased total adipose tissue and visceral adipose tissue weights. Thus, ALS-L123 was effective to prevent obesity and adiposity, suggesting that ALS-L1023 is useful to regulate obesity-associated metabolic disorders including T2D.

T2D is mainly characterized by obesity-associated insulin resistance and a progressive failure of pancreatic β -cells. In this study, HFD-fed obese sham mice exhibited increased levels of fasting serum glucose and insulin levels compared with FLD-fed mice. However, 0.8% ALS-L1023 significantly decreased fasting blood glucose levels and insulin levels. Similarly, 0.8% ALS-L1023 supplement significantly improved the impaired glucose tolerance at 30 and 90 min, indicating that ALS-L1023 may improve glucose tolerance in obese mice. These results suggest that ALS-L1023 prevents obesity-induced insulin resistance in female sham mice.

It is known that insulin resistance adaptively increases insulin secretion and if this compensation is inadequate, glucose intolerance and T2D develop (Kahn, 2003; Ahrén *et al.*, 2005; Bergman, 1989; Larsson and Ahrén, 1996; Ahrén, 2005). Insulin resistance, as in obesity, is also associated with expansion of β -cell mass, as shown in genetic models of obesity in rodents (Butler *et al.*, 2003; Bock *et al.*, 2003) and in studies of human autopsy pancreatic material (Butler *et al.*, 2003; Klöppel *et al.*, 1985). The dynamics in β -cell expansion are mainly believed to be a consequence of altered balance between β -cell apoptosis and proliferation, although there are also recent findings suggesting that neogenesis from progenitor cells in the pancreatic

ductal epithelium may contribute (Bouwens and Rooman, 2005; Butler *et al.*, 2007; Sachdeva and Stoffers, 2009; Ahrén *et al.*, 2010). The LFD-fed mice showed a normal pancreatic islet structure, whereas the size of pancreatic islets insulin-positive β -cell areas were markedly increased in HFD-fed mice compared with LFD-fed mice. Cells inside the pancreatic islets showed hyperplasia. Thus, it is likely that insulin resistance accompanying HFD feeding in female sham mice is followed by progressive β -cell expansion as evidenced by increased islet size and β -cell area in female sham mice (Ahrén *et al.*, 2010). In contrast, the size of pancreas was decreased to that in LFD-fed mice after 0.8% ALS-L1023 treatment. And insulin-positive cell density increased in both 0.4% and 0.8% ALS-L1023-treated mice compared with HFD-fed mice. These results demonstrate that administration of ALS-L1023 may improve islet morphology and decrease islet β -cell volume to the levels of LFD-fed mice. This histological result was consistent with the serum insulin levels.

Obesity is due to a chronic positive energy balance, which increases the amount of TGs in adipose tissue. However, the TG can also be stored in non-adipose tissue, such as muscle, liver, pancreas and heart. Indeed, obesity has been shown to lead to excessive deposition of TG in these organs, which is termed ectopic fat deposition or steatosis. Lipid droplets accumulate in the cytoplasm of the cells and an excessive accumulation of these lipids may lead to cell dysfunction or cell death, a phenomenon known as lipotoxicity (Unger and Orci L, 2001; Schaffer, 2003; Herpen and Schrauwen-Hinderling, 2008). In the present study, ALS-L1023 reduced fat accumulation in pancreas. Masson's trichrome staining showed fat accumulation in the pancreas and ectopic

deposition of the interlobular fat of HFD-fed mice. As the metabolic consequence of weight reduction, pancreatic lipid accumulation was decreased in ALS-L1023-treated mice. HFD-fed mice exhibited ectopic deposition of the interlobular fat accumulation in pancreas. However, treatment of mice with ALS-L1023 significantly decreased fat accumulation compared with HFD-fed mice.

The function of PPAR α in energy homeostasis is also related to the regulation of the mitochondrial β -oxidation (Viana *et al.*, 2011). PPAR α seems to affect carbohydrate metabolism by means of compensatory insulin secretion by the islets of Langerhans, influencing glucose regulation and lipid regulation (Viana *et al.*, 2011). In order to investigate the mechanism by which the inhibition of pancreatic steatosis by ALS-L1023 is associated with FA oxidation in pancreas, mRNA expression of genes for β -oxidation was measured. MCAD, VLCAD, CPT-1, PPAR α , AMPK α 1, and AMPK α 2 mRNA levels were increased in 0.4% and 0.8% ALS-L1023 groups compared with HFD-fed group in pancreas of sham mice.

Sterol regulatory elements binding proteins 1c (SREBP-1c) are a key transcription factor family that play an important role in adipogenesis, insulin sensitivity, and FA homeostasis (Lin and Lane, 1993; MacDougald *et al.*, 1995; Wu *et al.*, 1999; Spiegelman, 1999). By preventing lipid accumulation in adipose tissue, the selective downregulation of adipocyte SREBP-1c in obesity might promote the partitioning of free FAs toward other tissues, such as skeletal muscle, pancreas, or liver, where through 'lipotoxicity' they may impair insulin action and/or secretion (Unger and Orci, 2000; Unger and Orci, 2001; Tiano *et al.*, 2011). N. Yamada *et al.* was concluded that SREBP-1c has

a negative impact on insulin secretion and plays a physiological role in β -cells. Thus, N. Yamada *et al.* speculated that SREBP-1c, because of its function in de novo FA synthesis, responds to nutritional status and plays a regulatory role in insulin secretion and β -cell function (Shimano *et al.*, 2007). To determine whether ALS-L1023 inhibits the expression of lipogenic genes in female mice, the mRNA levels of PPAR γ , C/EBP α , aP2, SREBP-1c, FAS, and ACC were measured in pancreas of HFD-fed mice. SREBP-1c, ACC and aP2 mRNA levels were decreased by 0.8% ALS-L1023-treated-group. Although, FAS and C/EBP α mRNA levels were not decreased by ALS-L1023 group compared with HFD group. By contrast, PPAR γ mRNA levels shown increased disposition by ALS-L1023 group compared with HFD group. Pioglitazone, a PPAR γ agonist, decreased islet TG content and simultaneously restored the impaired insulin secretion in these animals (Matsui *et al.*, 2004; Herpen and Schrauwen-Hinderling, 2008). Overall, These data suggest that ALS-L1023 may pancreatic steatosis through modulating the expression of genes involved in FA β -oxidation and lipogenesis.

Obesity-induced diabetes is associated with low-grade inflammation in adipose tissue and macrophage infiltration of islets (Pejnovic *et al.*, 2013). Pancreatic inflammation was examined using a toluidine blue staining method an anti-CD68 antibody. To determine the mast cells and macrophages, respectively. In this study, mast cells, macrophages and mRNA levels of inflammation-related gene CD68 were increased in HFD-fed mice compared with LFD-fed mice. By contrast, ALS-L1023 decreased HFD-induced increases in mast cells, macrophages and mRNA levels compared with HFD alone. Therefore, inhibition of pancreatic inflammation

by ALS-L1023 may be caused by decreases in inflammatory cells and expression of inflammatory genes.

A number of studies have already addressed the relationships between inflammation and pancreatic fat accumulation or fibrosis in animal models of obesity or diabetes (Ehses *et al.*, 2007; Otani *et al.*, 2010). Sumio Kawata *et al.* demonstrated that intralobular fat accumulation in exocrine pancreatic tissue and lipid droplets in acinar cells are increased in ZDF rats under chronic intake of a HFD and that these conditions appear to lead to acinar cell injury and fibrosis (Matsuda *et al.*, 2014). In this study, levels of collagen by Masson's trichrome staining were much lower in pancreatic tissue from 0.4% and 0.8% ALS-L1023-treated mice than that from HFD-fed mice. The mRNA expression of fibrogenic genes including α -SMA, collagen1, and TGF β 1 are downregulated in 0.8% ALS-L1023-treated mice compared with HFD-fed mice. These results demonstrate that inhibition of fibrogenesis by ALS-L1023 may be due to the reduced of fibrogenic factors.

T2D occurs when pancreatic β -cells fail to compensate for the increased insulin demand in the context of obesity-associated insulin resistance. Thus, developing novel therapeutic strategies to prevent β -cell failure in the context of obesity is a major challenge. The likely mechanisms of early β -cell demise include fuel overload associated with dysfunctional lipid homeostasis and glucolipotoxicity, which leads to oxidative and endoplasmic reticulum stress, inflammation, and, eventually, β -cell apoptosis (Prentki and Nolan, 2006). In diabetic models, females are

relatively protected from β -cell failure (Liu and Mauvais-Jarvis, 2010; Tiano *et al.*, 2011). Apoptosis are upregulated and downregulated by apoptosis inducers (Bax and p53) and apoptosis inhibitors (Bcl-2 and Bcl-xL), respectively. In contrary to Bax, Bcl-xL and Bcl-2 normally exert an anti-apoptotic action in β -cells. Under the stimulation of FAs, Bcl-2 mRNA levels were significantly decreased in isolated human islet cells, while the levels of Bax remained unchanged (Cunha *et al.*, 2008; Haopeng and Xuejun, 2012). In addition, p53 protein levels were significantly downregulated by activate protein kinase B activation, which might also contribute to its ability to protect β -cells from apoptosis (Haopeng and Xuejun, 2012). p53 mRNA levels were significantly downregulated whereas Bcl-xL mRNA levels were significantly upregulated, in the pancreas of ALS-L1023-treated mice compared with HFD-fed mice.

2. Female OVX mice

In the next study, obesity and T2D were investigated in HFD-fed C57BL/6J female OVX mice, which is an animal model of human postmenopause. HFD-fed OVX mice had higher body weight, visceral adipose tissue weight, and visceral adipocyte size compared with LFD-fed OVX mice. This increases are greater in OVX mice than in sham mice. The body weight of OVX mice fed a HFD supplement with 0.4% ALS-L1023 was decreased compared with HFD-fed mice. In addition, adipose tissue weights and adipocyte size were decreased by 0.4% ALS-L1023 treatment in HFD-fed female OVX mice. However, body weight and adipose tissue weight of OVX mice fed a HFD supplement with 0.8% ALS-L1023 were not decreased compared with HFD-fed mice. In contrast, adipocyte size were decreased by 0.8% ALS-L1023

treatment in HFD-fed female OVX mice.

Estrogen deficiency also contributes to the development of insulin resistance and T2D in rodent models (Louet et al 2004). OVX rodents with low level of endogenous estrogen have elevated basal glucose levels and impaired glucose tolerance (Bailey et al 1980; Haifei and Kumar, 2012). Similarly, OVX mice exhibited elevated glucose levels during OGTT. However, ALS-L1023 lowered glucose levels at both concentrations. In particular, 0.8% ALS-L1023 supplement significantly improved the impaired glucose tolerance at 30 min although body weight and adipose tissue mass were not decreased by 0.8% ALS-L1023. This may be because 0.8% ALS-L1023 decreased visceral adipocyte size. It is known that adipocyte hypertrophy increases insulin resistance and secretes several molecules involved in the pathogenesis of insulin resistance and T2D (Kadowaki, 2000; Kubota *et al.*, 2009; Okuno *et al.*, 1998; Jeong and Yoon, 2009). However, ALS-L1023 were not decreased fasting blood glucose levels and increased insulin levels in female OVX mice.

The LFD-fed OVX mice showed a normal pancreatic islet structure, whereas the size of pancreatic islets was markedly increased in HFD-fed OVX mice compared with LFD-fed OVX mice. Cells inside the pancreatic islets showed hyperplasia that in HFD-fed OVX mice. In contrast, the pancreas morphology was restored to that in LFD-fed mice after 0.4% ALS-L1023 treatment. 0.4% ALS-L1023-treated group showed improved islet morphology but pancreatic islet size of 0.8% ALS-L1023-treated group were not different between HFD-group. Consistent with serum insulin levels, insulin-positive cells increased in both 0.4% and 0.8% ALS-L1023-treated

mice compared with HFD-fed OVX mice. Thus, ALS-L1023 improves islet morphology and insulin-secreting activity and their effects were not different between sham and OVX mice.

In the present study, ALS-L1023 reduced fat accumulation in pancreas. Masson's trichrome staining showed fat accumulation and ectopic deposition of the interlobular fat in the pancreas of HFD-fed OVX mice. As the metabolic consequence of weight reduction, pancreatic lipid accumulation were decreased in ALS-L1023-treated mice compared with HFD-fed mice. These results suggest that ALS-L1023 inhibits pancreatic steatosis.

Studies in humans and laboratory animals indicate that estrogen has a significant role in the adipose tissue regulation. It has been reported that ovariectomy increases adiposity in rodents, and administration of estrogen derivatives reduce fat deposition in these animals. Similarly, following menopause total body fat increases in women and of estrogen-replacement therapy attenuates the accumulation of fat in postmenopausal woman. D'Eon *et al.* reported in their OVX mice model of menopause, estrogen replacement upregulates PPAR δ mRNA expression. Estrogen replacement also upregulates PPAR α gene expression and increases lipid peroxidation in genetically PPAR α deficient mice (D'Eon *et al.*, 2005; Campbell *et al.*, 2003; Djouadi *et al.*, 1998; Tunca *et al.*, 2013).

In order to investigate the mechanism by which ALS-L1023 regulates pancreatic steatosis, mRNA expression of genes for β -oxidation was measured. However, mRNA expression of FA β -oxidation genes was not different between HFD group and ALS-L1023 group in female OVX mice. In contrast, ALS-L1023

inhibits the expression of lipogenic genes in OVX mice. C/EBP α and aP2 mRNA levels were decreased in ALS-L1023-treated mice compared with HFD-fed OVX mice. Therefore, these results indicate that ALS-L1023 suppresses OVX-induced hepatic steatosis through decreasing the expression of lipogenic genes, but not FA oxidation genes.

Pancreatic inflammation in female OVX mice was examined using the same methods as used in the experiments of female sham mice. In this study, mast cells, macrophages and mRNA levels of the inflammatory gene CD68 were reduced by ALS-L1023 compared with HFD. These results suggest that ALS-L1023 treatment improves HFD-induced pancreatic inflammation in female OVX mice and this process may be mediated through change in inflammatory gene expression.

HFD-fed OVX mice showed pancreatic inflammation as shown by increases in Masson's trichrome-stained collagen levels compared with LFD-fed mice. However, levels of collagen were much lower in pancreatic tissue from 0.4% and 0.8% ALS-L1023-treated mice than from HFD-fed OVX mice. The mRNA expression of fibrogenic genes including α -SMA and collagen1 were downregulated in ALS-L1023-treated OVX mice compared with HFD-fed OVX mice. These results demonstrate that ALS-L1023 inhibits fibrogenesis may be due to the inhibition of fibrogenic factors.

The ALS-L1023 also reduced the expression of apoptosis genes in HFD-fed OVX mice. Bax and p53 mRNA levels were decreased in ALS-L1023-treated mice compared with HFD-fed mice. Bcl-2 mRNA levels were increased in ALS-L1023-treated group compared with HFD group in female OVX mice.

In conclusion, these results demonstrate that the angiogenesis inhibitor

ALS-L1023 may prevent HFD-induced obesity and T2D in both female sham and OVX mice, and that these processes are regulated probably through the inhibition of pancreatic steatosis, inflammation, fibrosis, and apoptosis. In this study, HFD-induced obesity and T2D were more eminent in OVX mice than in sham mice. The effects of ALS-L1023 on obesity and T2D are greater in sham mice with functioning ovaries compared with OVX mice, maybe due to high estradiol concentrations in female sham mice.

V. REFERENCES

- Akhondzadeh S, Moroozian M, Mohammadi M, Ohadinia S, Jamshidi AH, Khani M (2003) Melissa officinalis extract in the treatment of patients with mild to moderate Alzheimer's disease : a double blind, randomised, placebo controlled trial. *J Neurol Neurosurg Psychiatry*. 74(7):863-866.
- Ahrén B (2005) Type 2 diabetes, insulin secretion and beta-cell mass. *Curr Mol Med*. 5(3):275-286.
- Ahrén B, Pacini G (2005) Islet adaptation to insulin resistance: mechanisms and implications for intervention. *Diabetes Obes Metab*. 7(1):2-8.
- Ahrén B (1999) Plasma leptin and insulin in C57BL/6J mice on a high-fat diet: relation to subsequent changes in body weight. *Acta Physiol Scand*. 165(2):233-240.
- Ahrén J, Ahrén B, Wierup N (2010) Increased β -cell volume in mice fed a high-fat diet: a dynamic study over 12 months. *Islets*. 2(6):353-6
- Ali NK (2014) "Chronic Pancreatitis Imaging". Medscape. Retrieved 5
- Bajaj M, Suraamornkul S, Piper P, Hardies LJ, Glass L, Cersosimo E, Pratipanawatr T, Miyazaki Y, DeFronzo RA (2004) Decreased plasma adiponectin concentrations are closely related to hepatic fat content and hepatic insulin resistance in pioglitazone-treated type 2 diabetic patients. *J Clin Endocrinol Metab*. 89(1):200-206.
- Bajaj M, Suraamornkul S, Pratipanawatr T, Hardies LJ, Pratipanawatr W, Glass L, Cersosimo E, Miyazaki Y, DeFronzo RA (2003) Pioglitazone reduces hepatic fat content and augments splanchnic glucose uptake in patients with type 2 diabetes. *Diabetes*. 52(6):1364-1370.
- Becker W, Kluge R, Kantner T, Linnartz K, Korn M, Tschank G, Plum L, Giesen K, Joost HG. (2004) Differential hepatic gene expression in a polygenic mouse model with insulin resistance and hyperglycemia: evidence for a combined transcriptional dysregulation of gluconeogenesis and FA synthesis. *J Mol Endocrinol*. 32(1):195-208.
- Bergman RN (1989) Lilly lecture 1989. Toward physiological understanding of glucose tolerance. Minimal-model approach. *Diabetes*. 38(12):1512-1527.
- Bock T, Pakkenberg B, Buschard K (2003) Increased islet volume but unchanged islet number in ob/ob mice. *Diabetes*. 52(7):1716-1722.
- Bouwens L, Rooman I (2005) Regulation of pancreatic beta-cell mass. *Physiol Rev*. 85(4):1255-1270.
- Brownlee M (2003) A radical explanation for glucose-induced beta cell dysfunction. *J Clin Invest*. 112(12):1788-1790.

Butler AE, Janson J, Bonner-Weir S, Ritzel R, Rizza RA, Butler PC (2003) Beta-cell deficit and increased beta-cell apoptosis in humans with type 2 diabetes. *Diabetes*. 52:102-110.

Butler AE, Janson J, Soeller WC, Butler PC (2003) Increased beta-cell apoptosis prevents adaptive increase in beta-cell mass in mouse model of type 2 diabetes: evidence for role of islet amyloid formation rather than direct action of amyloid. *Diabetes*. 52(9):2304-2314.

Butler PC, Meier JJ, Butler AE, Bhushan A (2007) The replication of beta cells in normal physiology, in disease and for therapy. *Nat Clin Pract Endocrinol Metab*. 3(11):758-768.

Campbell SE, Mehan KA, Tunstall RJ, Febbraio MA, Cameron-Smith D (2003) 17beta-estradiol upregulates the expression of peroxisome proliferator-activated receptor alpha and lipid oxidative genes in skeletal muscle. *J Mol Endocrinol*. 31(1):37-45.

Chiasson JL, Josse RG, Gomis R, Hanefeld M, Karasik A, Laakso M; STOP-NIDDM Trial Research Group (2002) Acarbose for prevention of T2D: the STOP-NIDDM randomised trial. *Lancet*. 359(9323):2072-2077.

Childs B (2005) Complete nurse's guide to diabetes care. Port City Press

Colditz GA, Willett WC, Rotnitzky A, Manson JE (1995) Weight gain as a risk factor for clinical diabetes mellitus in women. *Ann Intern Med*. 122(7):481-486.

Cunha DA, Hekerman P, Ladrière L, Bazarra-Castro A, Ortis F, Wakeham MC, Moore F, Rasschaert J, Cardozo AK, Bellomo E, Overbergh L, Mathieu C, Lupi R, Hai T, Herchuelz A, Marchetti P, Rutter GA, Eizirik DL, Cnop M (2008) Initiation and execution of lipotoxic ER stress in pancreatic beta-cells. *J Cell Sci*. 121(Pt 14):2308-2318.

David GG, Dolores MS (2011) Greenspan's Basic & Clinical Endocrinology. New York: McGraw-Hill Medical. pp. Chapter 17.

DeFronzo RA (1988) Lilly lecture 1987. The triumvirate: beta-cell, muscle, liver. A collusion responsible for NIDDM. *Diabetes*. 37(6):667-687.

DeFronzo RA (1997) Pathogenesis of type 2 diabetes : metabolic and molecular implications for identifying diabetes genes. *Diabetes Rev*. 5:177-5269.

D'Eon TM, Souza SC, Aronovitz M, Obin MS, Fried SK, Greenberg AS (2005) Estrogen regulation of adiposity and fuel partitioning. Evidence of genomic and non-genomic regulation of lipogenic and oxidative pathways. *J Biol Chem*. 280(43):35983-35991.

Diamond J (2003) The double puzzle of diabetes. *Nature*. 423(6940):599-602.

Dimitrova Z, Dimov B, Manolova N, Pancheva S, Ilieva D, Shishkov S (1993) Antiherpes effect of *Melissa officinalis* L. extracts. *Acta Microbiol Bulg.* 29:65–72.

Djouadi F, Weinheimer CJ, Saffitz JE, Pitchford C, Bastin J, Gonzalez FJ, Kelly DP (1998) A gender-related defect in lipid metabolism and glucose homeostasis in peroxisome proliferator-activated receptor α -deficient mice. *J Clin Invest.* 102(6):1083–1091.

Ehses JA, Perren A, Eppler E, Ribaux P, Pospisilik JA, Maor-Cahn R, Gueripel X, Ellingsgaard H, Schneider MK, Biollaz G, Fontana A, Reinecke M, Homo-Delarche F, Donath MY (2007) Increased number of islet-associated macrophages in type 2 diabetes. *Diabetes.* 56(9):2356–2370.

Flier JS (2004) Obesity wars: molecular progress confronts an expanding epidemic. *Cell.* 116(2):337–350.

Fox, Stuart Ira (2013) *Human Physiology*. McGraw-Hill Science/Engineering. pp.642

Ibid, pp. 643

Ibid, pp. 346 –347

Ibid, pp. 330–331

Geary N, Asarian L (2001) Estradiol increases glucagon's satiating potency in ovariectomized rats. *Am J Physiol Regul Integr Comp Physiol.* 281(4):R1290–4.

Gerich JE (1998) The genetic basis of T2D: impaired insulin secretion versus impaired insulin sensitivity. *Endocr Rev.* 19(4):491–503.

Guilherme A, Virbasius JV, Puri V, Czech MP (2008) Adipocyte dysfunctions linking obesity to insulin resistance and type 2 diabetes. *Nat Rev Mol Cell Biol.* 9(5):367–377

Haifei Shi, Shiva Priya Dharshan Senthil Kumar (2012) Sex Differences in Obesity-Related Glucose Intolerance and Insulin Resistance. *Glucose Tolerance*. DOI: 10.5772/52972

Hans-Georg Joost (2008) Pathogenesis, Risk Assessment and Prevention of T2D. *Obesity Facts.* 1:128 – 137

Haopeng Y, Xuejun L (2012) The role of FA metabolism and lipotoxicity in pancreatic β -cell injury: Identification of potential therapeutic targets *Acta Pharmaceutica Sinica B.* Vol 2, Iss 4, Pgs 396 – 402

Harmon JS, Stein R, Robertson RP (2005) Oxidative stress-mediated, post-translational loss of MafA protein as a contributing mechanism to loss of insulin gene expression in glucotoxic beta cells. *J Biol Chem.* 280(12):11107–11113.

Hulín I, Šimko F, Zlatoš L, Bernadič M, Ďuriš I, Maasová D, Ferenčík M, Štvrtinová V, Jakubovský J, Mladosičová B, Sapáková H (1997) *Pathophysiology*. Slovak

Academic Press. pp. 404~410

J Revis, S Keene (2006) Type II Diabetes in American Women over 40: Obesity and Menopause. The Internet Journal of Health. Volume 6 Number 1

Jeong S, Yoon M (2009) Fenofibrate inhibits adipocyte hypertrophy and insulin resistance by activating adipose PPARalpha in high fat diet-induced obese mice. *Exp Mol Med*. 41(6):397-405.

Joost HG (2008) Pathogenesis, risk assessment and prevention of T2D. *Obes Facts*. 1(3):128-137

Jürgens H, Schmolz K, Neschen S, Ortmann S, Blüher M, Klaus S, Tschöp M, Joost HG, Schürmann A (2006) Development of Diabetes in Morbidly Obese New-Zealand Obese (NZO) Mice Requires Dietary Carbohydrates: Evidence for an Essential Role of Glucose Toxicity in Beta-Cell Destruction. *Diabetologia*. 50:1481-1489.

Kadowaki T (2000) Insights into insulin resistance and type 2 diabetes from knockout mouse models. *J Clin Invest*. 106(4):459-465.

Kahn BB (1998) Type 2 diabetes: when insulin secretion fails to compensate for insulin resistance. *Cell*. 92(5):593-596.

Kahn SE (2003) The relative contributions of insulin resistance and beta-cell dysfunction to the pathophysiology of Type 2 diabetes. *Diabetologia*. 46(1):3-19.

Kharroubi I, Ladrière L, Cardozo AK, Dogusan Z, Cnop M, Eizirik DL (2004) Free FAs and cytokines induce pancreatic beta-cell apoptosis by different mechanisms: role of nuclear factor-kappaB and endoplasmic reticulum stress. *Endocrinology*. 145(11):5087-5096.

Kim JS, Park BY, Park EK, Lee HS, Hahm JC, Bae KW, Kim MY (2006) Screening of anti-angiogenic activity from plant extract. *Kor. J. Pharmacogn*. 37(4):253-257.

Klöppel G, Löhr M, Habich K, Oberholzer M, Heitz PU (1985) Islet pathology and the pathogenesis of type 1 and T2D revisited. *Surv Synth Pathol Res*. 4(2):110-125.

Knowler WC, Barrett-Connor E, Fowler SE, Hamman RF, Lachin JM, Walker EA, Nathan DM; Diabetes Prevention Program Research Group (2002) Reduction in the incidence of type 2 diabetes with lifestyle intervention or metformin. *N Engl J Med*. 346(6):393-403.

Kolb H, Mandrup-Poulsen T (2005) An immune origin of type 2 diabetes? *Diabetologia*. 48(6):1038-1050.

Kubota N, Terauchi Y, Miki H, Tamemoto H, Yamauchi T, Komeda K, Satoh S, Nakano R, Ishii C, Sugiyama T, Eto K, Tsubamoto Y, Okuno A, Murakami K, Sekihara H, Hasegawa G, Naito M, Toyoshima Y, Tanaka S, Shiota K, Kitamura T,

Fujita T, Ezaki O, Aizawa S, Kadowaki T (1999) PPAR gamma mediates high-fat diet-induced adipocyte hypertrophy and insulin resistance. *Mol Cell*. 4(4):597-609.

Kumar V, Fausto N, Abbas Abul K, Cotran Ramzi S, Robbins Stanley L. (2005) Robbins and Cotran Pathologic Basis of Disease (7th ed.). Philadelphia, Pa.: Saunders. pp. 1194 - 1195.

Lan H, Rabaglia ME, Stoehr JP, Nadler ST, Schueler KL, Zou F, Yandell BS, Attie AD (2003) Gene expression profiles of nondiabetic and diabetic obese mice suggest a role of hepatic lipogenic capacity in diabetes susceptibility. *Diabetes*. 52(3):688-700.

Larsson H, Ahrén B (1996) Failure to adequately adapt reduced insulin sensitivity with increased insulin secretion in women with impaired glucose tolerance. *Diabetologia*. 39(9):1099-1107.

Le May C, Chu K, Hu M, Ortega CS, Simpson ER, Korach KS, Tsai MJ, Mauvais-Jarvis F (2006) Estrogens protect pancreatic beta-cells from apoptosis and prevent insulin-deficient diabetes mellitus in mice. *Proc Natl Acad Sci U S A*. 103(24):9232-9237.

Leahy JL (1990) Natural history of beta-cell dysfunction in NIDDM. *Diabetes Care*. 13(9):992-1010.

Leiter EH, Coleman DL, Eisenstein AB, Strack I (1981) Dietary control of pathogenesis in C57BL/KsJ db/db diabetes mice. *Metabolism*. 30(6):554-562.

Leiter EH, Coleman DL, Ingram DK, Reynolds MA (1983) Influence of dietary carbohydrate on the induction of diabetes in C57BL/KsJ-db/db diabetes mice. *J Nutr*. 113(1):184-195.

Leonardi O, Mints G, Hussain MA (2003) Beta-cell apoptosis in the pathogenesis of human T2D. *Eur J Endocrinol*. 149(2):99-102.

Lin FT, Lane MD (1994) CCAAT/enhancer binding protein alpha is sufficient to initiate the 3T3-L1 adipocyte differentiation program. *Proc Natl Acad Sci U S A*. 91(19):8757-8761.

Liu S, Le May C, Wong WP, Ward RD, Clegg DJ, Marcelli M, Korach KS, Mauvais-Jarvis F (2009) Importance of extranuclear estrogen receptor-alpha and membrane G protein-coupled estrogen receptor in pancreatic islet survival. *Diabetes*. 58(10):2292-2302.

Liu S, Mauvais-Jarvis F (2010) Minireview: Estrogenic protection of beta-cell failure in metabolic diseases. *Endocrinology*. 151(3):859-864.

Louet JF, Smith SB, Gautier JF, Molokhia M, Virally ML, Kevorkian JP, Guillausseau PJ, Vexiau P, Charpentier G, German MS, Vaisse C, Urbanek M, Mauvais-Jarvis F (2008) Gender and neurogenin3 influence the pathogenesis of ketosis-prone diabetes.

Diabetes Obes Metab. 10(10):912-920.

MacDougald OA, Cornelius P, Liu R, Lane MD (1995) Insulin regulates transcription of the CCAAT/enhancer binding protein (C/EBP) alpha, beta, and delta genes in fully-differentiated 3T3-L1 adipocytes. *J Biol Chem.* 270(2):647-654.

Maedler K, Spinas GA, Dyntar D, Moritz W, Kaiser N, Donath MY. (2001) Distinct effects of saturated and monounsaturated FAs on beta-cell turnover and function. *Diabetes.* 50(1):69-76.

Mantzoros C.S (2006) Obesity and diabetes. Humana Press

Marguet D, Baggio L, Kobayashi T, Bernard AM, Pierres M, Nielsen PF, Ribet U, Watanabe T, Drucker DJ, Wagtmann N (2000) Enhanced insulin secretion and improved glucose tolerance in mice lacking CD26. *Proc Natl Acad Sci U S A.* 6;97(12):6874-6879.

Mark F, Lawrence SF, Lawrence JB, Marvin H (2009). Sleisenger & Fordtran's gastrointestinal and liver disease pathophysiology, diagnosis, management (9th ed.). St. Louis, Mo: MD Consult.

Martinez SC, Tanabe K, Cras-Méneur C, Abumrad NA, Bernal-Mizrachi E, Permutt MA (2008) Inhibition of Foxo1 protects pancreatic islet beta-cells against FA and endoplasmic reticulum stress-induced apoptosis. *Diabetes.* 57(4):846-859.

Matsuda A, Makino N, Tozawa T, Shirahata N, Honda T, Ikeda Y, Sato H, Ito M, Kakizaki Y, Akamatsu M, Ueno Y, Kawata S (2014) Pancreatic fat Accumulation, Fibrosis, and Acinar Cell Injury in the Zucker Diabetic Fatty Rat Fed a Chronic High-Fat Diet. *Pancreas.*

Matsui J, Terauchi Y, Kubota N, Takamoto I, Eto K, Yamashita T, Komeda K, Yamauchi T, Kamon J, Kita S, Noda M, Kadowaki T (2004) Pioglitazone reduces islet triglyceride content and restores impaired glucose-stimulated insulin secretion in heterozygous peroxisome proliferator-activated receptor-gamma-deficient mice on a high-fat diet. *Diabetes.* 53(11):2844-2854.

Mauvais-Jarvis F, Sobngwi E, Porcher R, Riveline JP, Kevorkian JP, Vaisse C, Charpentier G, Guillausseau PJ, Vexiau P, Gautier JF (2004) Ketosis-prone type 2 diabetes in patients of sub-Saharan African origin: clinical pathophysiology and natural history of beta-cell dysfunction and insulin resistance. *Diabetes.* 53(3):645-653.

National institutes of health (1998) Clinical Guidelines on the Identification, Evaluation, and Treatment of Overweight and Obesity in Adults--The Evidence Report. National Institutes of Health. *Obes Res.* 6 Suppl 2:S1S-209S.

Ogden CL, Carroll MD, Curtin LR, McDowell MA, Tabak CJ, Flegal KM (2006) Prevalence of overweight and obesity in the United States, 1999-2004. *JAMA.* 295(13):1549-1555.

Okuno A, Tamemoto H, Tobe K, Ueki K, Mori Y, Iwamoto K, Umesono K, Akanuma Y, Fujiwara T, Horikoshi H, Yazaki Y, Kadowaki T (1998) Troglitazone increases the number of small adipocytes without the change of white adipose tissue mass in obese Zucker rats. *J Clin Invest.* 101(6):1354-1361.

Otani M, Yamamoto M, Harada M, Otsuki M (2010) Effect of long- and short-term treatments with pravastatin on diabetes mellitus and pancreatic fibrosis in the Otsuka-Long-Evans-Tokushima fatty rat. *Br J Pharmacol.* 159(2):462-473.

Pejnovic NN, Pantic JM, Jovanovic IP, Radosavljevic GD, Milovanovic MZ, Nikolic IG, Zdravkovic NS, Djukic AL, Arsenijevic NN, Lukic ML (2013) Galectin-3 deficiency accelerates high-fat diet-induced obesity and amplifies inflammation in adipose tissue and pancreatic islets. *Diabetes.* 62(6):1932-1944

Petersen KF, Dufour S, Befroy D, Lehrke M, Hendler RE, Shulman GI (2005) Reversal of nonalcoholic hepatic steatosis, hepatic insulin resistance, and hyperglycemia by moderate weight reduction in patients with type 2 diabetes. *Diabetes.* 54(3):603-608.

Pick A, Clark J, Kubstrup C, Levisetti M, Pugh W, Bonner-Weir S, Polonsky KS (1998) Role of apoptosis in failure of beta-cell mass compensation for insulin resistance and beta-cell defects in the male Zucker diabetic fatty rat. *Diabetes.* 47(3):358-364.

Plum L, Kluge R, Giesen K, Altmüller J, Ortlepp JR, Joost HG (2000) Type 2 diabetes-like hyperglycemia in a backcross model of NZO and SJL mice: characterization of a susceptibility locus on chromosome 4 and its relation with obesity. *Diabetes.* 49(9):1590-1596.

Poitout V, Robertson RP (2002) Minireview: Secondary beta-cell failure in type 2 diabetes--a convergence of glucotoxicity and lipotoxicity. *Endocrinology.* 143(2):339-342.

Polotsky HN, Polotsky AJ (2010) Metabolic implications of menopause. *Semin Reprod Med.* 28(5):426-434

Prentki M, Nolan CJ (2006) Islet beta cell failure in type 2 diabetes. *J Clin Invest.* 116(7):1802-1812.

Reaven GM (1995) The fourth musketeer--from Alexandre Dumas to Claude Bernard. *Diabetologia.* 38(1):3-13.

Reimer MK, Ahrén B (2002) Altered beta-cell distribution of pdx-1 and GLUT-2 after a short-term challenge with a high-fat diet in C57BL/6J mice. *Diabetes.* 51 Suppl 1:S138-143.

Robertson RP, Zhang HJ, Pyzdrowski KL, Walseth TF (1992) Preservation of insulin mRNA levels and insulin secretion in HIT cells by avoidance of chronic exposure to

high glucose concentrations. *J Clin Invest.* 90(2): 320 - 325.

Rosenthal S (2005) *The Type 2 Diabetes Sourcebook for Women.* McGraw-Hill Education

Sachdeva MM, Stoffers DA (2009) Minireview: Meeting the demand for insulin: molecular mechanisms of adaptive postnatal beta-cell mass expansion. *Mol Endocrinol.* 23(6):747-758.

Schaffer JE (2003) Lipotoxicity: when tissues overeat. *Curr Opin Lipidol.* 14(3):281-287.

Scheen AJ (1996) Pathophysiology of type 2 diabetes. In: Kuhlman J, Puls W, eds, *Handbook of Experimental Pharmacology, Oral Antidiabetics* (Springer Verlag: Berlin) pp.7-42.

Scheen AJ (2001) Obesity and diabetes. In : *The management of obesity and related disorders* (Kopelman P.G., Ed.), Martin Dunitz Ltd, London, UK, pp.11-44.

Scheen AJ (2003) Pathophysiology of type 2 diabetes. *Acta Clin Belg.* 58(6):335-341.

Schulze MB, Hu FB (2005) Primary prevention of diabetes: what can be done and how much can be prevented? *Annu Rev Public Health.* 26:445-467.

Sewter C, Berger D, Considine RV, Medina G, Rochford J, Ciaraldi T, Henry R, Dohm L, Flier JS, O'Rahilly S, Vidal-Puig AJ (2002) Human obesity and type 2 diabetes are associated with alterations in SREBP1 isoform expression that are reproduced ex vivo by tumor necrosis factor- α . *Diabetes.* 51(4):1035-1041.

Shimano H, Amemiya-Kudo M, Takahashi A, Kato T, Ishikawa M, Yamada N (2007) Sterol regulatory element-binding protein-1c and pancreatic beta-cell dysfunction. *Diabetes Obes Metab. Suppl* 2:133-139.

Shlomo M, Kenneth SP, Henry MK (2012) *Williams textbook of endocrinology.* (12th ed.). Philadelphia: Elsevier/Saunders. pp. 1371 - 1435.

Sjöholm A, Nyström T (2006) Inflammation and the etiology of type 2 diabetes. *Diabetes Metab Res Rev.* 22(1):4-10.

Smyth S, Heron A (2006) Diabetes and obesity: the twin epidemics. *Nat Med.* 12(1):75-80.

Spiegelman BM (1998) PPAR- γ : adipogenic regulator and thiazolidinedione receptor. *Diabetes.* 47(4):507-514.

Spranger J, Kroke A, Möhlig M, Bergmann MM, Ristow M, Boeing H, Pfeiffer AF. (2003) Adiponectin and protection against T2D. *Lancet.* 361(9353):226-228.

Srinivasan K, Ramarao P (2007) Animal models in type 2 diabetes research: an

overview. Indian J Med Res.125(3):451-472.

Stumvoll M (2004) Control of glycaemia: from molecules to men. Minkowski Lecture 2003. Diabetologia. 47(5):770-781.

Surwit RS, Feinglos MN, Rodin J, Sutherland A, Petro AE, Opara EC, Kuhn CM, Rebuffé-Scrive M (1995) Differential effects of fat and sucrose on the development of obesity and diabetes in C57BL/6J and A/J mice. Metabolism. 44(5):645-651.

Surwit RS, Kuhn CM, Cochrane C, McCubbin JA, Feinglos MN (1988) Diet-induced type II diabetes in C57BL/6J mice. Diabetes. 37(9):1163-1167.

Tiano JP, Delghingaro-Augusto V, Le May C, Liu S, Kaw MK, Khuder SS, Latour MG, Bhatt SA, Korach KS, Najjar SM, Prentki M, Mauvais-Jarvis F (2011) Estrogen receptor activation reduces lipid synthesis in pancreatic islets and prevents β cell failure in rodent models of type 2 diabetes. J Clin Invest. 121(8):3331-3342.

TUNCA, Recai, DEVRIM, Alparslan K, SOZMEN, Mahmut, DAG, Serpil, GUNGOR, Orsan, IPEK, Emrah (2013) The Effects of Gemfibrozil and Ovariectomy on the Peroxisome Proliferator Activated Receptors (PPARs) in Mice with Experimentally Induced Obesity. Kafkas Universitesi Veteriner Fakultesi Dergisi, Vol. 19 Issue 5, p783.

Tuomilehto J, Lindstrom J, Eriksson JG, Valle TT, Hamalainen H, IlanneParikka P, Keinanen-Kiukaanniemi S, Laakso M, Louheranta A, Rastas M, Salminen V, Uusitupa M (2001) Finnish Diabetes Prevention Study Group: Prevention of T2D by changes in lifestyle among subjects with impaired glucose tolerance. N Engl J Med. 344:1343 - 1350.

Unger RH, Orci L (2000) Lipotoxic diseases of nonadipose tissues in obesity. Int J Obes Relat Metab Disord. 24 Suppl 4:S28-32.

Unger RH, Orci L (2001) Diseases of liporegulation: new perspective on obesity and related disorders. FASEB J. 15(2):312-321.

Unger RH (2003) Minireview: weapons of lean body mass destruction: the role of ectopic lipids in the metabolic syndrome. Endocrinology. 144(12):5159-5165.

van Herpen NA, Schrauwen-Hinderling VB (2008) Lipid accumulation in non-adipose tissue and lipotoxicity. Physiol Behav. 94(2):231-241.

Viana Abranches M, Esteves de Oliveira FC, Bressan J (2011) Peroxisome proliferator-activated receptor: effects on nutritional homeostasis, obesity and diabetes mellitus. Nutr Hosp. 26(2):271-279.

Vinay K, Nelso F, Abul A (2005). Robbins and Cotran Pathologic Basis of Disease (7th ed.). Philadelphia, Pa.: Saunders. pp. 1194 - 1195.

Wade GN (1975) Some effects of ovarian hormones on food intake and body weight in

female rats. *J Comp Physiol Psychol.* 88(1):183-193.

Wade GN, Gray JM, Bartness TJ (1985) Gonadal influences on adiposity. *Int J Obes.* 9 Suppl 1:83-92.

Wang Y, Rimm EB, Stampfer MJ, Willett WC, Hu FB (2005) Comparison of abdominal adiposity and overall obesity in predicting risk of type 2 diabetes among men. *Am J Clin Nutr.* 81(3):555-563.

Winzell MS, Ahrén B (2004) The high-fat diet-fed mouse: a model for studying mechanisms and treatment of impaired glucose tolerance and type 2 diabetes. *Diabetes.* 53 Suppl 3:S215-219.

Wong WP, Tiano JP, Liu S, Hewitt SC, Le May C, Dalle S, Katzenellenbogen JA, Katzenellenbogen BS, Korach KS, Mauvais-Jarvis F (2010) Extranuclear estrogen receptor- α stimulates NeuroD1 binding to the insulin promoter and favors insulin synthesis. *Proc Natl Acad Sci U S A.* 107(29):13057-13062.

Wrede CE, Dickson LM, Lingohr MK, Briaud I, Rhodes CJ (2002) Protein kinase B/Akt prevents FA-induced apoptosis in pancreatic beta-cells (INS-1). *J Biol Chem.* 277(51):49676-49684.

Wu Z, Rosen ED, Brun R, Hauser S, Adelmant G, Troy AE, McKeon C, Darlington GJ, Spiegelman BM (1999) Cross-regulation of C/EBP α and PPAR γ controls the transcriptional pathway of adipogenesis and insulin sensitivity. *Mol Cell.* 3(2):151-158.

Xu X, D'Hoker J, Stangé G, Bonn   S, De Leu N, Xiao X, Van de Casteele M, Mellitzer G, Ling Z, Pipeleers D, Bouwens L, Scharfmann R, Gradwohl G, Heimberg H (2008) Beta cells can be generated from endogenous progenitors in injured adult mouse pancreas. *Cell.* 132(2):197-207.

국문 요약

혈관신생억제제 ALS-L1023이 고지방식이 암컷 비만마우스에서 제2형 당뇨병에 미치는 효과

임 혜 숙

목원대학교 대학원 생물학과 동물학전공

지도교수 윤 미 정

비만은 고지혈증, 심혈관계 질환 및 제2형 당뇨병을 유발하는 중요한 위험인자이다. 또한 비만인구의 증가와 더불어 여러 종류의 대사증후군 유병률도 함께 증가하고 있다. 제1형 당뇨병은 자가면역 과정의 결과로 인한 베타세포의 손상 때문에 발생하나, 제2형 당뇨병은 복부비만과 연관성이 깊다. 비만으로 인한 대사증후군 중 하나인 제2형 당뇨병은 인슐린 작용저하가 주요 원인이며 나아가 췌장 베타세포 사멸로 인한 인슐린의 분비 결함으로 인해 혈당이 높아지는 대사질환이다. 특히, 비만 및 대사질환은 난소호르몬의 유 무에 따라 다르게 조절되는 것으로 알려져 있다. 따라서 본 연구에서는 난소 유 무에 따라 암컷 C57BL/6J 마우스를 두 그룹으로 나눈 후 고지방식이를 섭취시킨 비만마우스에서 복부비만 치료제인 혈관신생억제제 ALS-L1023이 암컷마우스의 제2형 당뇨병을 조절하는지 조사하고, 작용기전을 규명하고자 하였다.

1. 고지방식이 암컷 비만마우스

제2형 당뇨병은 복부비만과 밀접하게 연관되어 있으며, 이는 제2형 당뇨병에서 복부비만과 지방과다증의 중요성을 보여준다. 본 연구에서는 난소를 가진 고지방식이 암컷 비만 C57BL/6J 마우스에서 복부지방조직의 성장과 발달을 억제하는 혈관신생억제제 ALS-L1023의 제2형 당뇨병 조절효과를 조사하였다.

- 1) 저지방식이 마우스와 비교하여 고지방식이를 섭취한 마우스는 몸무게, 지방조직 무게가 증가하였으나, ALS-L1023을 처리한 고지방식이 마우스에서는 몸무게, 지방조직 무게, 지방세포 크기가 감소되었다.
- 2) 고지방식이 마우스에서는 혈당과 인슐린의 증가를 통해 인슐린 저항성이 나타났으나 0.8% ALS-L1023 처리로 혈당과 인슐린 수준이 모두 감소되었다.
- 3) 고지방식이를 섭취한 비만마우스는 경구내당성이 손상되었으나 0.8% ALS-L1023을 처리한 고지방식이 마우스에서는 손상된 경구내당성이 개선되었다.
- 4) 고지방식이를 섭취한 비만마우스와 비교하여 0.8% ALS-L1023을 처리한 고지방식이 마우스에서 췌장의 형태가 개선되었으며, 췌장의 크기도 저지방식이 마우스의 췌장 크기로 감소되었다. 또한, ALS-L1023의 처리에 의해 췌장의 인슐린 양성반응 세포의 강도가 증가되었다.
- 5) 고지방식이 비만마우스와 비교하여 ALS-L1023이 처리된 고지방식이 비만마우스에서 췌장의 지질 축적이 감소되었으며, 지질생성유전자 (aP2, SREBP-1c, ACC)의 mRNA 수준이 감소되었다. 반면, 0.8% ALS-L1023을 처

리한 고지방식이 비만마우스에서 지방산 β -산화 유전자 (MCAD, CPT-1, PPAR α , AMPK α 1, AMPK α 2) 의 mRNA 수준이 증가되었다.

- 6) ALS-L1023이 처리된 고지방식이 비만마우스에서 췌장의 염증반응을 조사한 결과 고지방식이 비만마우스와 비교하여 비만세포가 감소되었으며, 염증성 유전자인 CD68의 mRNA 발현이 감소되었다.
- 7) ALS-L1023이 처리된 고지방식이 비만마우스에서 췌장의 섬유화를 조사한 결과 고지방식이 비만마우스와 비교하여 콜라겐 수준이 감소되었으며, 섬유생성 유전자 (α -SMA, collagen α 1)의 mRNA 발현이 감소되었다.
- 8) 고지방식이 비만마우스와 비교하여 ALS-L1023이 처리된 고지방식이 마우스에서 췌장의 세포사멸 유도유전자 (p53)의 mRNA 수준이 감소된 반면, 췌장의 세포사멸 억제유전자 (Bcl-xL)의 mRNA 수준이 증가되었다.

2. 난소가 제거된 고지방식이 암컷 비만마우스

성호르몬인 에스트로젠은 몸무게, 체지방 분포, 당 대사와 인슐린 저항성을 조절하는 주요 조절인자이다. 폐경기 여성에서는 비만, 제2형 당뇨병과 같은 대사 증후군 위험성이 크게 증가하므로 난소를 제거한 C57BL/6J 마우스는 폐경기 여성의 동물모델로 적합하다. 따라서 본 연구는 폐경기 여성의 마우스 모델에서 비만과 관련된 대사증후군 중 하나인 제2형 당뇨병에서 ALS-L1023의 작용을 규명하고자 하였다.

- 1) 고지방식이를 섭취한 난소제거 비만마우스는 몸무게와 지방조직 무게가 증가하였으나, 0.4% ALS-L1023을 처리한 고지방식이 난소제거 마우스에서는

몸무게와 지방조직 무게가 감소되었다. 그러나 0.8% ALS-L1023을 처리한 고지방식이 난소제거 비만마우스의 경우에는 몸무게와 지방조직 무게가 감소되지 않았다.

- 2) 고지방식이 난소제거 비만마우스와 비교하여 0.4%와 0.8% ALS-L1023을 처리한 고지방식이 난소제거 마우스에서는 지방세포 크기가 통계적으로 유의하게 감소되었다.
- 3) 고지방식이를 섭취한 난소제거 비만마우스와 비교하여 ALS-L1023을 처리한 고지방식이 난소제거 마우스에서는 혈청 인슐린 농도가 증가되었다.
- 4) 고지방식이 난소제거 비만마우스와 비교하여 ALS-L1023을 처리한 고지방식이 난소제거 마우스에서는 손상된 경구내당성이 개선되는 경향을 보여주었다.
- 5) 고지방식이 난소제거 비만마우스와 비교하여 ALS-L1023을 처리한 고지방식이 난소제거 마우스에서는 췌장의 형태와 크기가 개선되었으며, 췌장의 인슐린 양성반응 강도가 증가되었다.
- 6) 고지방식이 난소제거 비만마우스와 비교하여 ALS-L1023을 처리한 고지방식이 난소제거 마우스에서는 췌장의 지질 축적이 감소되었으며 0.8% ALS-L1023 처리마우스에서 지질생성유전자 (C/EBP α , aP2, SREBP-1c)의 mRNA 수준이 감소되었다. 그러나 지방산 β -산화 유전자 (MCAD, VLCAD, AMPK α 1, AMPK α 2)의 mRNA 수준에는 변화가 없었다.
- 7) 고지방식이 난소제거 비만마우스와 비교하여 ALS-L1023이 처리된 마우스

에서 췌장의 비만세포가 감소되었으며, 염증성 유전자인 CD68의 mRNA 발현이 감소되었다.

8) 고지방식이 난소제거 비만마우스와 비교하여 ALS-L1023이 처리된 마우스에서 췌장의 섬유화와 섬유생성 유전자 (α -SMA, collagen α 1)의 mRNA 발현이 감소되었다.

9) 고지방식이 난소제거 비만마우스와 비교하여 ALS-L1023이 처리된 마우스에서 췌장의 세포사멸 유도유전자 (Bax, p53)의 mRNA 수준이 감소되었으나, 췌장의 세포사멸 억제유전자 (Bcl-2)의 mRNA 수준은 증가되었다.

이상의 결과로 보아, 혈관신생억제제 ALS-L1023은 고지방식으로 유발된 비만과 제2형 당뇨병을 개선시키며, 이는 복부비만, 췌장의 지방증, 섬유화, 염증, 세포사멸 억제를 통해 조절 되는 것으로 보인다. 본 연구에서 고지방식은 비만과 관련된 대사증후군인 제2형 당뇨병을 유도하였으며, 난소를 가진 암컷 비만마우스보다 난소제거 비만마우스에서 더욱 현저하게 발생하였다. 또한 비만과 제2형 당뇨병에 대한 ALS-L1023의 억제효과는 난소를 가진 암컷 정상마우스에서 더 큰 것으로 보이며, 그 이유는 고농도로 존재하는 estradiol의 부가효과 때문으로 생각된다.